

INFORMATION TO USERS

This manuscript has been reproduced from the microfilm master. UMI films the text directly from the original or copy submitted. Thus, some thesis and dissertation copies are in typewriter face, while others may be from any type of computer printer.

The quality of this reproduction is dependent upon the quality of the copy submitted. Broken or indistinct print, colored or poor quality illustrations and photographs, print bleedthrough, substandard margins, and improper alignment can adversely affect reproduction.

In the unlikely event that the author did not send UMI a complete manuscript and there are missing pages, these will be noted. Also, if unauthorized copyright material had to be removed, a note will indicate the deletion.

Oversize materials (e.g., maps, drawings, charts) are reproduced by sectioning the original, beginning at the upper left-hand corner and continuing from left to right in equal sections with small overlaps.

Photographs included in the original manuscript have been reproduced xerographically in this copy. Higher quality 6" x 9" black and white photographic prints are available for any photographs or illustrations appearing in this copy for an additional charge. Contact UMI directly to order.

**Bell & Howell Information and Learning
300 North Zeeb Road, Ann Arbor, MI 48106-1346 USA
800-521-0600**

UMI[®]

NOTE TO USERS

Page(s) not included in the original manuscript are unavailable from the author or university. The manuscript was microfilmed as received.

iv

This reproduction is the best copy available.

UMI

**EFFICIENCY OF PAHs REMOVAL FROM CLAYEY SOIL
USING SUPERCRITICAL FLUID EXTRACTION**

HAIFA EL-SADI

A THESIS

IN

**THE DEPARTMENT OF
BUILDING, CIVIL, AND ENVIRONMENTAL
ENGINEERING**

**Presented in Partial Fulfilment of the Requirements
For the Degree of Master of Applied Science**

**CONCORDIA UNIVERSITY
Montreal, Quebec, Canada**

January 1999

© Haifa El-Sadi 1999



**National Library
of Canada**

**Acquisitions and
Bibliographic Services**

395 Wellington Street
Ottawa ON K1A 0N4
Canada

**Bibliothèque nationale
du Canada**

**Acquisitions et
services bibliographiques**

395, rue Wellington
Ottawa ON K1A 0N4
Canada

Your file Votre référence

Our file Notre référence

The author has granted a non-exclusive licence allowing the National Library of Canada to reproduce, loan, distribute or sell copies of this thesis in microform, paper or electronic formats.

The author retains ownership of the copyright in this thesis. Neither the thesis nor substantial extracts from it may be printed or otherwise reproduced without the author's permission.

L'auteur a accordé une licence non exclusive permettant à la Bibliothèque nationale du Canada de reproduire, prêter, distribuer ou vendre des copies de cette thèse sous la forme de microfiche/film, de reproduction sur papier ou sur format électronique.

L'auteur conserve la propriété du droit d'auteur qui protège cette thèse. Ni la thèse ni des extraits substantiels de celle-ci ne doivent être imprimés ou autrement reproduits sans son autorisation.

0-612-39099-3

Canada

ABSTRACT

Efficiency of PAHs removal from clayey soil using supercritical fluid extraction

The clay soil has specific properties that cause difficulty in the contaminated site assessment and the remediation process. The difficulty in extraction of HOC (hydrophobic organic compounds) from clay material was reported. Therefore, the SFE (supercritical fluid extraction) has a potential to substitute classical methods. The efficiency of using SFE (ISCO 200 model) for clay soil (illite) was investigated.

SFE tests were performed on various compositions of clayey soils. Phenanthrene was used to examine the extraction efficiency of PAHs from clayey soil. Phenanthrene concentration in soil specimen was determined by UV. Carbon dioxide was chosen as the supercritical fluid and 5% (mol) methanol was used as a modifier. The highest recovery (72%) from clay was obtained at a pressure of 55 kPa (8000 psi) and temperature of 150 °C with modifier when dynamic time of 30 min was applied. The impact of pressure (5000 to 8000 psi), temperature (50 to 150 °C) and time (static and dynamic) were discussed.

The extraction efficiency of phenanthrene from soil was modeled. The model accounts for effective diffusion of the phenanthrene in the solid pores, axial dispersion in the fluid phase and external mass transfer to the fluid phase from the particle surface. This model, involving partial differential equations, was solved using the finite difference. The model showed the relationship between diffusivity, mass transfer coefficient and properties of porous media (clay texture). Solubility of phenanthrene in carbon dioxide was calculated. The porous media analysis was reported by an electron microscopy and an image analysis. The developed model can be applied for more precise analysis necessary for contaminated site assessment as well as for evaluation of the remediation technology efficiency.

ACKNOWLEDGMENTS

I wish to express my gratitude and deep appreciation to my supervisor Dr. Maria Elektorowicz who provided guidance and encouragement throughout this research project. Mr. Ron Parisella deserves my warmest thanks for his cooperation and help. My deep gratitude to my husband whose love for steering me in the right direction. I am especially grateful to my family especially Wael for their advice. Lovingly dedicated to Omar, Ahmed and Sara, my kids.

TABLE OF CONTENTS

LIST OF FIGURES	viii
------------------------	-------------

LIST OF TABLES	ix
-----------------------	-----------

CHAPTER 1

Introduction	1
1.1 Statement of the problem	1
1.2 Separation process	5
1.3 Objectives	5

CHAPTER 2

Literature Review	6
2.1 Soil composition	6
2.2 Characteristic of illite soil	7
2.3 Contaminated soil - interaction	10
2.3.1 Adsorption mechanism	11
2.3.1.1 Physical adsorption (van der waals forces)	12
2.3.1.2 Hydrogen bonding	12
2.3.1.3 Ion exchange	13
2.3.1.4 Cationic exchange	13
2.3.1.5 Anion exchange	14
2.3.1.6 Chemisorption	14
2.3.2 Clay adsorption	14
2.3.3 Effect of adsorbate structure on adsorption	15
2.3.3.1 Aliphatic hydrocarbons	15
2.3.3.2 Aromatic hydrocarbons	16
2.4 Polycyclic aromatic hydrocarbons contaminant	16

NOTE TO USERS

Page(s) not included in the original manuscript are unavailable from the author or university. The manuscript was microfilmed as received.

iv

This reproduction is the best copy available.

UMI

TABLE OF CONTENTS (cont'd)

2.4.1. Mechanisms of formation	16
2.5 Extraction techniques	
2.5.1 SFE and other technologies	17
2.5.2 SFE process	19
2.5.2.1 SFE process description	19
2.5.2.2 Theory of supercritical fluid applications	20
2.5.2.3 SFE design considerations	21
2.5.2.4 Parameters affecting on SFE efficiencies	22
2.5.2.5 Modifiers	24
2.5.2.6 Collection solvent	26

CHAPTER 3

Methodology	27
3.1 Materials	27
3.1.1 Soil specimens	27
3.1.2 Phenanthrene	29
3.2 Equipment Supercritical fluid extraction (SFX 220)	30
3.3 Extraction test	30
3.4 Analysis	33
3.4.1 UV analysis of an extracted analyte from soil specimens	35
3.4.2 Microscopic analysis of specimens	35

CHAPTER 4

Experimental Results	37
4.1 Introduction	37
4.2 Extraction with modifier from illite (S1)	37
4.3 Extraction without modifier from illite (S1)	37

TABLE OF CONTENTS (cont'd)

4.4 Extraction with modifier from soil specimen (S2)	38
4.5 Extraction without modifier from soil specimen (S2)	39
4.6 Extraction with modifier from soil specimen (S3)	39
4.7 Extraction without modifier from soil specimen (S3)	39
4.8 Comparison between specimens S1, S2, S3	40
4.9 Extraction without modifier from sand	41

CHAPTER 5

Modeling of supercritical fluid of extraction phenanthrene from soil	71
5.1 Literature survey	71
5.2 Model description	72
5.3 Solution technique	74
5.4 Verification of the model	77
5.4.1 Case1- SFE extraction over 30 min	77
5.4.2 Case1- SFE extraction over 20 min	79
5.4.3 Case1- SFE extraction over 10 min	79
5.5 Solubility	80

CHAPTER 6

Discussion of the effect of SFE technological parameters on the removal efficiencies	89
6.1 Introduction	89
6.2 Physical matrix effects	89
6.3 Properties of supercritical fluid carbon dioxide	90

TABLE OF CONTENTS (cont'd)

6.4 The use of modifier in SFE	91
6.5 Temperature effect on SFE efficiencies	91
6.6 Pressure effects on SFE efficiencies	92
6.7 Effect of the time	92
6.8 Collection solvent	93
6.9 Effect of diffusion and dispersion phenomena	93
6.10 Effect of mass transfer	94
6.11 Effect of solubility	94
6.12 Effect of equipment dimensions on extraction efficiency	95
6.13 Sensitivity of the model	95

CHAPTER7

Conclusion and recommendation	96
--------------------------------------	-----------

REFERENCES	98
-------------------	-----------

APPENDICES	103
-------------------	------------

LIST OF TABLES

Table 2.1 Polycyclic aromatic hydrocarbons in the environment	17
Table 2.2 Modifiers that have been used in SF technology with CO ₂	26
Table 3.1 Physico-chemical characteristics of illite	29
Table 3.2 Physico-chemical properties of soil	29
Table 3.3 Type of specimens and its extraction condition	33
Table 5.1 Comparison between the concentrations	80
Table 5.2 The effect of the particle size on the axial dispersion	80
Table 4.1 Condition; clay 100%, no modifier	105
Table 4.2 Condition; clay 100%, modifier	106
Table 4.3 Condition; clay 60% and sand 40%, no modifier	107
Table 4.4 Condition; clay 60% and sand 40%, modifier	108
Table 4.5 Condition; clay 20% and sand 80%, no modifier	109
Table 4.6 Condition; clay 20% and sand 80%, modifier	110
Table 4.7 Condition; sand 100%, modifier	110
Table A5.2 The output results from the program in 30 min	113
Table A5.3 The output results from the program in 20 min	113
Table A5.4 The output results from the program in 10 min	113
Table A5.5 The output from the program in the radial co-ordinate	114

LIST of FIGURES

Figure 1.1 Movement of LNAPLs into the subsurface	2
Figure 1.2 Movement of DNAPLs into the subsurface	4
Figure 2.1 Main components of the soil solid phase	7
Figure 2.2 Schematic diagram of the structures of illite	8
Figure 2.3 Diagrammatic sketch of the structure of muscovite	9
Figure 2.4 Charge distribution in muscovite	9
Figure 2.5 Pressure-temperature diagram for a pure CO ₂	20
Figure 3.1 Schematic diagram for experimental program	28
Figure 3.2 Phenanthrene's structure	30
Figure 3.3 Dual syringe pump system for modifier SFE	32
Figure 3.4 Sequence of extraction events	34
Figure 4.1 Recovery of phenanthrene from specimen S1 vs. temperature	42
Figure 4.2 Recovery of phenanthrene from specimen S1 vs. temperature	43
Figure 4.3 Recovery of phenanthrene from specimen S1 vs. time	44
Figure 4.4 Recovery of phenanthrene from specimen S1 vs. time	45
Figure 4.5 Recovery of phenanthrene from specimen S1 vs. temperature	46
Figure 4.6 Recovery of phenanthrene from specimen S1 vs. time	47
Figure 4.7 Recovery of phenanthrene from specimen S2 vs. temperature	48
Figure 4.8 Recovery of phenanthrene from specimen S2 vs. temperature	49
Figure 4.9 Recovery of phenanthrene from specimen S2 vs. time	50
Figure 4.10 Recovery of phenanthrene from specimen S2 vs. time	51
Figure 4.11 Recovery of phenanthrene from specimen S2 vs. temperature	52
Figure 4.12 Recovery of phenanthrene from specimen S2 vs. time	53
Figure 4.13 Recovery of phenanthrene from specimen S3 vs. temperature	54
Figure 4.14 Recovery of phenanthrene from specimen S3 vs. temperature	55
Figure 4.15 Recovery of phenanthrene from specimen S3 vs. time	56
Figure 4.16 Recovery of phenanthrene from specimen S3 vs. time	57

Figure 4.17 Recovery of phenanthrene from specimen S3 vs. temperature	58
Figure 4.18 Recovery of phenanthrene from specimen S3 vs. time	59
Figure 4.19 Recovery of phenanthrene from specimen S3 vs. temperature	60
Figure 4.20 Recovery of phenanthrene from specimen S1,S2,S3 vs. temp.	61
Figure 4.21 Recovery of phenanthrene from specimen S1,S2,S3 vs. temp.	62
Figure 4.22 Recovery of phenanthrene from specimen S1,S2,S3 vs. time	63
Figure 4.23 Recovery of phenanthrene from specimen S1,S2,S3 vs. time	64
Figure 4.24 Recovery of phenanthrene from specimen S1,S2,S3 vs. time	65
Figure 4.25 Recovery of phenanthrene from specimen S1,S2,S3 vs. temp.	66
Figure 4.26 Recovery of phenanthrene from specimen S1,S2,S3 vs. temp.	67
Figure 4.27 Recovery of phenanthrene from specimen S1,S2,S3 vs. time	68
Figure 4.28 Recovery of phenanthrene from specimen S1,S2,S3 vs. time	69
Figure 4.29 Recovery of phenanthrene from specimen S4 vs. temperature	70
Figure 5.1 Concentrations of phenanthrene obtained from model and exp.	82
Figure 5.2 A micrograph of non contaminated illite	83
Figure 5.3 A micrograph of contaminated illite	84
Figure 5.4 A micrograph of an extracted soil at p=8000 psi, T=150°C	85
Figure 5.4a Image of contaminated illite with phenanthrene	86
Figure 5.5 A micrograph of an extracted soil at p=5000 psi, T=50 °C	87
Figure 5.6 A micrograph of an extracted soil at p=8000 psi, T=50 °C	88
Figure A3.1 Chart showing % clay, silt, sand in the soil	104

Notation

f_{oc} = the fraction organic carbon content of the soil

k_{oc} = proportionality constant characteristic of the specific chemical.

K_p = the partition coefficient

C = concentration of phenanthrene in bulk fluid, mg/ml

C_a = concentration at the surface of the particle, mg/kg

ε = void fraction

u = superficial velocity in the cartridge, m/s

D_L = axial dispersion coefficient, m^2/s

k_m = mass transfer coefficient, m/s.

L = cartridge length, m.

Z = vertical coordinate along the axis of cartridge.

C_i = concentration in pores, mg / ml

D_e = effective diffusivity in the porous media, m^2/s

r = radial coordinate from center of particle, m.

n = porosity of media

ρ = density of particles, mg/cm^3 .

k_d = first-order desorption rate constant, $cm^3/mg.s$

k'_a = pseudo first-order adsorption rate constant, $cm^3/mg.s$

C_a = adsorbed concentration, mg / ml.

D_m = the molecular diffusivity

R' = the radius of the solute molecule

K = the Boltzmann constant, $1.38 \cdot 10^{-23} \text{ joule/}^\circ\text{K} = 1.38 \cdot 10^{-23} \text{ kg.m}^2/\text{s}^2 \cdot ^\circ\text{K}$

μ = the solvent viscosity

T = the temperature of the system

μ_c = the reduced viscosity

p_C = the critical pressure (atm.)

T_C = the critical temperature ($^\circ\text{K}$)

M = molecular weight of carbon dioxide

μ_r = the viscosity of the solvent (CO_2) (micropoises = 10^6 g /cm. sec.)

V = the total volume.

V_s = the volume of the particle.

n = the porosity

ϵ = the void fraction

τ_p = the tortuosity factor .

r_p = the particle radius, m.

k_m = the mass transfer coefficient.

Y_2 = the solubility of phenanthrene in carbon dioxide

P_i^{sat} = the vapor pressure, kPa .

ϕ_i^v = the fugacity at vapor pressure kPa

ϕ_2^v = the fugacity at the pressure of the system kPa.

p = the pressure of the system kPa.

v_i^{os} = the molal volume, $\text{m}^3/\text{kg} \cdot \text{m}^3$

R = ideal gas constant

T = the temperature of the system, $^\circ\text{K}$

CHAPTER 1

INTRODUCTION

1.1 . Statement of the problem

The increasing use of organic compounds by the industrial, manufacturing and agricultural segments of the world, and the general distribution and use of toxic or potentially toxic materials by the general public have led to contamination of some surface and ground water supplies.

The transport vehicles for pollutants are air, rain, surface and groundwater, sediment, and living organisms. A growing concern has arisen in recent years about the fate of toxic compounds in soils. Soil is often a receptacle of these compounds, and there is potential danger that they may reach the groundwater in original or altered but still toxic forms. Hydrophobic organic compounds (HOC) are recognized as a primary issue regarding contaminated subsurface in Quebec. Transports of contaminants in subsurface liquids that do not readily dissolve in water and can exist as a separate fluid phase are known as nonaqueous phase liquids (NAPLs). Generally, NAPLs are subdivided into two classes: those that are lighter than water (LNAPLs like benzene, toluene); and those with a density greater than water (DNAPLs, like PCBs, polychlorinated biphenyls). The migration of NAPL depends on the quantity released, the physical properties of the surface and the structure of the soil through which the contaminant moves. Potential consequences of the LNAPL spill is shown in Fig. 1.1

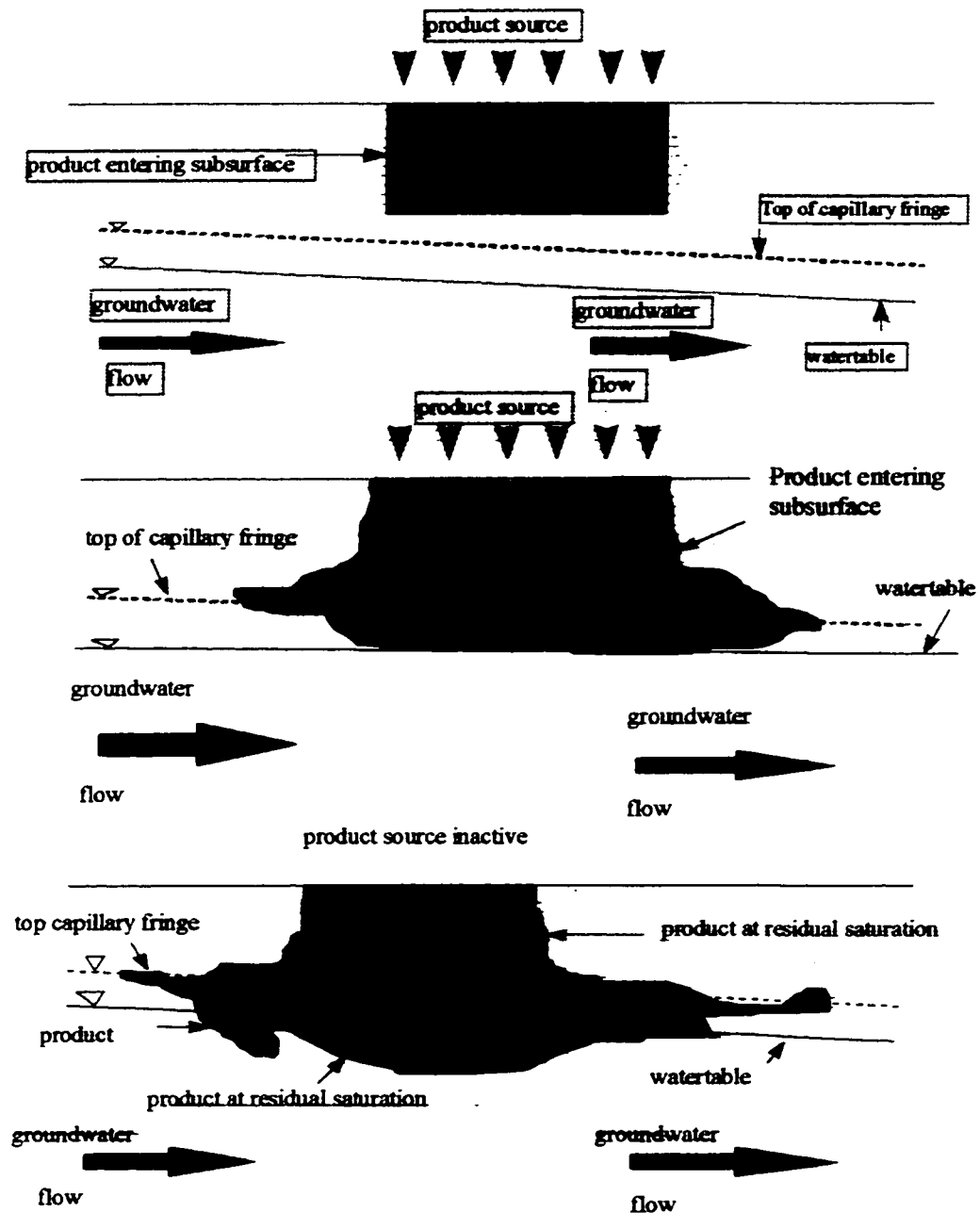


Figure 1.1 Movement of LNAPLS into the subsurface: (a) distribution of LNAPL after small volume has been spilled; (b) depression of the capillary fringe and water table; (c) rebounding of the water table as LNAPL drains from overlying pore space. [1]

The extent of movement depends on both the porosity and the permeability of the soil. For dry soils, bonding between the NAPL and soil solid would be different from moist soils because of the presence of (water) hydration layers surrounding the soil particles.

DNAPLs (e.g. trichloroethylene, phenanthrene) have great penetration capability in the subsurface because of their relatively low solubility, high density and low viscosity. The insoluble DNAPLs do not mix with water and therefore remain as separate phases. The potential impact of DNAPL's on subsurface versus the spilled volume is shown in Fig.1.2.

This review has been conducted to gain more understanding the behavior of hydrophobic organic compounds in subsurface, which can influence on the improvement of contaminant removal method. Organic chemicals that are nonvolatile are more difficult to remove from the soil mostly due to the fact that they do not change readily from one phase to another. These chemicals include polycyclic aromatic hydrocarbons (PAHs).

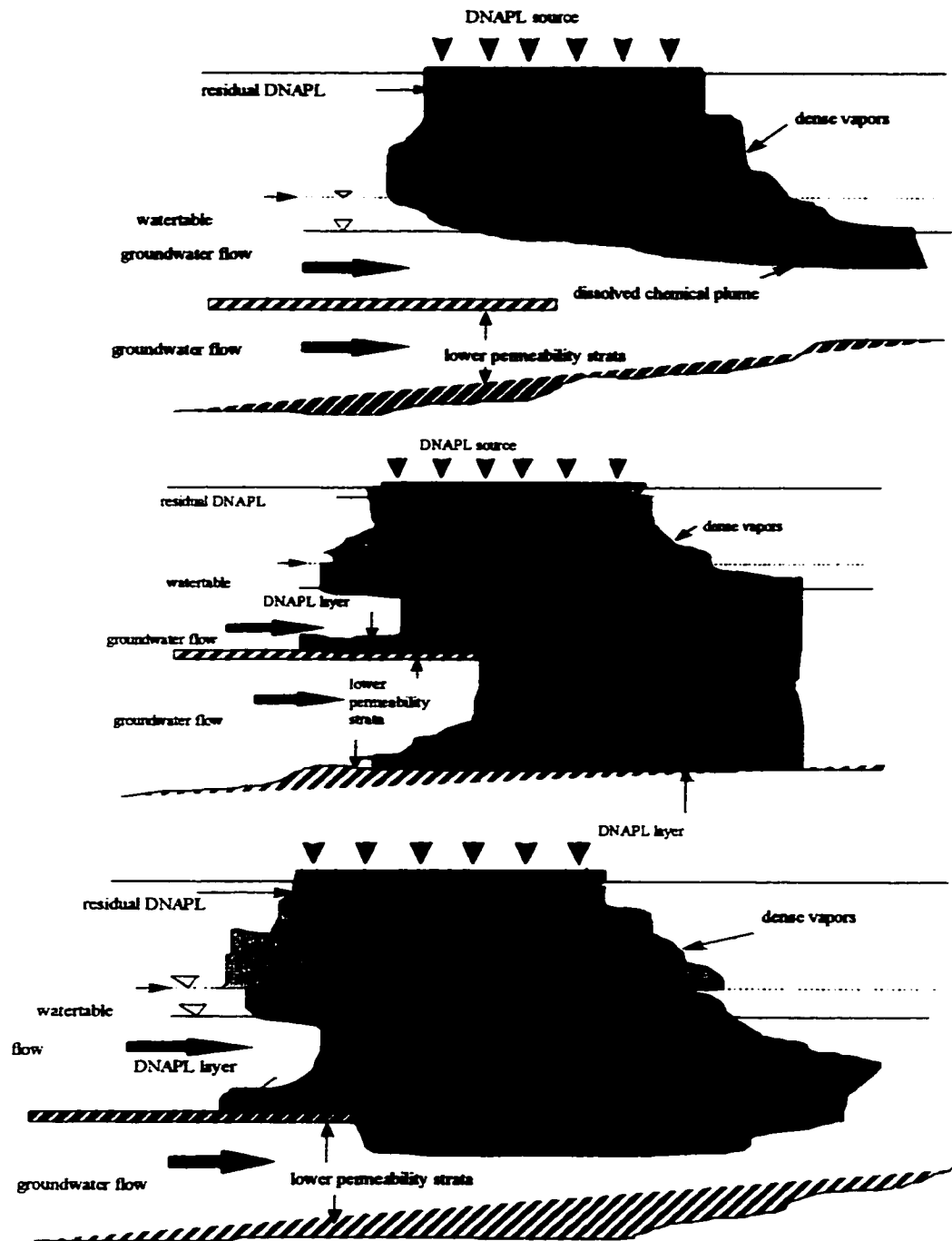


Figure 1.2. Movement of DNAPLs into the subsurface: (a) distribution of DNAPL after small volume has been spilled; (b) distribution of DNAPL after overate volume has been spilled; (c) distribution of DNAPL after large volume has been spilled [1].

The removal of PAHs from the soil requires specific techniques. The successful of these techniques depend on the degree of the analytical accuracy. Through the last years, analytical chemistry has developed powerful techniques that can separate, identify and quantify a large number of sample compounds in an acceptable time. Supercritical fluid extraction (SFE) has even been able to participate in certification procedures on environmental matrices. Further evidence of the growth of analytical SFE is the rapid advance in instrumentation. Then fluid solvents predominantly in the critical and supercritical ranges are of considerable interest for many fields. The removal of PAHs soil using SFE has a high potential application for soil analysis and soil remediation technique. Every extraction process (including SFE) requires a detailed knowledge of many thermodynamic and transports properties like solubility, viscosity, diffusion coefficient etc. This knowledge is particularly important in the case of a complex matrix of clayey soil. A previous work [2] was conducted to study the efficiency of SFE in the removal of phenanthrene from clay materials such as kaolinite, montmorillonite and illite. However, the results were not satisfactory for illite. Considering the above-mentioned facts, it is necessary to advance the knowledge of SFE system in order to make it more useful in soil remediation domain.

1.2 Objectives

The focal point of this study is to:

- (1) Examine the impact of the technological parameters on extraction efficiency of PAHs (phenanthrene) including the investigation of extraction pressure, temperature, and extraction time for SFE.
- (2) Develop model for extraction efficiency of phenanthrene from illite soil using SFE.

CHAPTER 2

LITERATURE REVIEW

This chapter reviews the clayey soil mineralogy and behaviors as well as PAHs properties in order to understand the contaminant-soil interaction. A review also includes the different types of extractions and the effect of SFE parameters on the contaminant extraction.

2.1. Soil composition

The inorganic part of the soil consists largely of alumina silicates. The inorganic components of soil range from highly crystalline to amorphous (Fig.2.1) Most clay minerals are quasi crystalline. The crystal sizes are smaller and they have more substitutions, e.g. of H^+ for K^+ , than primary minerals. The secondary minerals are layer silicates, and comprise the major portion of the clay-sized fraction material in soils. The organic component of soils ranges from relatively unaltered plant tissues to highly humidified material (humus). The humus fraction is bonded to mineral soil surfaces to form the material that determines soil characteristics. Topsoils are formed by alteration of inorganic and organic parent materials. The soil constituents consist of soil solids, fluid, and a gaseous phase. These phases provide the greatest opportunities for interactions with the contaminants in soil [3].

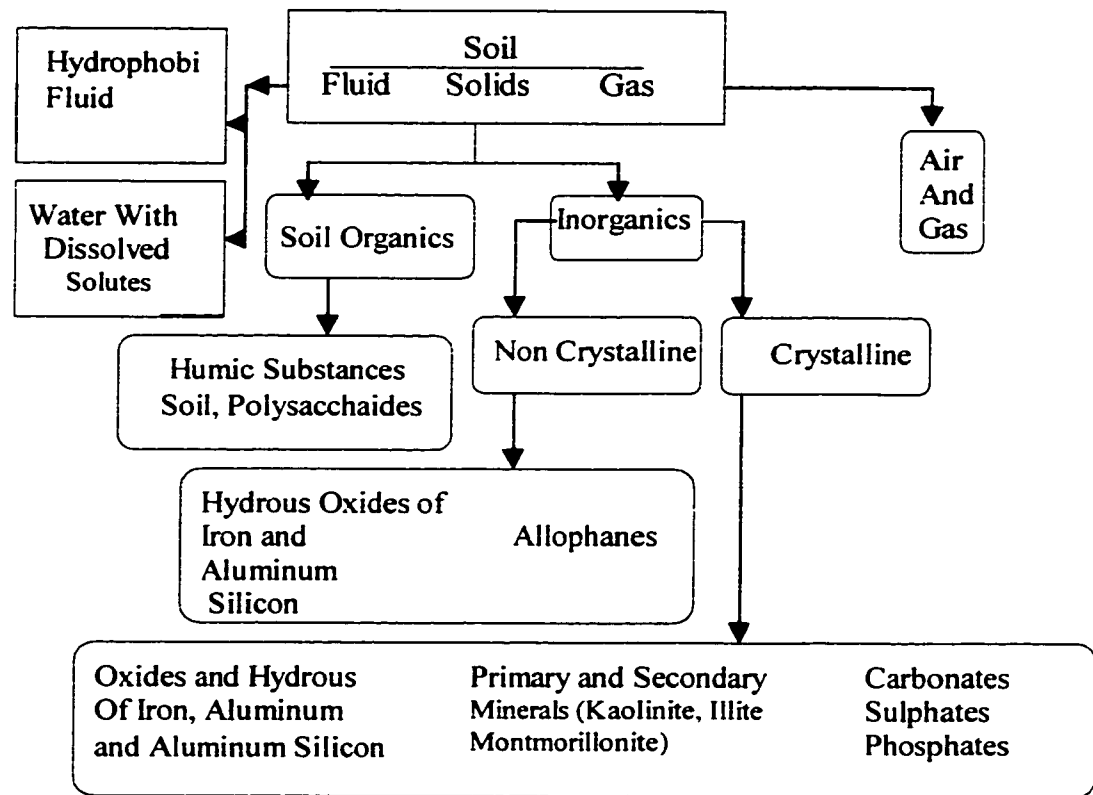
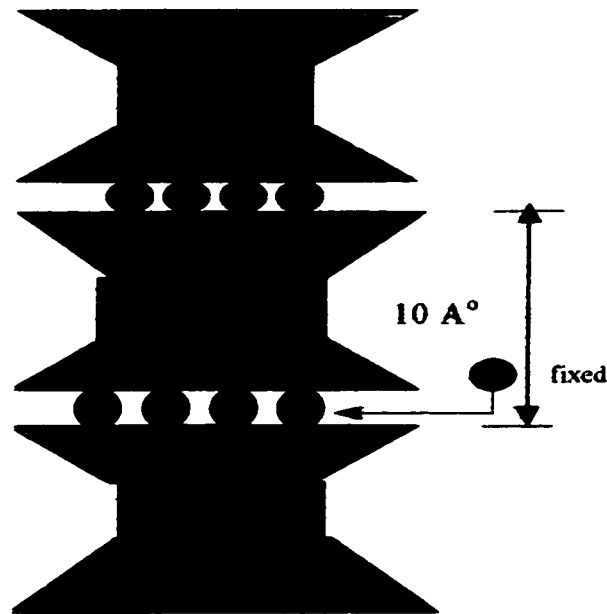


Figure 2.1. Main components of soil solid phase [3].

2.2 Characteristic of illite soils

Soil particles range in size from gravel, sand, silt, to clay in terms of the size. Clay particles are mainly plate-shaped as shown in Fig.2.2, the basic structures for illite are the tetrahedra in each silica sheet and octahedra in aluminum sheet. Clays are consisted of small crystalline particles containing mainly hydrous aluminum silicates, where all or part of the aluminum in the crystal would be replaced by magnesium or iron [4]. The most commonly occurring clay mineral found in the soils encountered in engineering practice has a structure similar to that of muscovite mica, and is termed “illite” or hydrous mica. A diagrammatic three-dimensional sketch of the muscovite structure is shown in Fig. 2.3. The structural configuration as well as charge distribution is

shown in Fig.2.4. Thus, the cation exchange capacity of illite is less than that of montmorillonite, amounting to 25-meq/100 g.



Al - aluminium sheet,

K - potassium

▾ silicon

Figure 2.2. Schematic diagram of the structures of illite.

The flaky illite particles may have a hexagonal outline if well crystallized. The long axis dimension ranges from 0.1 μm or less to several micrometers and the plate thickness may be as small as 30 \AA . Values of specific surface in the range of about 65 to 100 m^2/g have been reported for illite. The interlayer bonding by potassium is sufficiently strong that the basal spacing of illite remains fixed at 10 \AA in the presence of polar liquids. Illite usually occurs as very small, flaky particles mixed with other clay and nonclay materials. Illite deposits of high purity have not been located, as has been the case for kaolinite and montmorillonite.

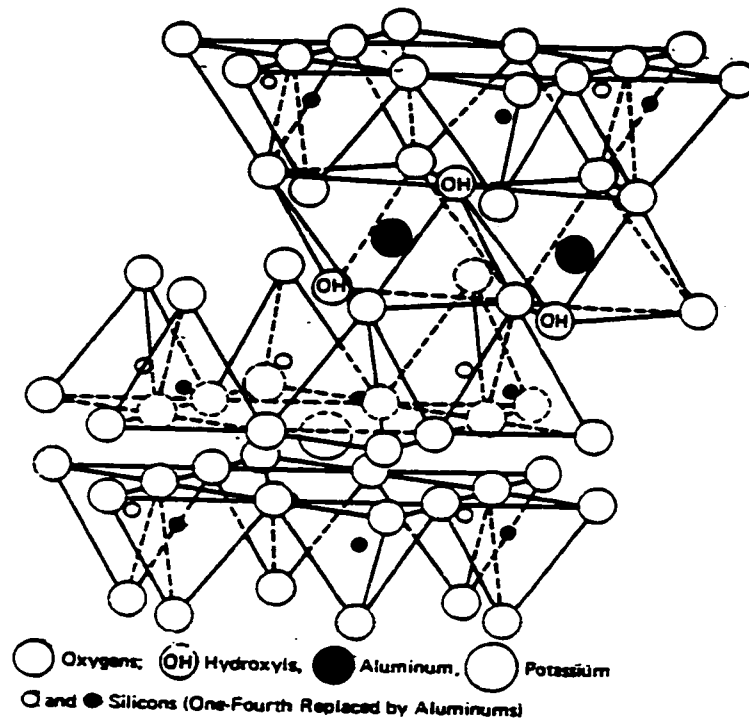


Figure 2.3. Diagrammatic sketch of the structure of muscovite [4].

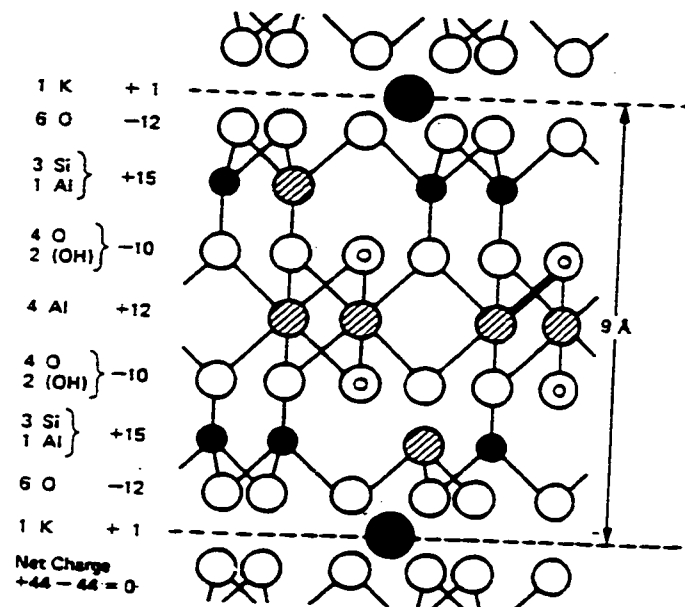


Figure 2.4. Charge distribution in muscovite [4].

As illite is distinguished from the montmorillonite; primarily by the absence of interlayer swelling with water or organic compound. Substitutions occur predominantly in the tetrahedral sheet. Cations, which compensate the net negative layer charge, are usually potassium ions. Since the layers do not part upon the addition of water, the potassium ions between the layers are not available for exchange- they are fixed. Only the potassium ions on the external surfaces can be exchanged for other cations. The illite is derived from the prototypes by variations in both the tetrahedral and octahedral substitutions. The swelling index character of illite equal 0.4 is attributed to a specific electrostatic linking effect of the layers by the potassium ions. These ions are of the right size to establish a favorable 12-coordination with opposite hexagonal oxygen rings of adjoining layers, being embedded in the space created by opposite holes. Illite contains 7 % carbonate which acts as cementing material between particles (chapter 3). Isomorphous substitution in the illite structure is extensive. The charge deficiency in illite is 1.3 to 1.5 per unit cell. In illite the charge deficiency is located primarily in the silica sheets and is balanced partially by the nonexchangeable potassium ions between layers. The illites are derived from the prototypes by variations in both the tetrahedral and octahedral substitutions.

Potassium montmorillonites behaves differently when compared to illites regarding the swelling characteristics. In the first place, in illites there will be more links per unit area because of the larger amount of potassium ions - possibly one and one-half times as many as in montmorillonites. Secondly, the links in montmorillonites may be weaker, since the negative lattice charge is concentrated more in the octahedral sheet and hence at a greater distance from the potassium ions than in illites, which have predominant tetrahedral substitution [4].

2.3 Contaminated soil-interaction

Extraction efficiency is related to reactions occurring between contaminants and soil constituents. The partition of immiscible liquid among liquid, solid and gases phase is the principle transport of organic contaminant in soil. Partition to the solid soil components is called sorption and govern the contaminant in soil.

The dominant mechanism of sorption of organics is the hydrophobic bond between a chemical and natural organic matter. The extent of sorption can be reasonably estimated if the organic carbon content of the soil is known by using the following expression: $K_p = k_{oc} f_{oc}$ (where f_{oc} is the fraction organic carbon content of the soil, k_{oc} is a proportionality constant characteristic of the specific chemical and K_p is the partition coefficient). The adsorption processes are governed by the surface properties of the soil, and physical chemical properties of a contaminant. [3]

2.3.1 Adsorption mechanisms

In general, adsorption is exothermic in nature, whereas desorption is endothermic. The process of adsorption can be divided into three-stage [5]:

- 1- External diffusion—diffusion through solution to the external surface of the solid.
- 2- Internal diffusion—diffusion within the pores of the adsorbent (this stage is important only for porous materials).
- 3- Adsorption at the surface—it is rapid in physical adsorption.

2.3.1.1 Physical adsorption (van der Waals forces)

Physical adsorption results from electrostatic interactions between atoms, ions and molecules due to the electron fluctuations that produce instantaneous

dipoles. The energy of adsorption due to van der Waals interactions is low (1-2 cal/mol) for atoms and small molecules, only slightly greater than that of kinetic motion (0.6 cal/mol) at 25 C⁰ [6]. The van der Waals interactions are weak and decrease very rapidly with the distance between the interacting species. The van der Waals forces are operative in all adsorbate-adsorbent interactions. These forces are important for adsorption of large molecules whose configuration conforms spatially to the adsorbing surface [7]. As such, these interactions are significant for ions in close contact with the surface or with adjacent adsorbed ions. Since van der Waals interactions are additive, heats of adsorption increase as the number of atoms in the molecule increase. On the basis of adsorption isotherms and X-ray analysis, Singhal and Singh [8] concluded physical adsorption was the primary mechanism of adsorption of Nemagon on bentonite. Greenland et al. [9] showed the importance of cation shape in determining the extent of van der Waals interactions for adsorption of amino acids and peptides by montmorillonite and illite.

2.3.1.2 Hydrogen bonding

Hydrogen bonding is a partial charge transfer interaction [10]. The energy of adsorption in hydrogen bonding systems may vary from 0.5 to 15 cal /mol [11]. Hydrogen bonding becomes very significant for large molecules or polymers in forming relatively stable complexes. Hydrogen bonding can occur on clay surfaces with the surface oxygen and protons of adsorbed water. Organic compounds with carbonyl groups are adsorbed on clay as a result of hydrogen bonding between the double-bonded oxygen of the carbonyl group and a hydrogen atom of the clay lattice [12]. Hydrogen bonding between water and oxygen of the silicate lattice is weaker than water-water hydrogen bonding [13].

Organic substances that are native to soil are also adsorbed to clays by hydrogen bonding; for example, humic acid is held on clay surfaces by hydrogen bonding to a water molecule in the primary hydration of the adsorbed cation on the exchange surface [14].

2.3.1.3 Ion exchange

Ion exchange is a process in which one type of ion is taken from a solution in exchange for another type contained or adsorbed on a solid. The coulombic forces of interionic attraction are very large (50 cal/mol) in the absence of solvent. However, in the presence of solvent, ion exchange is influenced by the solvation of the adsorbent in the region of the adsorption site and by the solvation of the adsorbate ion [15].

2.3.1.3.1 Cationic exchange

Many organic molecules are positively charged by protonation and are adsorbed on clays depending on the cation exchange capacity (CEC) of the clay minerals. Exchange reactions produce no net change in energy and are generally temperature-independent. Clay minerals differ in CEC and in their capacity to adsorb organic cations. Adsorption of organic compounds in amounts less than the CEC has been attributed to the covering of more than one exchange site by large molecules.

The adsorption of organic cations on clays is related to the molecular weight of the organic cation [16]. Large organic cations are adsorbed more strongly than inorganic cations by clays because cations are longer and have higher molecular weights [17].

2.3.1.3.2 Anion exchange

Anion exchange reactions are not as well defined as cation exchange reactions in soils. Anions are adsorbed either electrostatically or with a degree of chemical bonding by a wide range of soil materials [18]. Anion and cation exchange in kaolinite should be approximately equal since both occur at the broken edges of the clay. However, in montmorillonite CEC is mainly due to isomorphous substitution, and anion exchange is only a small fraction of CEC. Anionic surfactants are adsorbed by kaolinite, illite, and montmorillonite [19].

2.3.1.4 Chemisorption

Chemisorption is exothermic with energy range of 30-190-cal/mol [20]. The adsorption data of Nemgon on acid-and base-saturated illites indicates chemisorption [21]. For kaolinite, the adsorption occurred on the edges, whereas for montmorillonite, the adsorption was on both planar and lateral sites. In chemisorption, the first layer is chemically bonded to the surface [4] and additional layers are held by van der Waals force interactions only. Chemisorption at room temperature is usually a slower process than physical adsorption.

2.3.2 Clay adsorption

Adsorption of organic compounds by clay minerals is a complex process and not known very well yet. It differs for various types of clays because of different CEC, the strength of the negative charge, the specificity of adsorption sites and the nature of the cation on the exchange surface [22]. When an organic compound is adsorbed on a clay mineral, the ion-exchange property of the latter change [23]. Some organic compounds with high polarity form two or more molecular layers between the clay plates. Less polar compounds form only single layers.

An organic compound must have some polarity in order to penetrate into the basal surfaces of montmorillonite [24]. Exchangeable cations are adsorbed on the exterior surfaces of clays. In 2:1 clay (ex. montmorillonite, illite) cations and water molecules are also adsorbed on interlayer surfaces. This phenomenon does not occur in 1:1 clays (ex. kaolinite). Consequently 2:1 clays have a larger capacity to adsorb cations than 1:1 clays. Clay minerals in many ways resemble synthetic cation exchange resins, but behave differently due to the presence of aluminum in the lattice structure. Aluminum atoms can accommodate both tetrahedral and octahedral coordination with oxygen. Aluminum may move from positions within the crystalline lattice to an exchangeable position, and vice versa, and form amphoteric hydroxides with water at the clay surface. Clayey soil consist of the mixture of different type of clay material as well as not crystalline forms (Fig. 2.1) so solid phase-contaminant interaction may be mainly governed by the presence of amorphous matter.

2.3.3 Effect of adsorbate structure on adsorption

Adsorption is influenced by characteristic of organic compound, especially by chemical structure and placement or position of functional groups.

2.3.3.1 Aliphatic hydrocarbons

Aliphatic hydrocarbons are nonpolar compounds. Since aliphatic hydrocarbons lack polarity, they are poor competitors with water for adsorption sites on the exchange complex. Their adsorption can be gaseous by van der Waals forces, predominantly on the external surfaces of clay minerals [25]. Witt [26] concluded that unsaturated hydrocarbon gases such as ethylene and propylene were adsorbed in greater amounts by soil than the saturated hydrocarbon gases such as methane, ethane, and propane.

2.3.3.2 Aromatic hydrocarbons

Aromatic compounds are nonpolar or very weakly polar and sorption of such non-polar compounds are either absent or proceed very slowly. Aromatic molecules can interact with clay surfaces through their π electron [27]; for example, benzene forms a stable complex through its π electrons with Cu on clay. Another study [28], showed that the saturating cation might not influence the adsorption of nonpolar organic molecules.

2.4. Polycyclic aromatic hydrocarbons contaminant

Polycyclic aromatic hydrocarbons (PAHs) were recognized as a primer source of contamination by Ministry of the Environment and Wildlife in Quebec [29]. The presence of phenanthrene was observed in most contaminated site.

2.4.1. Mechanisms of formation

The generation of PAH during thermal decomposition of organic materials is based on at least two different mechanisms: (1) incomplete combustion or pyrolysis and (2) a process of carbonization, e.g., during formation of mineral oil or coal. The more completely an organic material, e.g., a fossil fuel, can be combusted with the appropriate amount of oxygen to carbon dioxide and water, the smaller is the amount of PAH formed as a by-product. During an incomplete combustion, an oxygen deficiency occurs in micro-oranges and thus pyrolysis conditions build up, i.e., in these micro-oranges the amount of oxygen necessary for a complete combustion is lacking. Thus during “incomplete” combustion a pyrolysis of fuel takes place in micro-oranges beside the “complete” combustion to CO_2 and H_2O . When considering pyrolysis, thermal decomposition under a

protective gas, as a separate process, the interrelations of temperature, type of material, amount of PAH, and profile of PAH can best be seen [30].

Table 2.1. Polycyclic Aromatic Hydrocarbons which occur Most Frequently in the Environment.

IUPAC designation	Chemical formula	Molecular weight	Boiling point °C
Fluorene	C ₁₃ H ₁₀	166	293
Phenanthrene	C₁₄H₁₀	178	338.4
Anthracene	C ₁₄ H ₁₀	178	340
Fluoranthene	C ₁₆ H ₁₀	202	383.5
Pyrene	C ₁₆ H ₁₀	202	393.5
2,13-benzofluoranthene	C ₁₈ H ₁₀	226	431.8
Tetraphene	C ₁₈ H ₁₂	228	437.5
Triphenylene	C ₁₈ H ₁₂	228	438.5
Chrysene	C ₁₈ H ₁₂	228	441

The hydrogen may or may not be substituted by variety of groups: Cl, I, NO, CN. They can be readily degraded, are extremely resistant or yield undesirable intermedial forms. Factors, which can influence the degradation rate are: number of rings, number of substitutions, type and position of substitutions groups, nature of atoms in heterocyclic compounds.

2.5 Extraction techniques

2.5.1 SFE and other extraction technologies

Some of the current commercially available supercritical fluid extraction systems may provide in the laboratory safer and more cost-effective than Soxhlet

extraction of contaminants from waste and environmental matrices. It is anticipated that the popularity of SFE will increase significantly when SFE hardware becomes more popular among companies and that the systems will be able to demonstrate comparable performance to Soxhlet for extraction of contaminants from waste and environmental solid matrices. SFE systems are field transportable and process components will take up considerably less space in a mobile laboratory than conventional extraction technologies such as Soxhlet. Application in the off-line mode allows extracts to be analyzed by a variety of field transportable chromatographic and spectrometric techniques, enhancing the characterization capabilities of field laboratories. This capability is particularly advantageous where characterization is needed onsite for decision-making as remediation takes place. The performance of a commercially available SFE system was compared to baseline extraction technology (ex. Soxhlet extraction) in laboratory tests conducted in the latter part of FY 1993 at Pacific Northwest Laboratory [31]. The tests incorporated Hanford sediments spiked with tributylphosphate and lard oil, organic chemicals co-disposed with carbon tetrachloride in large quantities to the ground at Hanford's 200 West Area. The FY 1993 study evaluated only one SFE design on the commercial market and therefore the data may not be fully representative of the performance of all SFE systems on the market relative to the baseline technology.

Based on 34 SFE and 64 Soxhlet extraction's conducted in the FY 1993 tests at Pacific Northwest Laboratory, a commercial SFE system using a non-variable restrictor and solvent trapping was found to give mixed performance relative to Soxhlet extraction. The accuracy of Soxhlet was 50%, but the SFE accuracy was #90.5% to 98.5%. SFE was found to be less labor intensive (15-min/sample vs. 85 min/sample) and provide more rapid turn-around time (2-hr. vs. 27-35 hr.) than Soxhlet extraction. In addition, while it was shown that Soxhlet extraction produced significant liquid waste (2,560 ml of solvent/8samples) and some solid waste (40 g/ 8 samples).

The SFE process did not produce a liquid waste and its solid waste is likely to be non-hazardous. SFE produced significantly less solvent releases to the

atmosphere (on a per sample basis) than Soxhlet extraction (105 ml/8 samples vs 640 ml/8 samples).

The SFE system tested in FY 1993 released comparable concentration levels of hazardous chemicals to the air during its time of operation. Soxhlet extraction for example released concentration levels of methylene chloride of 21 mg/m³ to the air over a period of 21 hr. at a hood flow rate of 107 ft³/min. For SFE, the concentration of methylene chloride was calculated to be 110 mg/m³ over a period of 40 min at the same hood flow rate. While SFE extraction efficiency of analytes from aged soils was demonstrated to be high and comparable to Soxhlet extraction, recovery of the analytes by SFE was low relative to Soxhlet (40% - 54% lower) due to poor solvent trapping efficiency [31].

2.5.2 SFE process

2.5.2.1 SFE process description

In SFE, the contaminant stream is introduced into an extraction vessel into which the extraction fluid, pressurized and heated to the critical point in a compressor, is continuously loaded. The organic contaminant in the contaminated stream dissolves in the supercritical fluid. The supercritical fluid (SCF) is then expanded by passing it through a pressure reduction valve. The expansion of the SCF lowers the solubility of the organic contaminant in the SCF and, thus, results in the separation of the organic contaminant from the extracting fluid. The SCF is then recompressed and recycled to the extraction vessel. The temperature can be reduced at a constant pressure by passing the SCF through a heat exchanger. The end result is also a reduction in the solubility of the organic contaminant in the SCF and the separation of both components. A blower is used instead of a compressor, and the separated extracting fluid entering the process vessel is heated in the same heat exchanger used to cool the exiting SCF [32]. The most common choices of the supercritical fluid are carbon dioxide, N₂O, freon etc.

2.5.2.2 Theory of supercritical fluid applications

Fluid is normally divided into two phases: liquids and gases. However, at elevated temperatures and pressures, a point is reached where this distinction is no longer discernible, and the saturated liquid and saturated vapor states are identical. This is termed the critical point. An SCF is a single-phase fluid at temperature and pressure above the critical point. An SCF has properties between those of the liquid and gas phases. As a result of these properties, organic compounds are highly soluble in SCFs and can easily transfer to the SCF from their original medium [32].

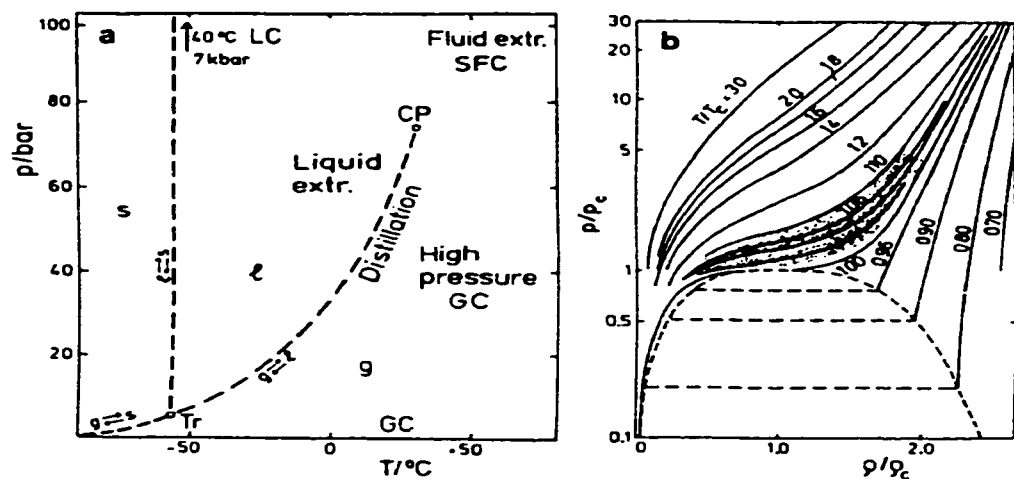


Figure 2.5 Pressure-temperature diagram for a pure carbon dioxide

(2.5a: p = pressure, T = absolute temperature, 2.5b: p = density, CP = critical point, p_c , T_c , ρ_c critical pressure, temperature and density, Tr = triple point, l = liquid, g = gaseous, s = solid) [33]

In Fig.2.5a the pressure-temperature diagram of carbon dioxide is presented. On the vapor pressure curve (lg) a liquid (l) and a gaseous (g) phase coexist. With increasing pressure the vapor pressure curve rises and ends at the critical point CP (T_c :304.21 °K, p_c :73.825 bar, and ρ_c :466 kg m⁻³) where the two

coexisting phases (l and g) become identical. With decreasing pressures it ends at the triple point Tr (T: 216.58 °K, p: 5.185 bar) where solid, liquid and gaseous carbon dioxide are in equilibrium.

In Fig.2.5 the ranges of temperatures and pressures are additionally marked where separation methods (such as SFE, SFC (supercritical fluid chromatography)) are normally performed. Here SFE has to be attributed to conditions of temperatures and pressures exceeding the critical values respectively. [33]

2.5.2.3 SFE system design considerations:

Among the many decisions to be made in designing an SCF extraction system is the selection of solvent. Separation of the SCF from the feed stream depends on the difference in density of the two fluids. For SFE, reactions between the solvent and solute would be undesirable. The toxicity associated with various solvents have led to increase the use of CO₂ as an SCF. The lower the critical temperature and pressure of the SCF, the process is less expensive. Additional design considerations include (1) the ability of the waste to be pressurized, (2) the potential to form char, and (3) the removal of the solids produced. If the waste is a solid, slurry, or suspension, the solid particles must be reduced to less than 100 µm in diameter, which is the particle size limit for high-pressure pump [32].

Combining efficient extraction of PAHs from soil matrix and the impact of various technological parameters should be evaluated. Parameter values that should be tested include type of supercritical fluid, pressure of extraction, temperature of extraction, temperature of restrictor, collection solvent, type and concentration of modifier.

2.5.2.4 Parameters affecting SFE efficiency

- **Extraction temperature and pressure**

Pressure and temperature are the most important physical parameters in SFE. The effects of temperature and pressure have been studied for PAHs from highly contaminated soil, were extracted with pure CO₂ at conventional (50 °C) and high (200 °C) temperatures. At 50 °C, raising the extraction pressure (350-650 atm) had no effect on extraction efficiencies from any of the samples. High recoveries were obtained in 40 min from the highly contaminated soil [34]. The trends in extraction efficiencies with increasing boiling point (and molecular weight) for the highly contaminated soil are more difficult to evaluate because of the poor reproducibility of the certified concentration, but no strong trend in recovery with increasing boiling point was observed for the species with boiling points between 250 and 500 °C when the extraction pressures were either 350 or 650 atm [34].

The maximum extraction efficiency occurs at higher pressures and temperatures [35].

- **Restrictor temperature**

Restrictors are a critical element in the SFE system because of decompression that takes place there, and the extraction fluid changes from a supercritical fluid to a gas [34]. Some investigations have suggested that heavy hydrocarbons can precipitate out of the fluid on the restrictor walls and eventually plug the SFE outlet restrictor [37], due to their higher molecular weight and lower solubility in pure CO₂ [36]. In addition, the plugging of restrictor could take place because of the samples contain water, which is extracted along with the hydrocarbons and freezes at the restrictor outlet [37]. Consequently the restrictor should be heated to prevent plugging from water or heavy hydrocarbons. However, the heating restrictor also increases the temperature of the SFE effluent

and subsequently the collection solvent, which can lead to low collection efficiencies of more volatile fuel components [31]. A restrictor temperature of 90 or 100 °C provided good fluid flow rates with little plugging up to moisture levels of ~30 wt % (based on sand) [41]. At 130 and 200 °C good recovery is obtained with solvent trap and no difference was observed between the more and less volatile. At a restrictor temperature of 250 °C, the recovery for all PAHs are decreased [36].

- **Fluid choices in SFE**

In practice, more than 90% of all analytical SFE is performed with carbon dioxide (CO₂) for several practical reasons. Apart from having relatively low critical pressure (74 kPa) and temperature (32 °C), CO₂ is non-toxic, not flammable and low explosive, chemically relatively inactive, available in high purity at relatively low cost, is easily removed from the extract, and creates no environmental problems when used for analytical purposes. In the supercritical state, CO₂ has a polarity comparable to liquid pentane and is, therefore, best suited for lipophilic compounds. The main drawback of CO₂ is its lack of polarity for the extraction of polar analytes. The second most common choice of extraction fluid for analytical SFE has been N₂O. This fluid was considered better suited for polar compounds because of its permanent dipole moment [38].

Unfortunately, this fluid has been shown to cause violent explosions when used for samples having high organic content and should, therefore, be used only when absolutely necessary [39]. Other more exotic supercritical fluids, which have been used for environmental SFE, are SF₆ and Freons. SF₆ is a very polar molecule and as a supercritical fluid, it has been shown to selectively extract aliphatic hydrocarbons up to around C-24 from a mixture containing both aliphatic and aromatic hydrocarbons [40]. Freons, especially CHClF₂ (Freon-22), has on several occasions been shown to increase the extraction efficiency compared to extraction with CO₂.

Hawthorne et al. [41] showed that CHClF_2 extracted PCBs from a river sediment with higher efficiency than pure CO_2 or CO_2 modified with methanol (MeOH). For PAHs from petroleum waste sludge and a railroad bed soil, CHClF_2 gave dramatically improved recoveries when compared to CO_2 and N_2O . In contrast, Klink et al. [42] did not experience any significant difference in the extraction efficiency between CO_2 and CHClF_2 for the extraction of sediment. Although supercritical water has often been used for the destruction of hazardous organic [43], the high temperature and pressure needed ($T > 374\text{ }^\circ\text{C}$ and $P > 221\text{ bar}$) together with the corrosive nature of water at these conditions, has limited the possible practical applications in environmental analysis [44].

2.5.2.5 Modifiers

Modifiers or cosolvents are often used for environmental applications with real world samples [45]. First of all, cosolvents can change the solvating power of the extraction fluid. Several phenomena may affect supercritical fluid extraction. These include solute and modifier polarity, physical and chemical state of the solute and the matrix, solubility of the solute in the modifier, miscibility of the modifier-supercritical fluid mixture under a wide variety of temperature and pressure conditions.

- **Solute-modifier interactions**

Many mechanisms have been proposed to explain the effect of modifiers on the extraction of solutes from various substrates. The first of these is the consideration of the solubility of the solute in modified supercritical fluid [46]. Molecular group interactions between modifiers and solutes that give rise to hydrogen bonding have been suggested as a potential influence of modified supercritical fluids in SFE [47].

- **Modifier-matrix interaction**

Matrix swelling resulting from the interaction of the modifier and the matrix has also been proposed as a predominate interaction in SFE [48]. A relationship between the interaction of the modifier with the matrix and the rate of mass transfer of the solute from the matrix can be developed. Swelling in soils is governed by the distribution of cations, anions, and repulsive electric forces between the charged particles of the soil. The range of spacing on the basal planes varies with exchangeable cations and the degree of interlayer solvation.

The presence of these large organic ions alters the clay dispersibility and allows for swelling of the lattice structure [49]. Greater recoveries from clay with different types of modifiers were enhanced by matrix swelling. [50]. Table 2.2 shows a listing of the various modifiers that have been used in supercritical fluid technology [51]. Practically, modifiers have been introduced in a number of ways in SFE.

The most effective way of delivering a modifier for SFE is by directly adding the modifier as a liquid to the sample matrix before filling the extraction vessel or while the sample matrix is already in the vessel but prior to the extraction. In this respect, the modifier is isolated from the actual primary supply pump thereby not contaminating the pump with the modifier [51].

Table 2.2. Modifiers that have been used in supercritical fluid technology with carbon dioxide as the primary supercritical fluid.

1,4-Dioxane	Diethyl ether
2-Butanol	Dimethyl sulfoxide
n-Butanol	Ethanol
t-Butanol	Ethyl acetate
Acetonitrile	n-Heptanol
Carbon disulfide	n-Hexane
Carbon tetrachloride	Methanol
Chloroform	2-Methoxyethanol
n-Decanol	n-Pentanol
n-Propanol	Water

Extraction using CO₂ with modifiers (ex. methanol 5% (mol)) at high temperature could be the most efficient SFE method for extracting PAHs from environmental sample [52].

2.5.2.6 Collection solvent

The collection solvent greatly influences the extraction result. If the analyte trapping is insufficient, one can get the impression that the extraction is incomplete. It was investigated, that methylene chloride and acetone are good collection solvent for PAHs extraction [53].

CHAPTER 3

Methodology

The investigation of SFE technological parameters was done at two stages: experimental and modeling. Results from both stages were used to assess SFE efficiency of the phenanthrene from clayey soil. The experimental stage was performed on specimens prepared from various soil compositions. The modeling of phenanthrene extraction from SFE is observed in chapter 5. Figure 3.1 shows research program including the specimens preparation, the SFE extraction tests, analysis of extracted specimens, modeling of the extraction process and assessment of the method.

3.1 Materials

3.1.1 Soil specimens

Specimens for experimental tests were prepared with illite and fine sand (0.06-0.2 mm) in various ratios 100% Clay (S1), 60% Clay and 40% sand (S2), 20% Clay and 80% sand (S3), and 100% sand (S4). These specimens represent the various, soils (Figure A.3.1-Appendix A3). Prepared specimens were dried in oven at 105 °C for 8 hours. Specimens have been spiked with phenanthrene (500-mg phenanthrene/kg dry soil) and left for swelling (24 hours) in the desecrator before the extraction.

Illite was purchased from Debro Chemicals, Montreal, Canada. Illite used for the test was analyzed and characterized as shown in Table 3.1

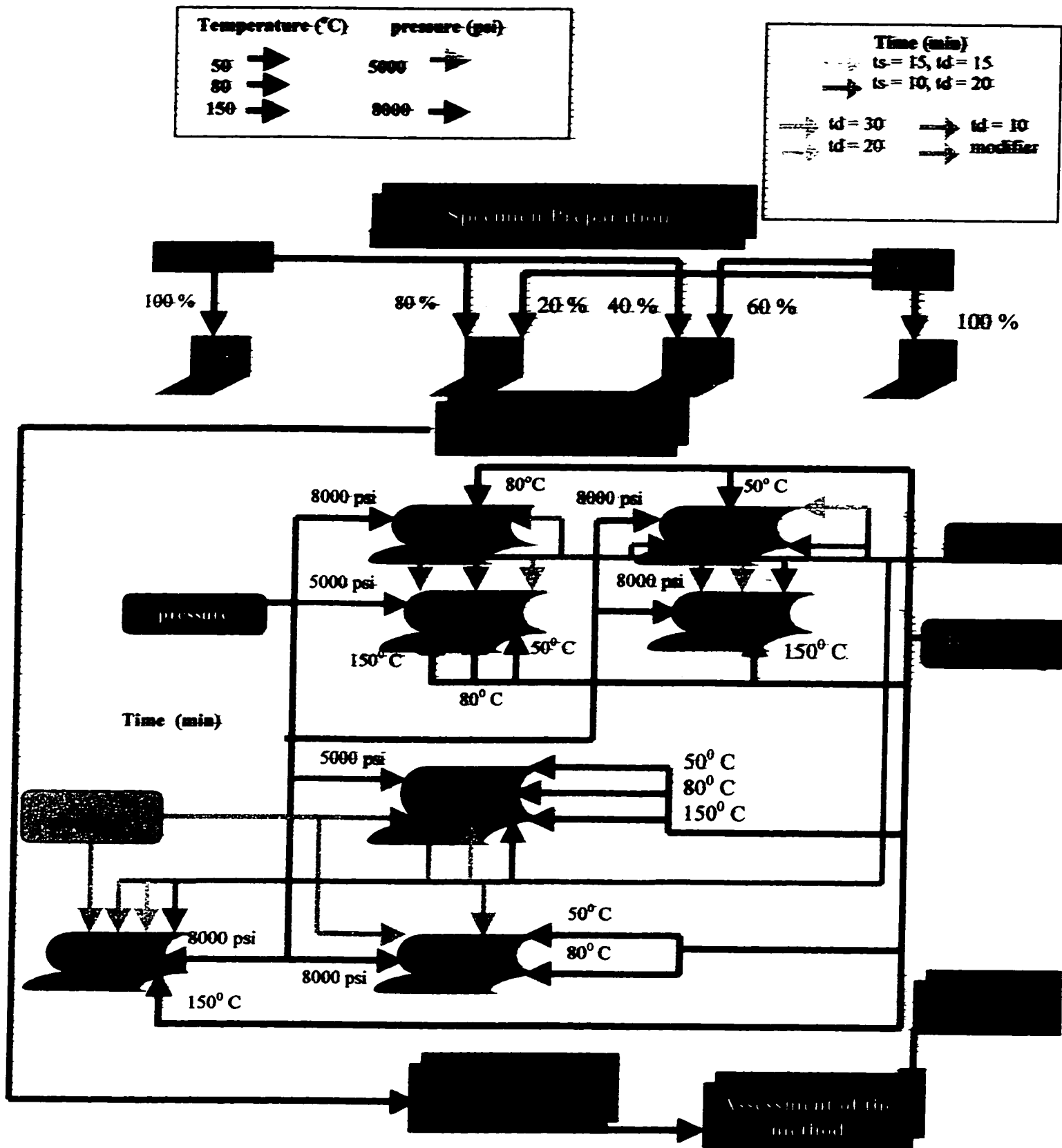


Figure. 3.1. Schematic Diagram for Experimental Program (td - dynamic time, ts - static time)

Table 3.1. Physico-chemical characteristics of illite

Characteristics of Illite	
Type of layering	2:1
Swelling index (after ref.)	0.4
CEC (meq/100 g)	21
Specific surface (m ² /g) (after ref.)	75-125
PH	7.9
Cl- (ppm)	245
Sulphate (ppm)	12.3
Iron in pore fluid (ppm)	<0.1
Carbonate (% CaCO ₃ by weight)	7.5
Organic matter (%)	2.7
Kjeldahl-N (%)	0.005

Pure silica sand, with particle diameter 0.06-0.2 mm was used in this investigation. The physical-chemical properties for the sand are shown in Table 3.2. More than 360 specimens were prepared to be tested.

Table 3.2. Physico-chemical properties of sand

Properties of Sand	
Specific gravity [g/cm ³]	2.64
Void ratio	0.74-0.9
Dry unit weight [kN/m ³]	14
Permeability	7.2*10 ⁻²
Cation exchange capacity [meq/100g]	-----

3.1.2 Phenanthrene

Soil specimens were spiked with phenanthrene, polynuclear aromatic hydrocarbon, commonly found on contaminated sites. Polynuclear aromatic hydrocarbons (PAH) are groups of aromatic rings containing only carbon and hydrogen. Phenanthrene consists of three benzene rings [62]. The physico - chemical characteristics of phenanthrene are shown in Table 3.3.

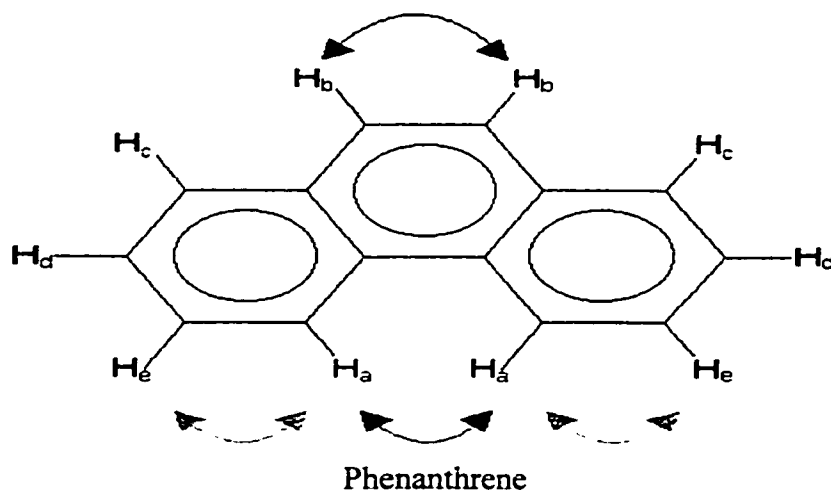


Figure 3.2. Phenanthrene structure

Table 3.3 Phenanthrene's Characteristics

-Chemical Formula: $C_{14}H_{10}$	-Molecular weight: 178.23
-Melting point ($^{\circ}C$): 100.5	-Boiling point ($^{\circ}C$): 338
-Heat of vaporization kJ / mol: 52.7	-Molecular connectivity X: 4.815
-Henry Constant $Atm.m^3 / mol$: $2.7.10^{-4}$	-Molar volume ($cm^3 mol$): 199
-Enthalpy of fusion (kJ / mol) : $16.7+0.3$	-Vapor pressure (Pa): 0.020
-Solubility (g / m^3): 1.1	-Log k_{ow} : 4.57
-Density (g / cm^3 at $20^{\circ}C$): 1.174	- Critical temperature ($^{\circ}K$): 869.25

All various soil compositions were spiked of the same concentration of phenanthrene (2.35 mg / ml).

3.2. Equipment supercritical fluid extraction (SFX 220)

The SFX 200 Extraction System used in laboratory tests consists of an SFX 220 Extractor, an SFX 200 Controller, and an ISCO Model 100 DX syringe pumps. Both the pumps and the extractor are connected to a SFX 200 Controller which controls all pumping and extraction operations. The SFX 220 Extractor is a bench top, dual chamber (cartridge filter with a 5/8-inch diameter filter element), supercritical fluid extraction device, which fits on top of an SFX 200 Controller. The extractor incorporates six motor actuated valves, which are controlled by the SFX 200 Controller. The fluid source for the extractor is supplied by a D series pump and the other pump for the modifier. The SFX 220's unique, pressure safe design prevents over pressurization or cross-contamination of chambers. Fused silica tubing with inner diameter 50 μm , 30 cm long was used, as outlet restrictor, allowing analytes to be conveniently collected in the test tubes. A vent valve allows rapid depressurization of the chamber after the extraction is completed. Figure 3.2 shows a basic SFE setup for modified supercritical carbon dioxide.

. Extracted analyte was collected outside of the oven at room temperature by placing the outlet end of the restrictor into a 30-ml vial containing 7-10 ml of hexane.

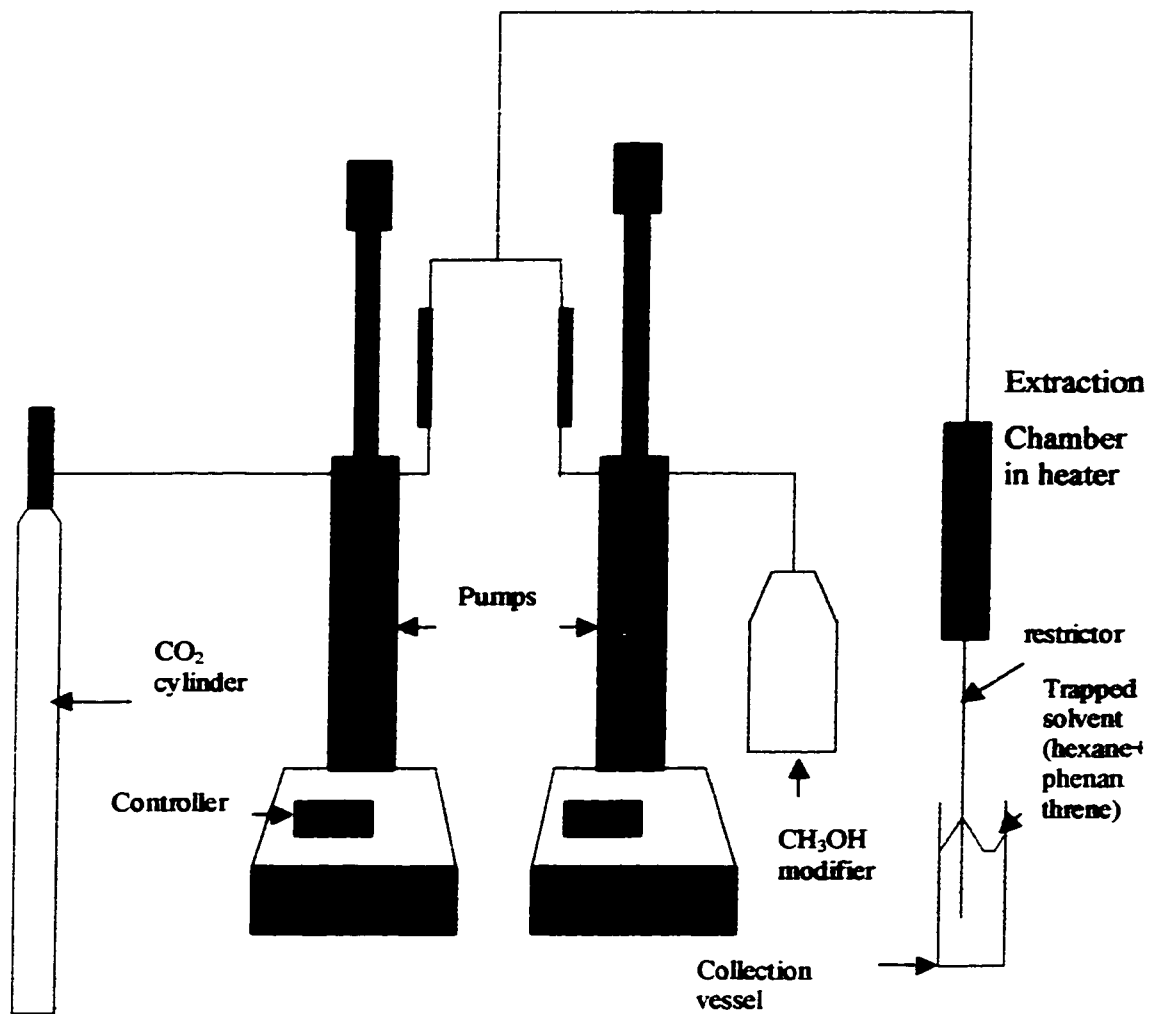


Figure 3.2. Dual syringe pump system for modifier SFE. Pumps are connected with back pressure control valves and mixing tee.

3.3 Extraction Test

For each type of specimens, extractions were performed at different conditions. The supercritical fluid extraction was performed by placing 3g of contaminated soil into a 10-ml cartridge body. Various dynamics times (10, 20, 30 min) were applied during the tests with modifier. In addition, combination of static and dynamic extraction time was used. Using SFC grade carbon dioxide and modifier with 5% mol methanol were used which were pressurized at 5000 psi (34.48 kPa) and 8000 psi (55.1 kPa). Figure 3.3 shows the extraction run sequence; Table 3.4 demonstrates the type of specimens and conditions of extraction.

Table 3.4 Type of specimens and its extraction conditions.

Test No.	Quantity of specimens	Type of specimen	Conditions of extraction			Modifier (Methanol) (mol)
			Pressure in psi (kPa)	Temperature (°C)	time (min)	
1	12	S1, S2, S3	8000 (55.15)	80	30	No
	8	S4	5000 (34.4)	50, 80, 150	td=10, 30	
2	108	S1, S2, S3	5000 (34.4)	50, 80, 150	ts=15, td=15 ts=10, td=20 td=30	No
	24	S4	5000 (34.4)	50, 80, 150	td=10, 30	
3	36	S1, S2, S3	8000 (55.15)	50	ts=15, td=15 ts=10, td=20 td=30	No
4	36	S1, S2, S3	8000 (55.15)	150	td=10, 20, 30	No
5	108	S1, S2, S3	5000 (34.4)	50, 80, 150	td=10, 20, 30	5%
6	24	S1, S2, S3	8000 (55.15)	50, 80	td=30	5%
7	36	S1, S2, S3	8000 (55.15)	150	td=10, 20, 30	5%
	4	S4	5000 (34.4)	50	td=30	5%

S1 = 100% clay, S2 = 60% clay and 40% sand, S3 = 20% clay and 80% sand, S4 = 100% sand
ts = static time, td = dynamic time

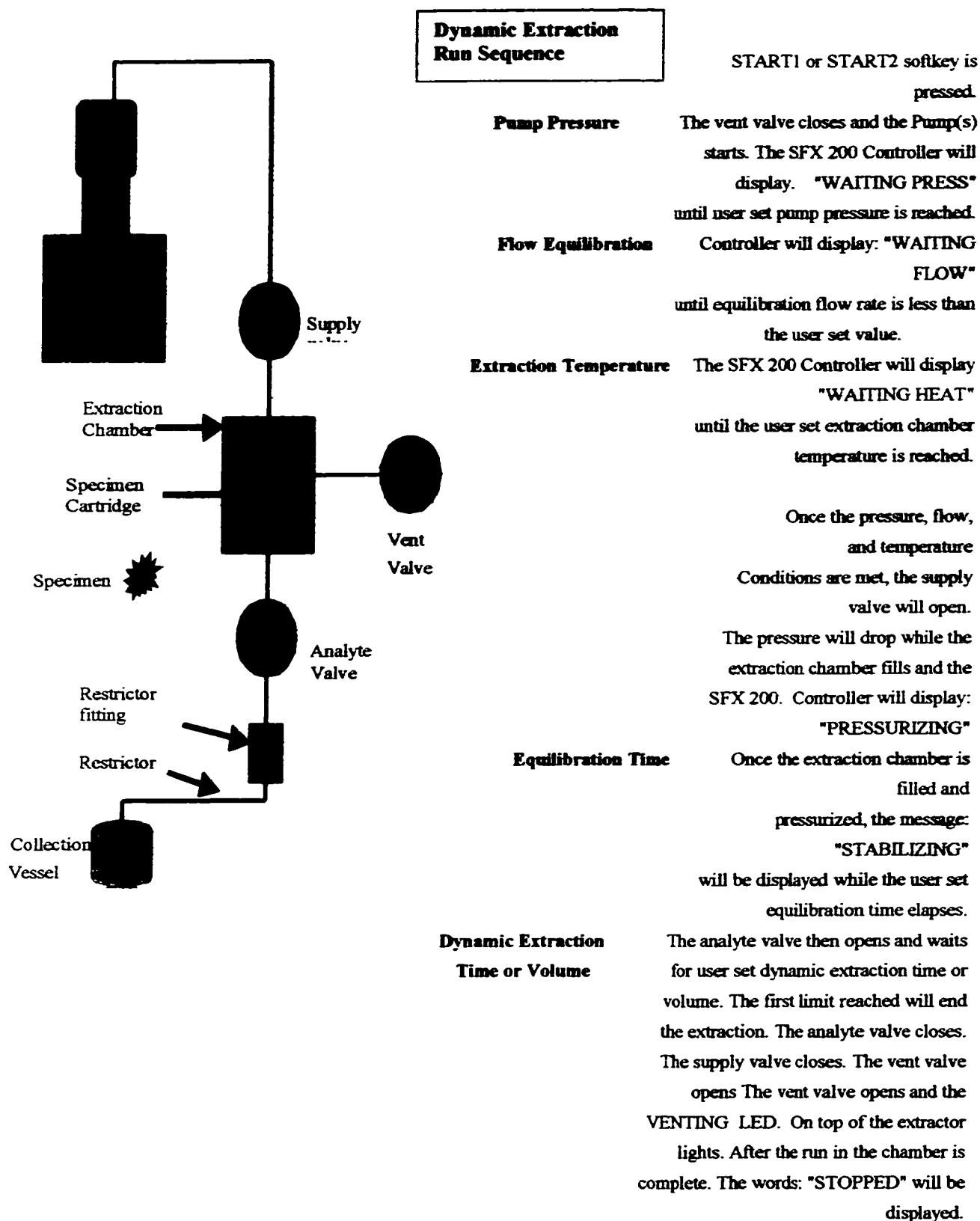


Figure 3.3. Sequence of extraction process.

3.5 Analysis

3.5.1. UV analysis of an extracted analyte from soil specimens

Lambda 2 UV / VIS (Perlen-Elmer) spectrometer was used to analyze the concentrations of extracted phenanthrene in collection vials of SFE (C). Detection of wavelength 292.4 nm in UV spectrum showed the presence of phenanthrene. Extraction efficiency was evaluated by the ratio:

$(V_t.C / V_{ph}.C_i)$. 100% where V_t is the trapped volume, V_{ph} is the volume of phenanthrene (ml), C is the extracted concentration and C_i is the initial concentration in mg / ml.

3.5.2 Microscopic analysis of specimens

In order to observe the influence of various extraction parameters on the fine porous media, some specimens were subjected to microscopic analysis.

The following specimens have been subjected to microscopic analysis:

- i) **Sample 1-** illite without contaminant (Fig.5.2).
- ii) **Sample 2-** contaminated illite with phenanthrene without extraction (Fig.5.3).
- iii) **Sample 3-** non-disturb illite after extraction at the following conditions: $p = 8000$ psi, $T=150$ °C, $t_d = 30$ min (Fig.5.4).
- iv) **Sample 4-** non-disturb illite after extraction at $p = 5000$ psi, $T=50$ °C, $t_s = 15$ min / $t_d = 15$ min (Fig.5.5).
- v) **Sample 5-** non-disturb illite after extraction at $p = 8000$ psi, $T=50$ °C, $t_s = 15$ min / $t_d = 15$ min (Fig.5.6).

Hitachi scanning electron microscope (SEM S 520) was used to obtain micrographes of above-mentioned samples. Specimens were dehydrated, placed on stubs and coated with 10 nm of gold in a sputter cotter (polaram. E 5100).

The microscopic image was further analyzed. The image analysis of micrograph shown in Figure 5.4 was performed in order to measure particle size and voids after extraction (Figure 5.4.a)

CHAPTER 4

EXPERIMENTAL RESULTS

4.1 Introduction

The phenanthrene recovery from various soil specimens (S1, S2, S3, and S4) is shown in Tables A4.1 to A4.6 in Appendix 4. The following sections present the efficiency of phenanthrene extraction related to different technological parameters of SFE. In nearly all cases, the results were within the average deviations 1 to 12.

4.2 Extraction with modifier from illite (S1)

Illite specimens was subjected to extraction pressures (5000, 8000 psi) at temperature of $T=50\text{ }^{\circ}\text{C}$, $80\text{ }^{\circ}\text{C}$, and $150\text{ }^{\circ}\text{C}$. Table A4.1 in Appendix 4 shows the recovery of phenanthrene from illite in above-mentioned conditions.

The pressure of 5000 psi, at $T = 150\text{ }^{\circ}\text{C}$ and $t_d = 30\text{ min}$ of phenanthrene the recovery reached 58%, as shown in Figure 4.3. By increasing pressure to 8000 psi in the same temperature and time, a slight increase of the recovery up to 72% was observed. Although, Figure 4.2 shows that at $T = 150\text{ }^{\circ}\text{C}$, $p = 8000\text{ psi}$ and 5000 psi where t_d decreased to 10-min. Extraction yielded low recovery value. While improved recovery is observed over 20-min dynamic time of extraction. Figure 4.1 shows the dependence of the recovery on dynamic extraction. In this figure the recovery at $T = 50\text{ }^{\circ}\text{C}$, $p = 5000\text{ psi}$ increased with dynamic time. It should be noted that the recovery $t_d = 30\text{ min}$, $T = 50\text{ }^{\circ}\text{C}$ is higher when $p=5000\text{ psi}$ than the recovery at $p= 8000\text{ psi}$. As dynamic time for $T = 150\text{ }^{\circ}\text{C}$ and $p = 8000\text{ psi}$ increased to $t_d = 60\text{-min}$ a decrease recovery appeared.

No significant recovery was observed at extraction temperature = $80\text{ }^{\circ}\text{C}$, for $t_d = 10, 20, 30\text{ min}$ when $p = 5000\text{ psi}$ was applied. However, a distinct increase in the recovery appeared by raising the pressure to 8000 psi, where t_d was 30 min.

4.3 Extraction without modifier from illite (S1)

Low extraction recovery yielded for $t_s = 15$ min / $t_d = 15$ min and $t_s = 10$ min / $t_d = 20$ min at $T = 50, 80, 150$ °C, $p = 5000$ psi. Recovery yielded little increase only in $t_d = 30$ min at $T = 150$ °C, $p = 5000$ psi (Figure 4.5).

For $p = 8000$ psi and $t_d = 30$ min the extraction yielded increase in recovery over a combination of $t_s = 15$ min / $t_d = 15$ min or use $t_s = 10$ min / $t_d = 20$ min at $T = 50$ °C (Figure 4.6). Although no modifier has been used, the increase of temperature to 150 °C, $p = 8000$ psi and different time raised the recovery (Figure 4.4). The SFE 200 does not have a mode, which permits to use a combination of modifier and static time.

4.4 Extraction with modifier from soil specimen S2

For extraction temperatures of $T = 50, 80, 150$ °C, $p = 5000$ psi, no significant recovery was observed for all $t_d = 10, 20, 30$ min (Figure 4.7). Although the use of a modifier the extraction at $T = 50, 80$ °C gave low recovery, comparable to $T = 150$ °C, a distinct increase in the recovery appeared with increasing t_d from 10 min to 30 min.

As shown in Figure 4.8, for the technological conditions such as $t_d = 30$ min and $T = 150$ °C the recovery increased as pressure raised to $p = 8000$ psi. A distinct decrease in the recovery appeared by raising the pressure to 8000 psi where $T = 150$ °C for dynamic time from 10 to 30 min (Figure 4.9).

4.5 Extraction without modifier from soil specimen (S2)

Figure 4.10 demonstrates no change in recovery at $T = 150$ °C, $p = 8000$ psi for different dynamic extraction time. Specimen S2 is a mixture of 60% clay with 40% sand. As shown in Figure 4.11, this specimen subjected to phenanthrene extraction considering different times $t_d = 30$ min, $t_s : t_d = 15:15$ min,

ts : td = 10 : 20 at T = 50 and 80 °C when p = 5000 psi, no significant recovery was observed. The use of td = 30 min yielded little increase in recovery comparable to the ratio ts : td = 15:15 min, ts : td = 10 : 20 at T = 150 °C and p = 5000 psi. Figure 4.12 demonstrates that the use of td = 30 min yielded little decrease in recovery comparison to ts : td = 15:15 min, ts : td = 10 : 20 ratio at T = 50 °C, p = 8000 psi. At the extraction temperature T = 150 °C, p = 8000 psi with increasing the time, the recovery of phenanthrene increased.

4.6 Extraction with modifier from soil specimen (S3)

The results shown in Figure 4.13 demonstrate that extractions with modified carbon dioxide at T = 50 and 80 °C, by applying pressure = 5000 psi were no significant for all extraction times. The increase of extraction temperature to T = 150 °C and td = 20 min, increase the phenanthrene recovery. Such high recovery was observed by increasing extraction time to 30 min.

The results in Figure 4.14 demonstrate, an increase of recovery of phenanthrene by raising the temperature to 150 °C, p = 8000 psi when td = 30 min. Figure 4.15 shows that the time of extraction have impact on the phenanthrene recovery at extraction pressure = 8000 psi, T = 150 °C, while at p = 5000 psi the recovery increase with raising the time from 10 min to 30 min.

4.7 Extraction without modifier from soil specimen (S3)

The recovery of phenanthrene at T = 150 °C, p = 8000 psi yielded increase with increasing from td = 10 min to 20 min, but no change in recovery was observed with increasing td = 20 min to 30 min (Figure 4.16).

As shown in Figure 4.17, for both temperatures 50 and 80 °C, p = 5000 psi at extraction time ts : td = 15:15 min, ts : td = 10 : 20 ratio to compare to td = 30 min the extraction is insignificant. The increase of temperature (150 °C) under the same pressure for td = 30 min yielded little increase in recovery.

The recoveries in Figure 4.18 shows that 30 min appeared a distinct increase over $t_s : t_d = 15:15$ min, $t_s : t_d = 10 : 20$ when the pressure was 8000 psi and $T = 50^\circ\text{C}$, while at $p = 5000$ psi no change in recovery was observed.

4.8 Comparison between specimens (S1, S2, S3)

- **Combined pressure and time effect with modifier:**

Increase the pressure yielded an increase in the recovery by raising the dynamic time for clay (S1) material, but no change yielded for sand clay mixtures ($S2 = 40:60$, $S3 = 80:20$) as shown in Figure 4.22 and 4.23.

- **Temperature and time effect with modifier**

For clay the recovery increase as time t_d increase for temperatures 50°C and 150°C , $p = 5000$ psi. For the mixture S2, S3, it is observed that the recovery increase at 150°C , but no change was observed at 50°C with time increase. At 80°C no change yielded for all types specimens as shown in Figures 4.19, 4.20, and 4.21.

- **Pressure and time effect without modifier**

The increase of extraction time does not change the recovery rate where samples are at the highest-pressure 8000 psi and temperature 150°C (Figure 4.24).

- **The effect of static / dynamic time and dynamic time without modifier**

For extraction time $t_s : t_d = 15:15$ min no change in the recovery was observed for clay and S3 at $T = 50, 80$ and 150°C , $p = 5000$ psi. However the increase in recovery appeared for mixture 40:60 (S2) when temperature rose to 150°C , as shown in Figure 4.25.

For $t_d = 30$ min ($T = 150^\circ\text{C}$, $p = 5000$ psi) an increase in the recovery for all the specimens was observed, but no change is shown at $T = 50, 80^\circ\text{C}$ (Figure 2.26). A distinct increase in recovery was observed for specimen S3 for the time of extraction $t_s : t_d = 15:15$ min at $p = 5000$ psi, $T = 50^\circ\text{C}$ (Figure 4.27).

4.9 Extraction without modifier from sand (S4)

The high recovery 71% of phenanthrene was observed at $T = 50$ when low pressure (5000 psi) and low dynamic time ($t_d = 10$ min) was applied without modifier (Figure 4.29). It should be noted that the recovery did not increase by raising the dynamic time from 10 min to 30 min at $T = 50$ °C and pressure $p = 5000$ psi. A distinct decrease in the recovery appeared by raising the pressure from 5000 psi to 8000 psi.

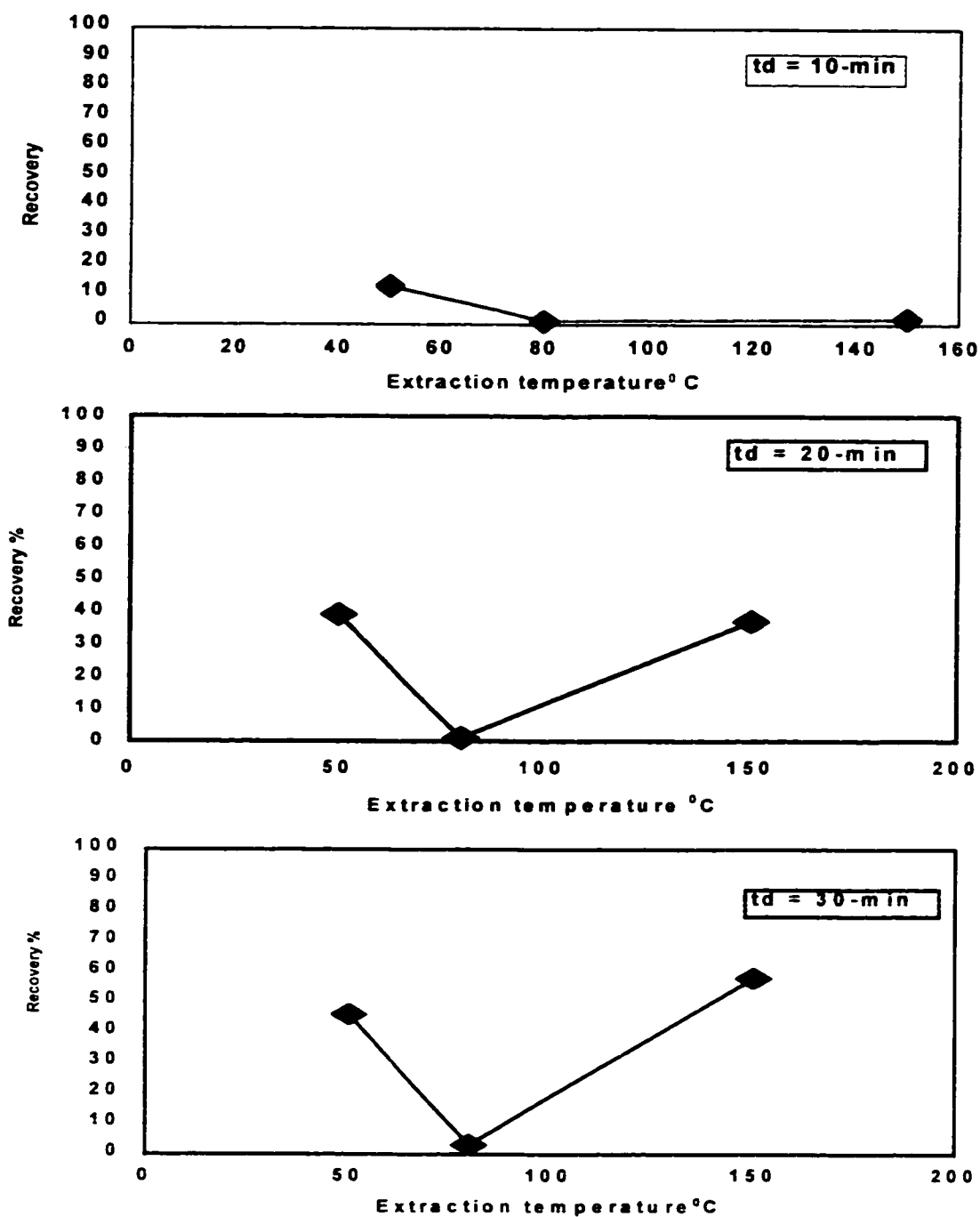


Figure 4.1. Recovery of phenanthrene from specimen S1 vs. extraction temperature 50, 80, 150 °C. **Conditions:** modifier: 5% (mol) methanol at p = 5000 psi, td = 10, 20, 30 min

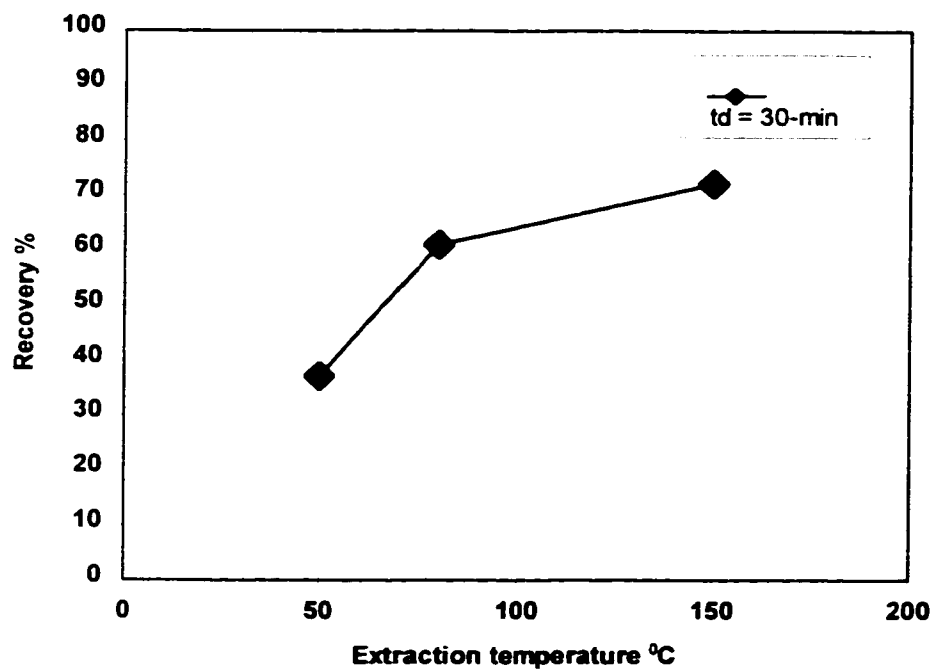


Figure 4.2. Recovery of phenanthrene from specimen S1 vs. extraction temperature, $T = 50\text{ }^{\circ}\text{C}$, $80\text{ }^{\circ}\text{C}$, $150\text{ }^{\circ}\text{C}$.

Conditions: modifier 5% (mol), $p = 8000\text{ psi}$, $td = 30\text{-min}$.

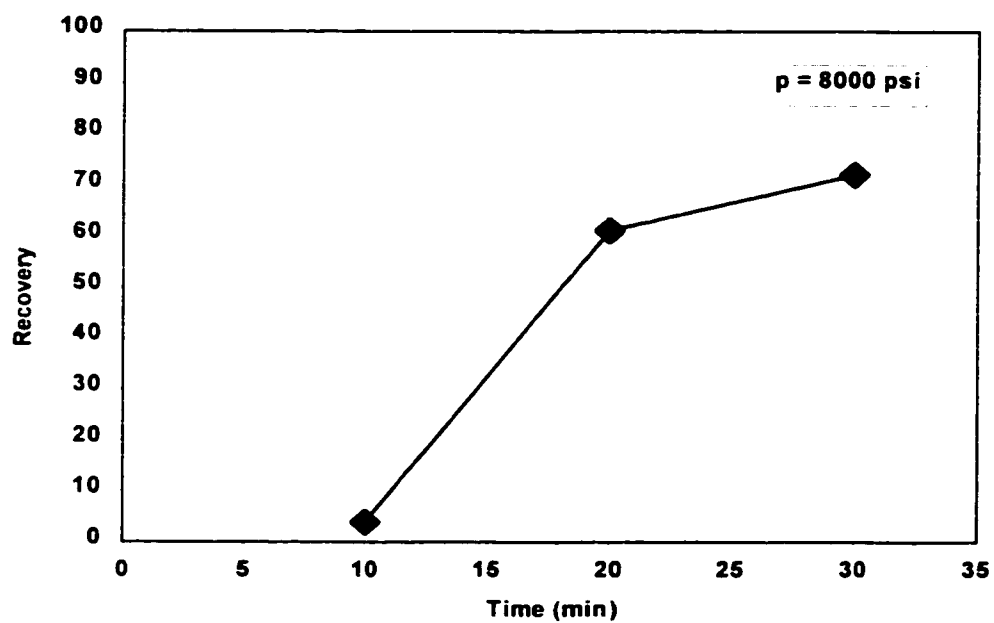
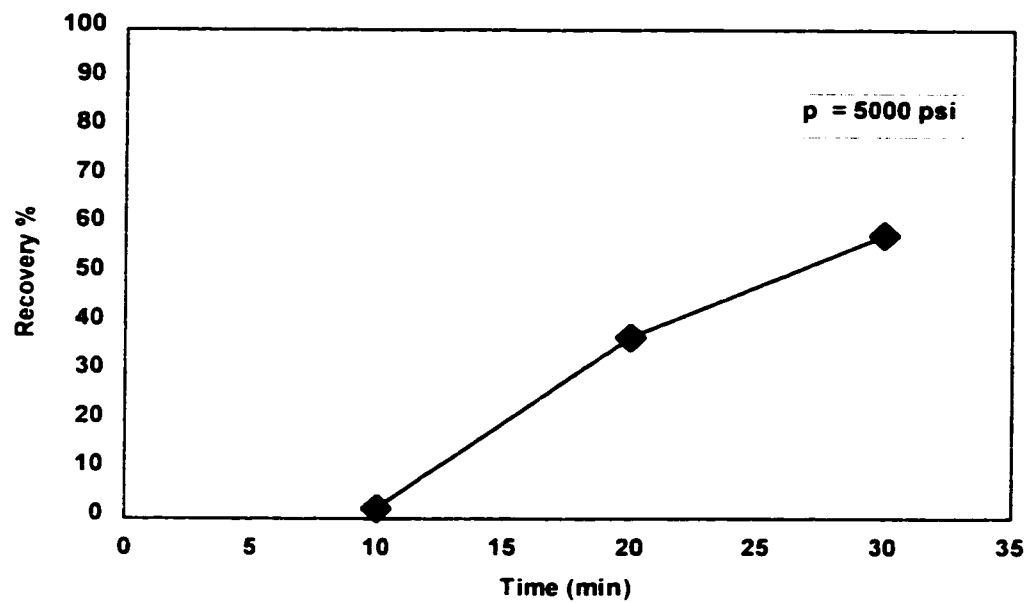


Figure 4.3. Recovery of phenanthrene from specimen S1 vs. dynamic time.
Conditions: modifier 5% (mol), $T = 150 \text{ }^{\circ}\text{C}$, $p = 5000 \text{ psi}$ (top), $p = 8000 \text{ psi}$ (bottom).

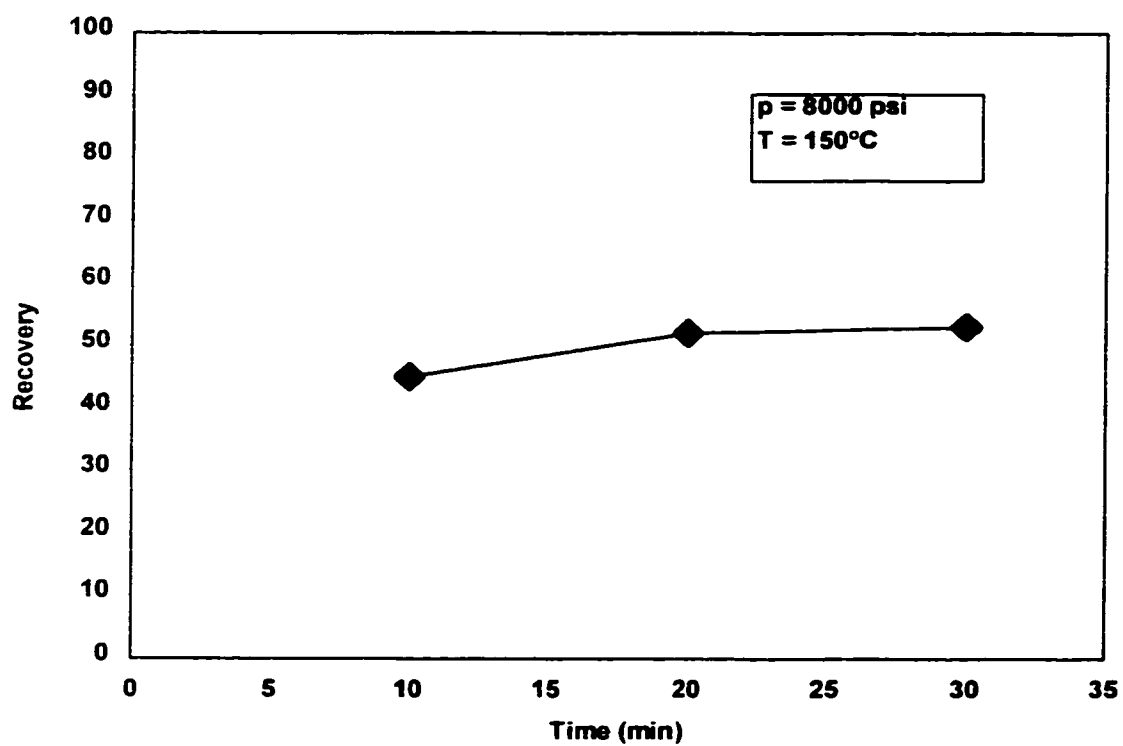


Figure 4.4. Recovery of phenanthrene from specimen S1 vs. dynamic time (td).

Conditions: without modifier, $T = 150^\circ\text{C}$, $p = 8000 \text{ psi}$.

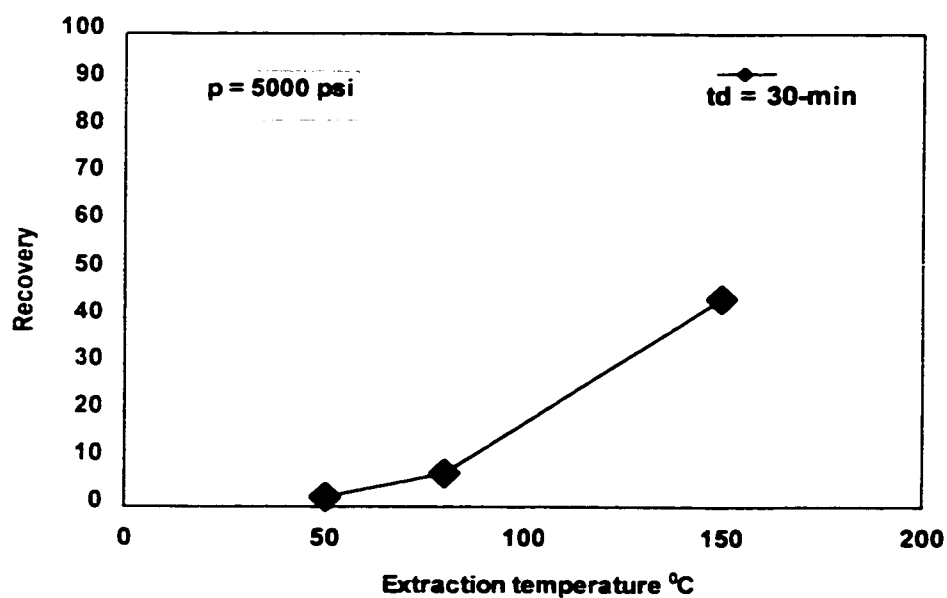
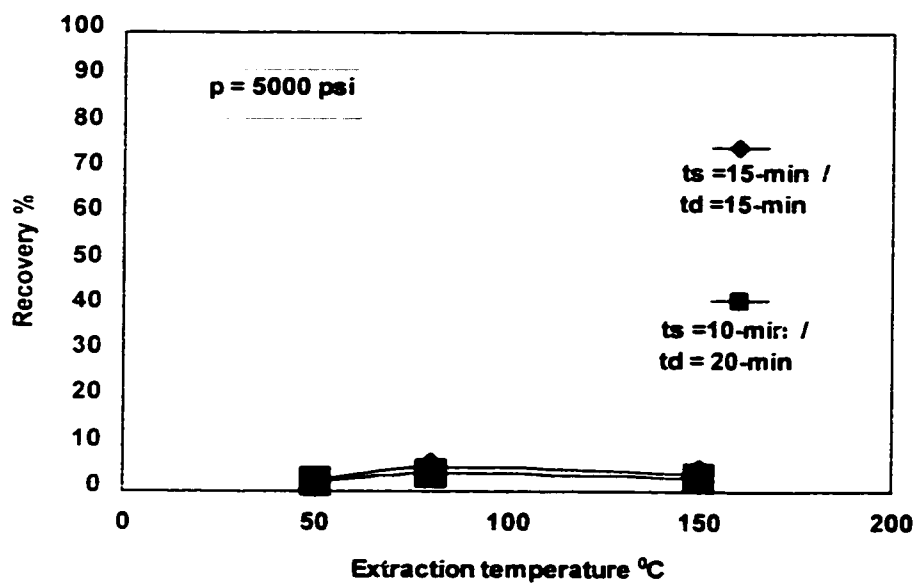


Figure 4.5. Recovery of phenanthrene from specimen S1 vs. extraction temperature.

Condition: without modifier, $p = 5000 \text{ psi}$, $t_s:t_d = 15:15 \text{ min}$, $t_s:t_d = 10:20$ (top) and $t_d = 30 \text{ min}$ (bottom).

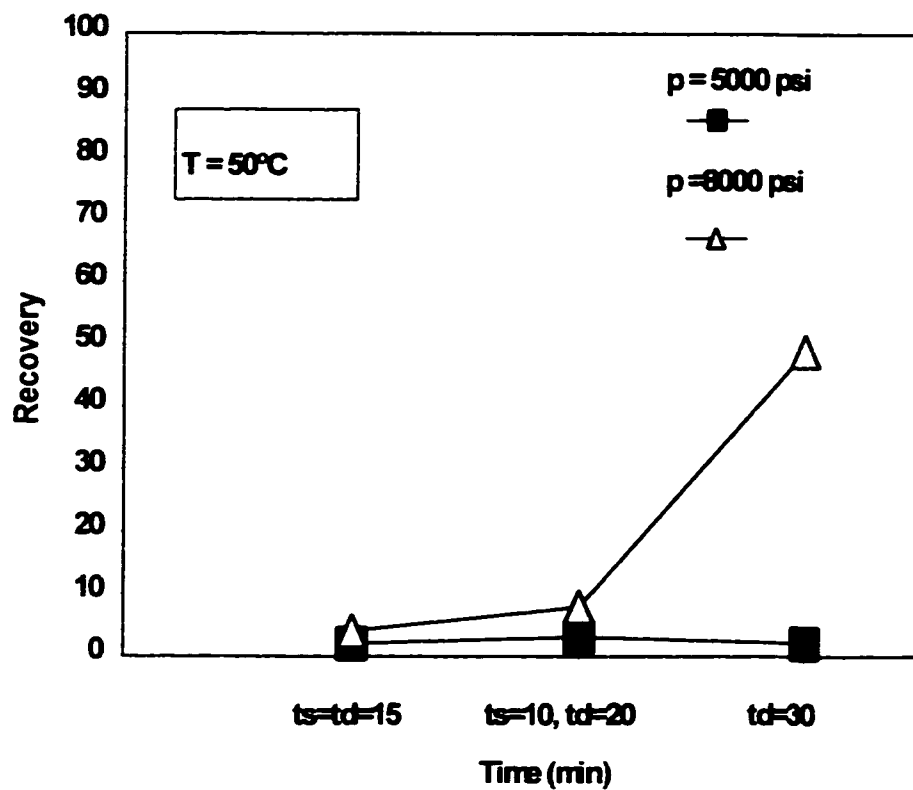


Figure 4.6. Recovery of phenanthrene from specimen S2 vs. time.

Conditions: without modifier, $T = 50\text{ }^{\circ}\text{C}$, using different $p = 5000$ psi and 8000 psi.

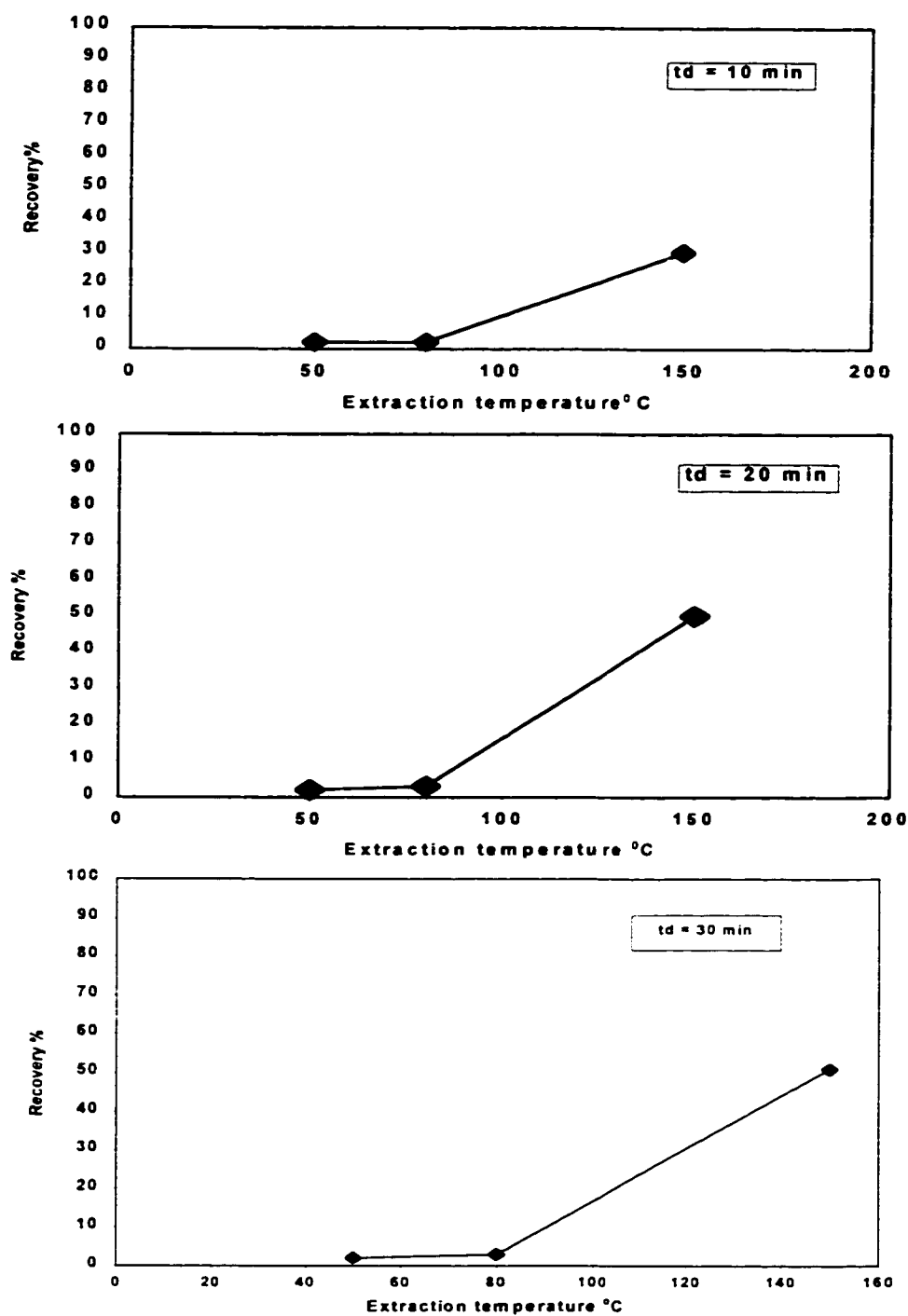


Figure 4.7. Recovery of phenanthrene from specimen S2 5% vs. extraction temperature, $T = 50, 80, 150^{\circ}\text{C}$. **Conditions:** with modifier 5% (mol) methanol, $p = 5000$ psi, $td = 10, 20, 30$ min.

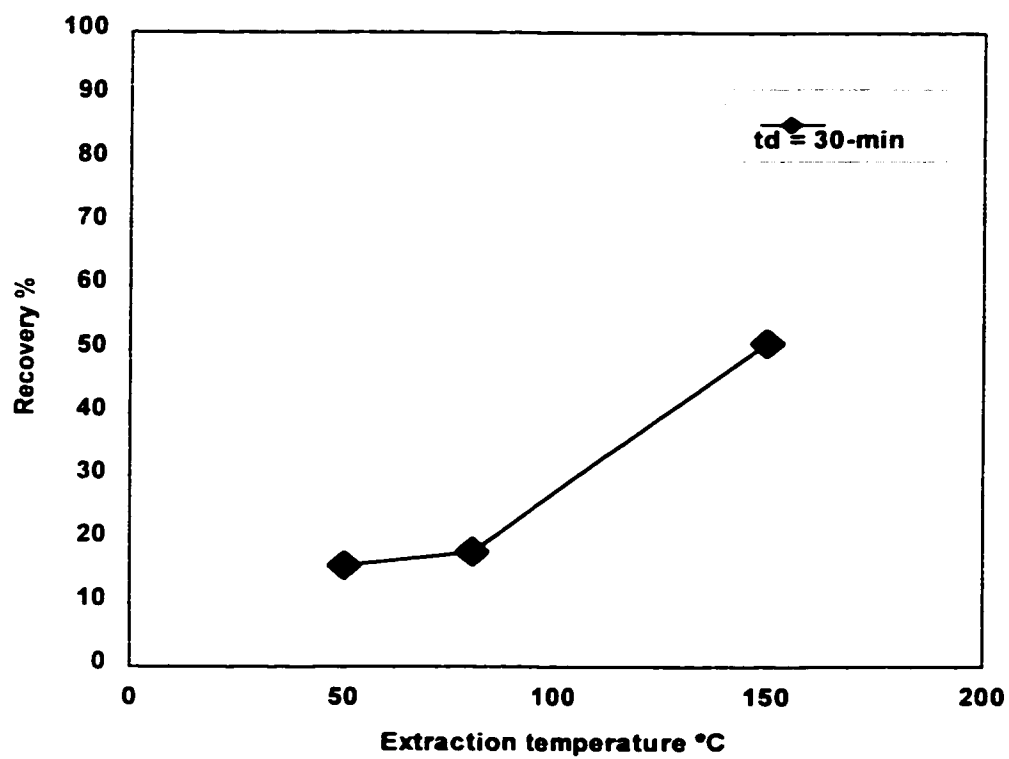


Figure 4.8. Recovery of phenanthrene from specimen S2 vs. extraction temperature, $T = 50, 80, 150\text{ }^{\circ}\text{C}$.

Conditions: with modifier 5% (mol) methanol, $p = 8000\text{ psi}$, $td = 30\text{-min}$.

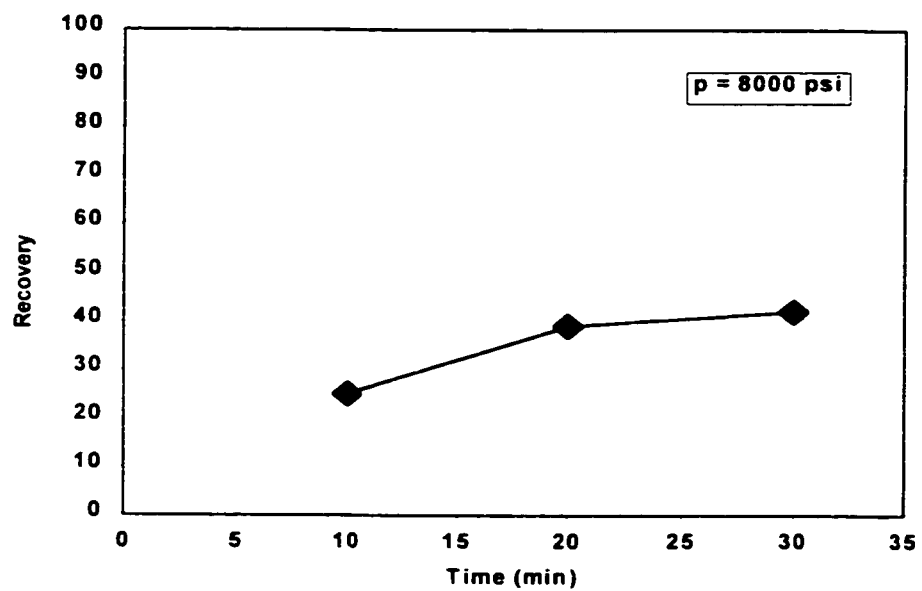
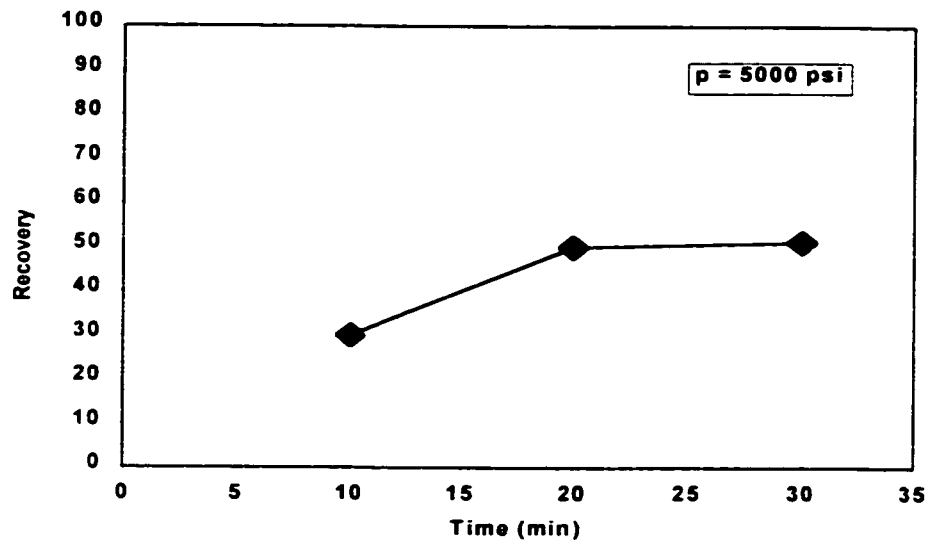


Figure 4.9. Recovery of phenanthrene from specimen S3 vs. dynamic time. **Conditions:** with modifier 5% (mol) methanol, $T = 150 \text{ }^{\circ}\text{C}$, $p = 5000 \text{ psi}$ (top), $p = 8000 \text{ psi}$ (bottom).

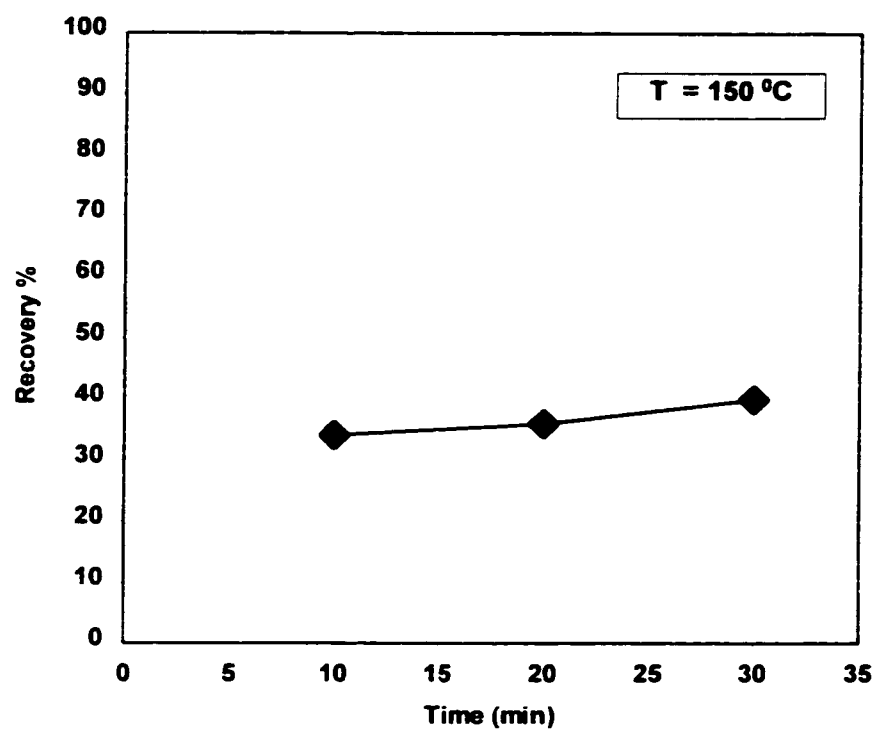


Figure 4.10. Recovery of phenanthrene from specimen S2 vs. dynamic time.

Conditions: without modifier, $T = 150\text{ }^{\circ}\text{C}$, $p = 8000\text{ psi}$.

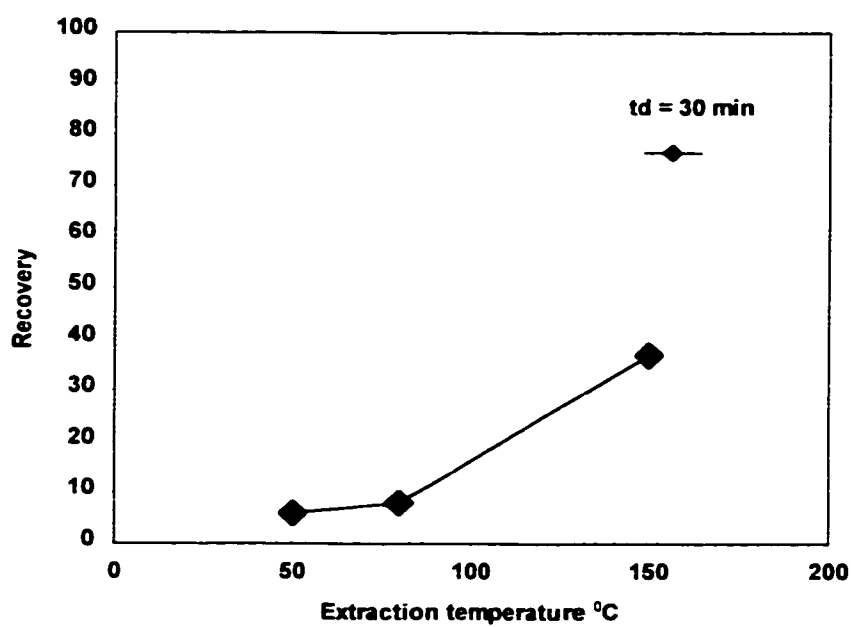
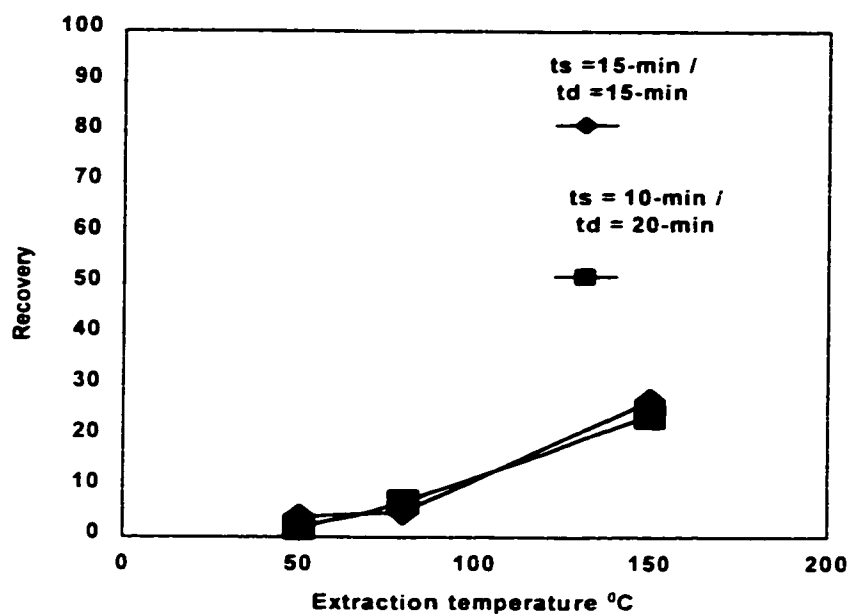


Figure 4.11. Recovery of phenanthrene from specimen S2 vs. extraction temperature. **Conditions:** without modifier, $p = 5000$ psi, $ts:td = 15:15$ and $10:20$ (top), $td = 30$ -min (bottom).

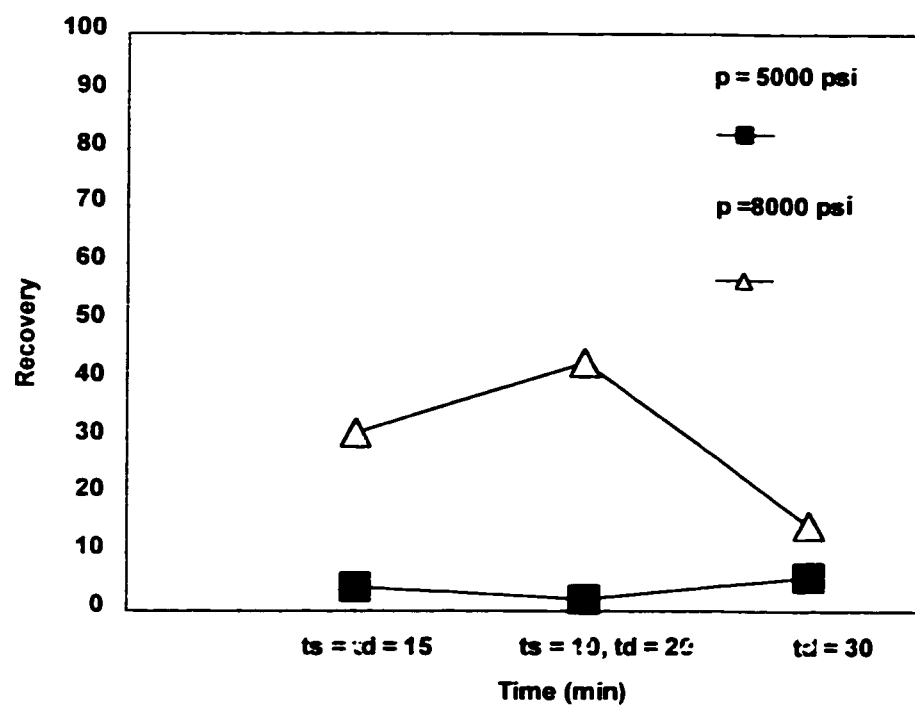


Figure 4.12. Recovery of phenanthrene from specimen S2 vs. time.
Conditions: without modifier, $T = 50\text{ }^{\circ}\text{C}$, $p = 5000\text{ psi}$ and 8000 psi .

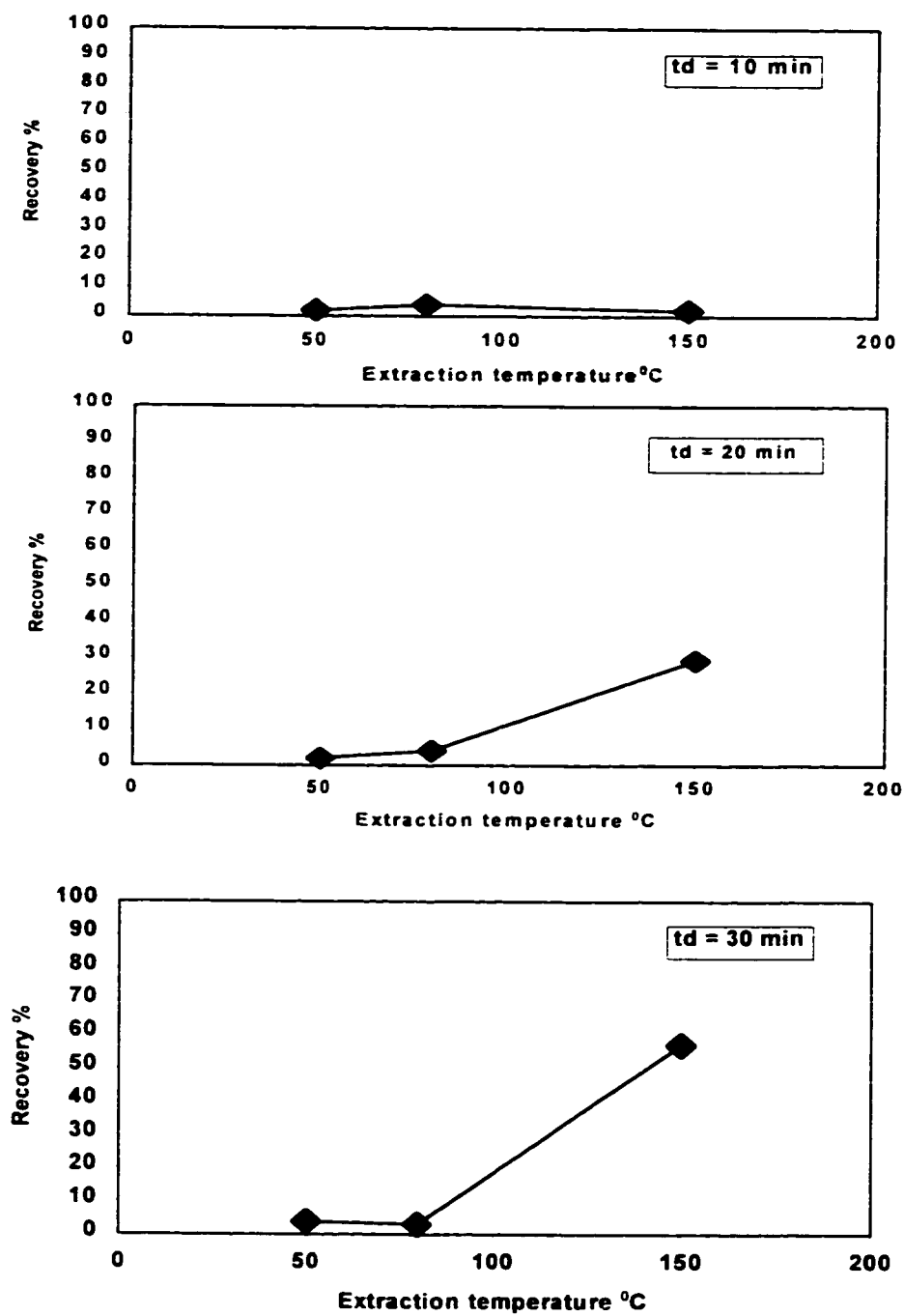


Figure 4.13. Recovery of phenanthrene from specimen S3 vs. extraction temperature, $T = 50, 80, 150\text{ }^{\circ}\text{C}$. **Conditions:** with modifier 5% (mol) methanol, $p = 5000\text{ psi}$, $td = 10, 20, 30\text{ min}$.

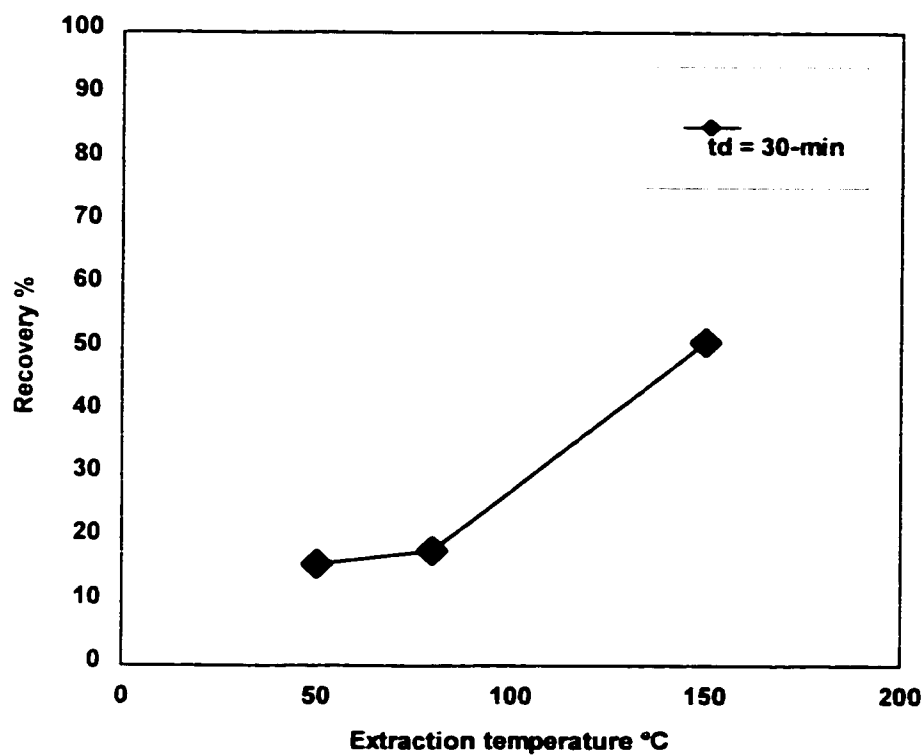


Figure 4.14. Recovery of phenanthrene from S3 vs. extraction temperature, $T = 50, 80, 150\text{ }^{\circ}\text{C}$

Conditions: with modifier 5% (mol) methanol, $p = 8000\text{ psi}$, $td = 30\text{-min}$.

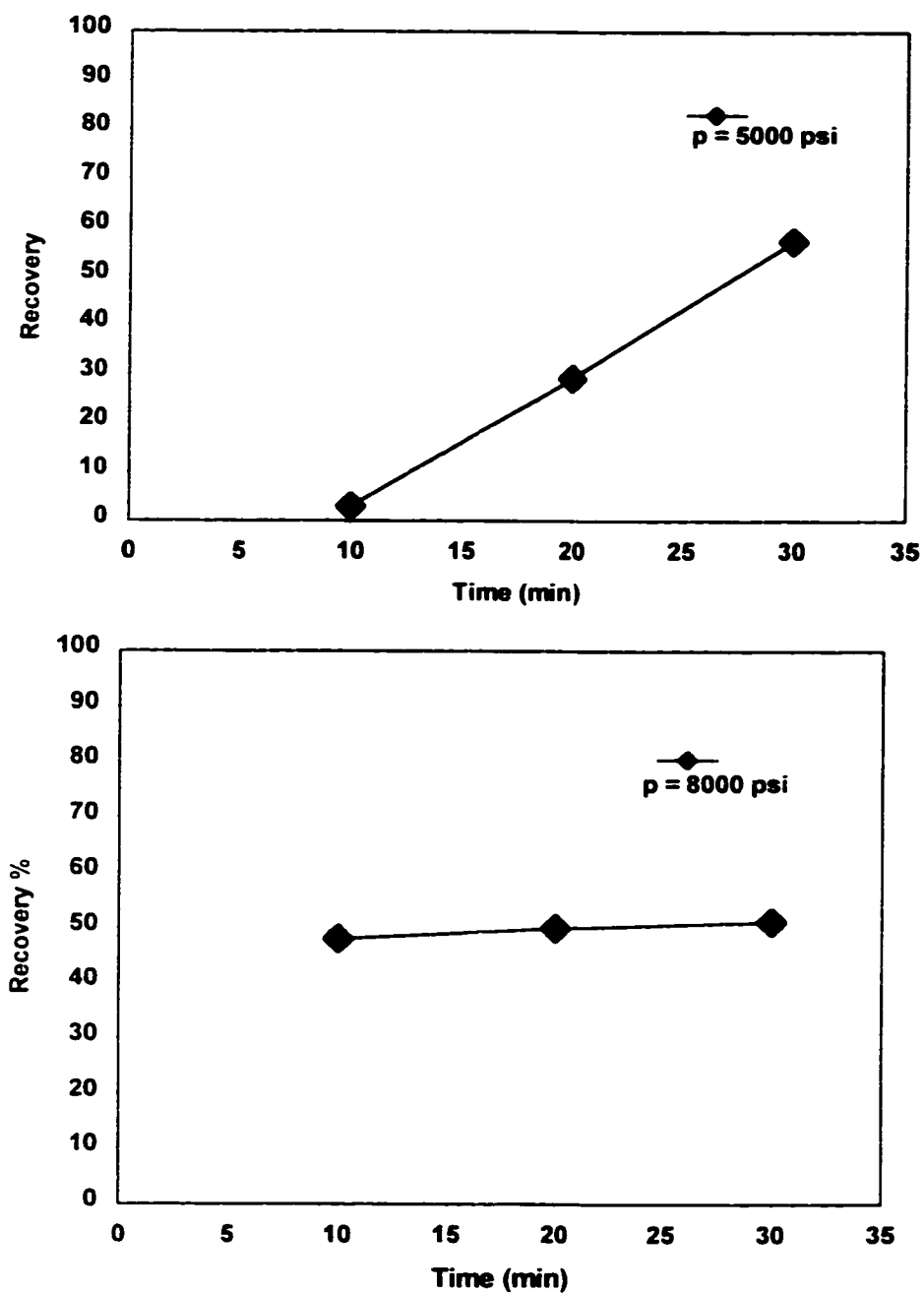


Figure 4.15. Recovery of phenanthrene from specimen S3 vs. $t_d = 10, 20, 30$.
Conditions: with modifier 5% (mol) methanol, $T = 150$ °C, $p = 5000$ psi (top), $p = 8000$ psi (bottom).

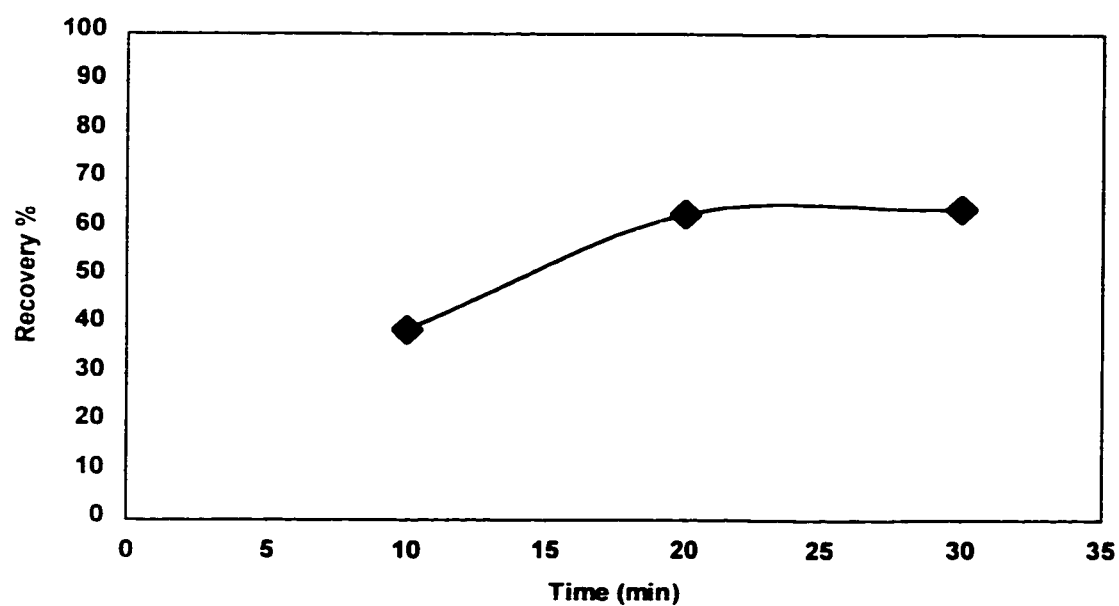


Figure 4.16. Recovery of phenanthrene from S3 vs. $t_d = 10, 20, 30$ min.

Conditions: without modifier, $T = 150\text{ }^{\circ}\text{C}$, $p = 8000\text{ psi}$.

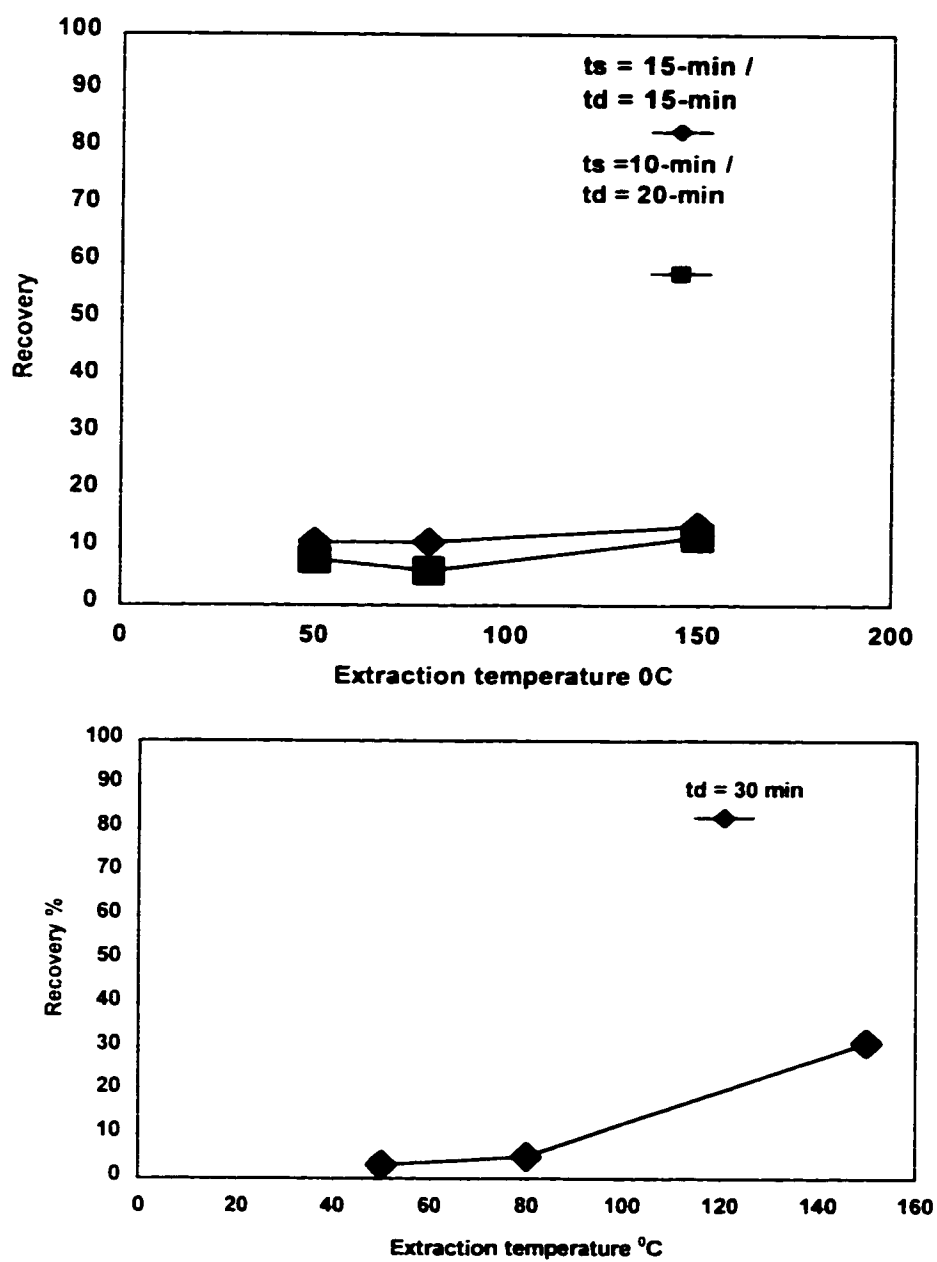


Figure 4.17. Recovery of phenanthrene from specimen S3 vs. extraction temperature.

Conditions: without modifier, $p = 5000$ psi, $ts:td = 15 : 15$ and $10:20$ (top), $td = 30$ (bottom).

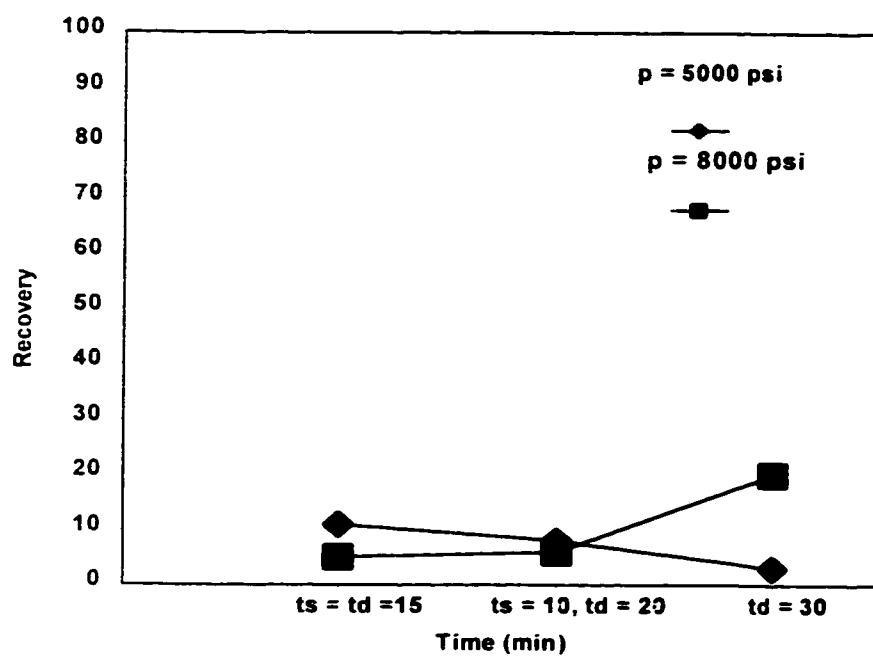


Figure 4.18. Recovery of phenanthrene from S3 vs. time.

Conditions: without modifier, $T = 50$ °C, $p = 5000$ psi and 8000 psi.

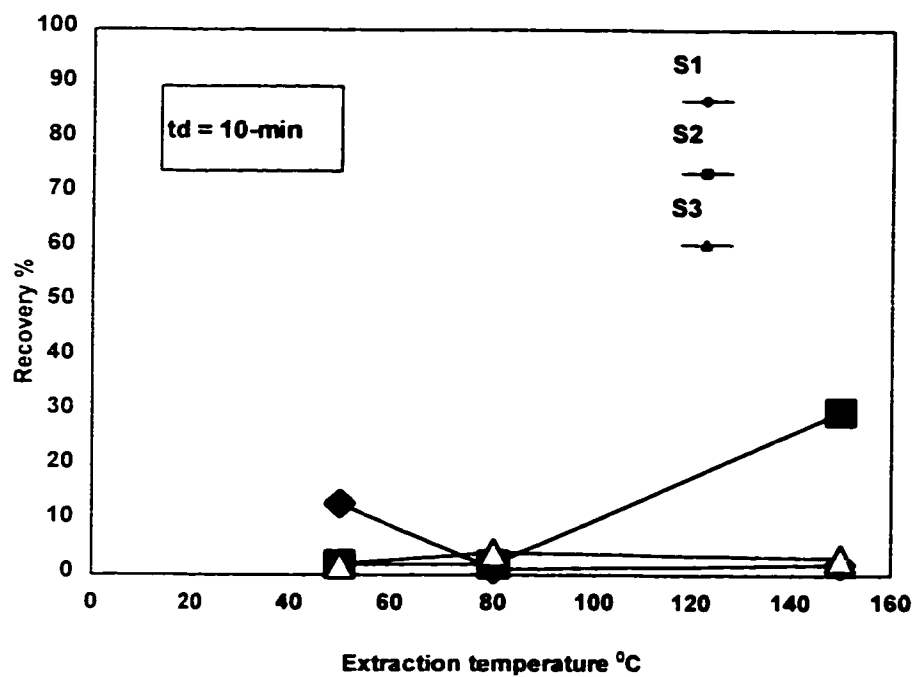


Figure 4.19. Recovery of phenanthrene from S1 (100% clay), S2 (60% clay and 40% sand), S3 (20% clay and 80%) vs. extraction temperature, $T = 50, 80, 150$ °C.

Conditions: with modifier 5% (mol) methanol, $p = 5000$ psi, $td = 10$ -min.

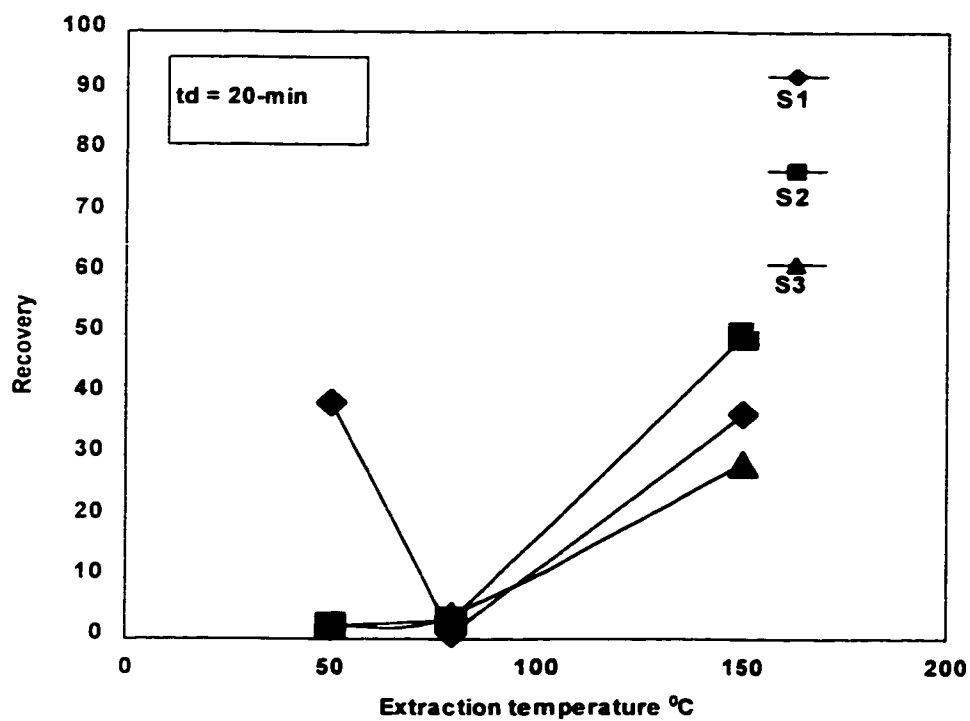


Figure 4.20. Recovery of phenanthrene from specimen S1, S2, S3 vs. extraction temperature, $T = 50, 80, 150\text{ }^{\circ}\text{C}$.

Conditions: modifier 5% (mol) methanol, $p = 5000\text{ psi}$, $td = 20\text{-min}$

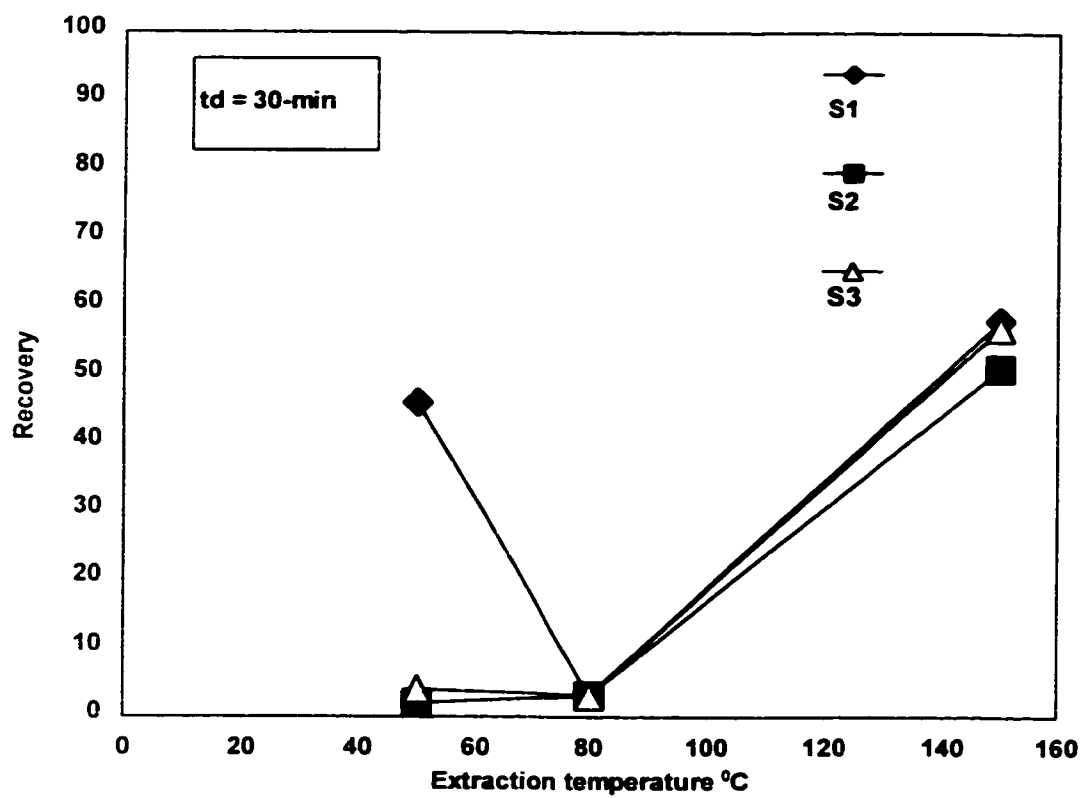


Figure 4.21. Recovery of phenanthrene from specimen S1, S2, S3 vs. extraction temperature, $T = 50, 80, 150\text{ }^{\circ}\text{C}$

Conditions: modifier 5% (mol) methanol, $p = 5000\text{ psi}$, $td = 30\text{-min}$.

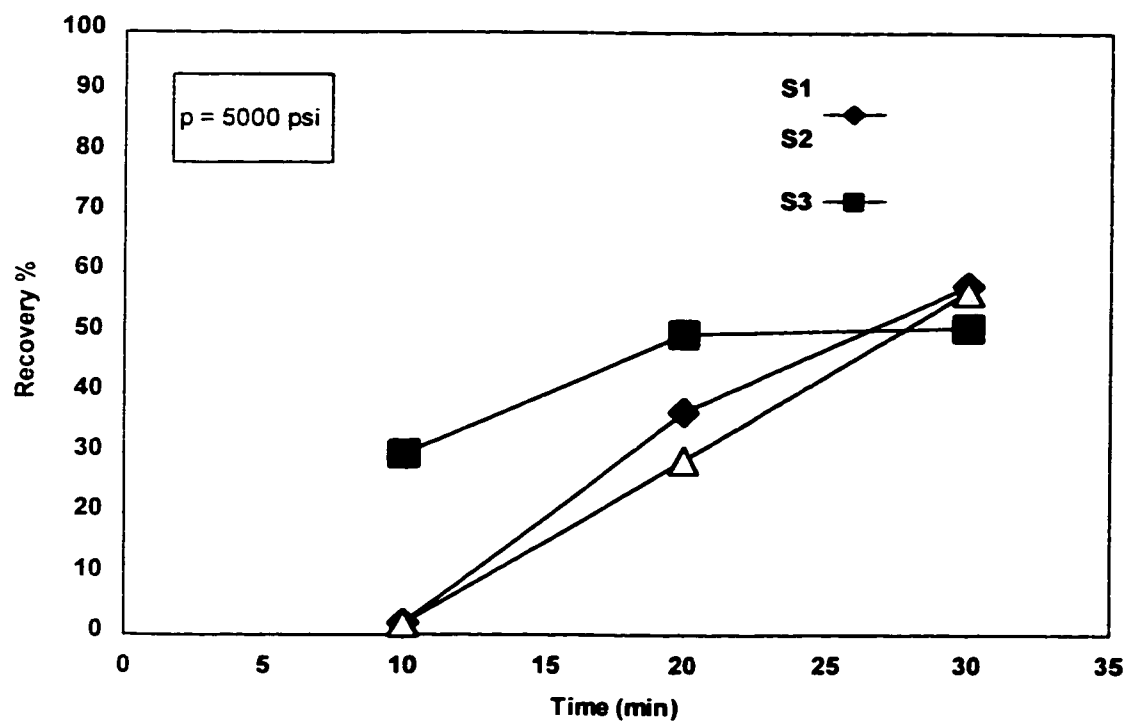


Figure 4.22. Recovery of phenanthrene from specimens S1, S2, S3 vs. dynamic time.

Conditions: modifier 5% (mol) methanol, $T = 150 \text{ }^{\circ}\text{C}$, $p = 5000 \text{ psi}$.

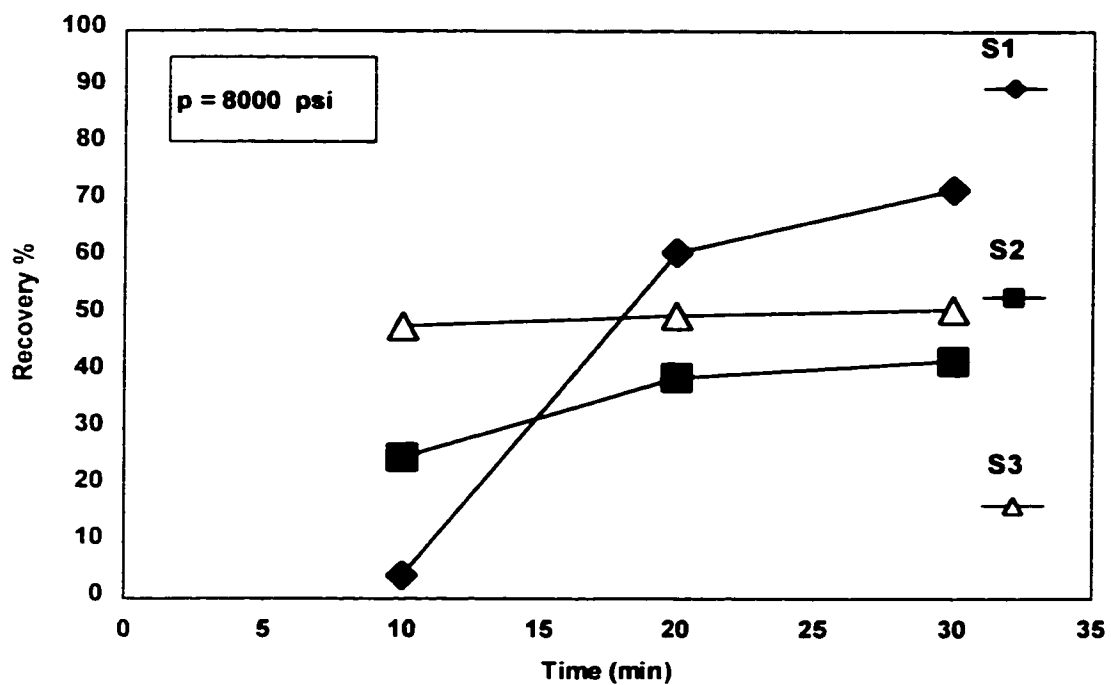


Figure 4.23. Recovery of phenanthrene from specimens S1, S2, S3 vs. dynamic time.

Conditions: with modifier 5% methanol, $T = 150 \text{ }^{\circ}\text{C}$, $p = 8000 \text{ psi}$.

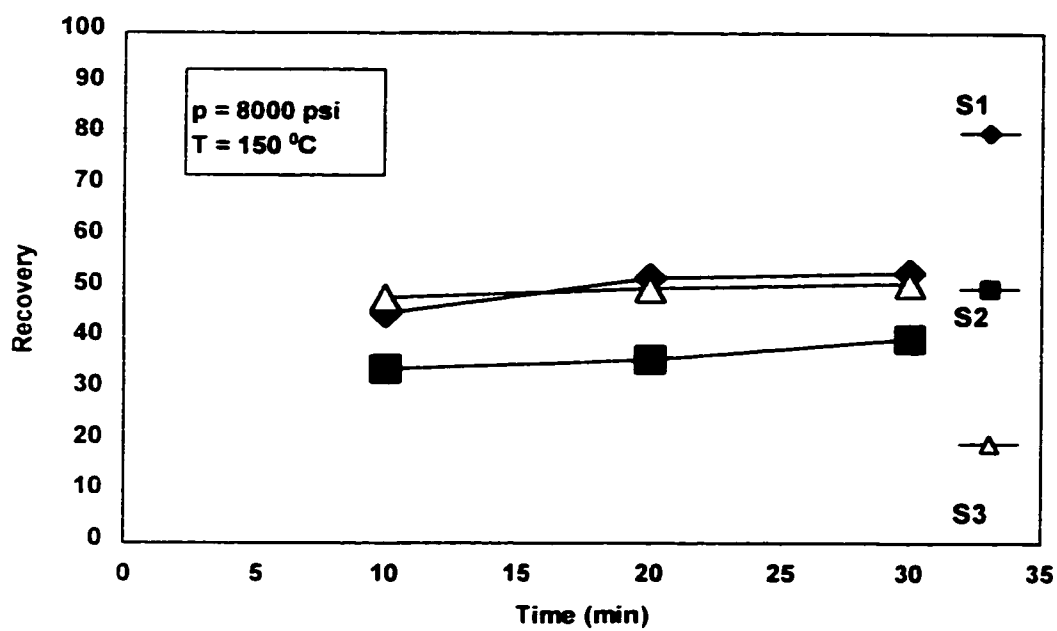


Figure 4.24. Recovery of phenanthrene from specimens S1, S2, S3 vs. dynamic time.

Conditions: without modifier, $T = 150 \text{ }^{\circ}\text{C}$, $p = 8000 \text{ psi}$.

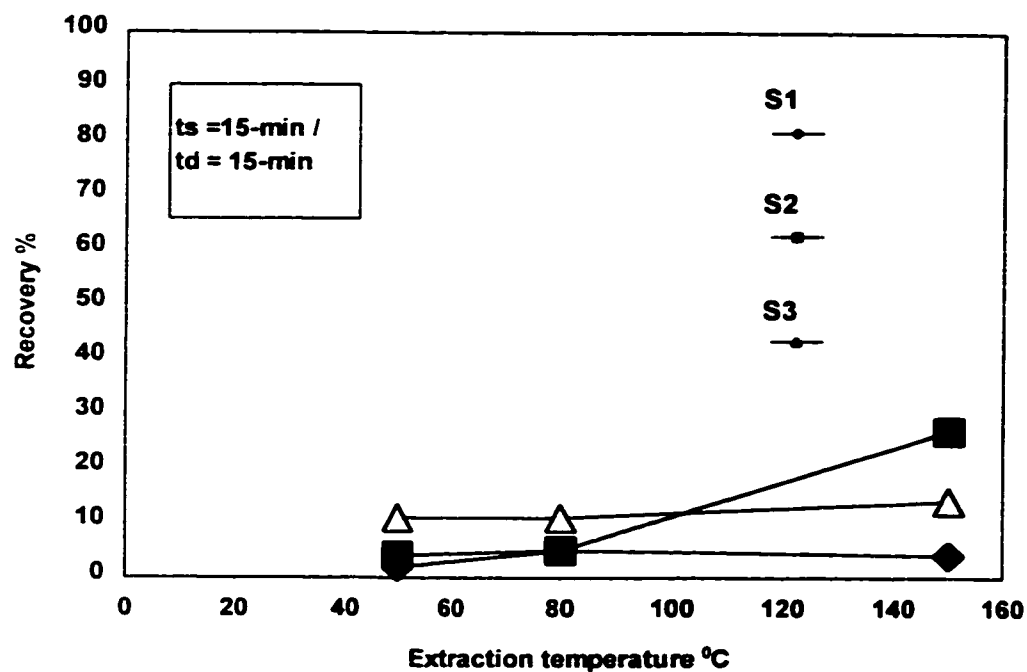


Figure 4.25. Recovery of phenanthrene from specimens S1, S2, S3 vs. extraction temperature

Conditions: without modifier, $p = 5000$ psi, $ts:td = 15:15$.

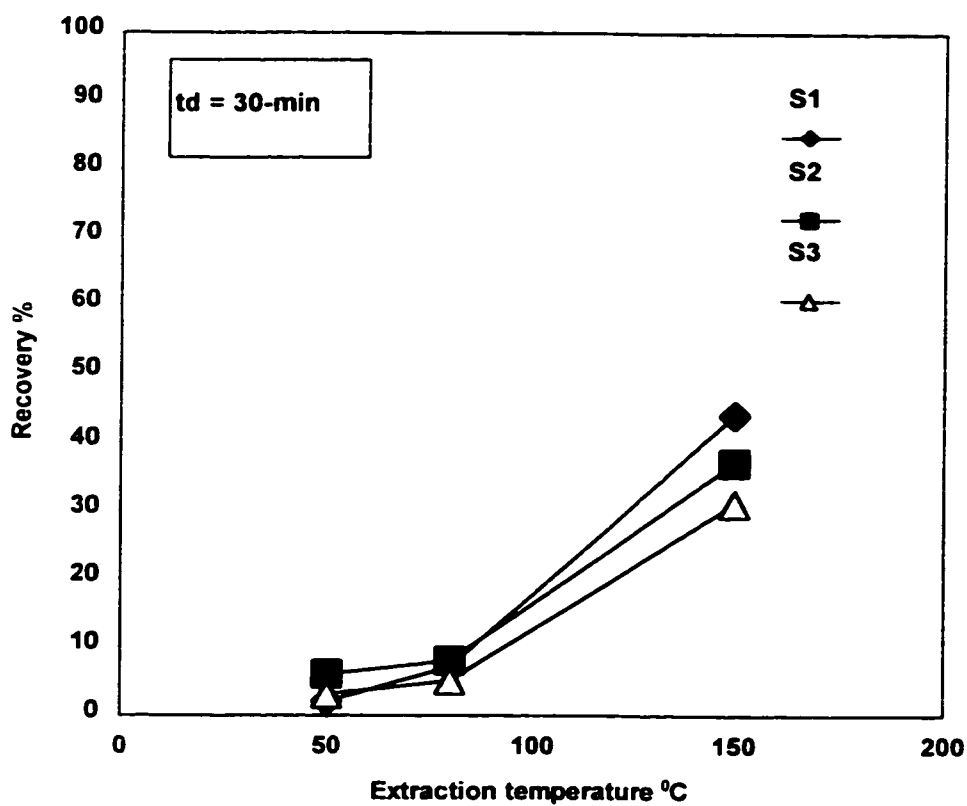


Figure 4.26. Recovery of phenanthrene from specimens S1, S2, S3 vs. extraction temperature $T = 50, 80, 150\text{ }^{\circ}\text{C}$.

Conditions: without modifier, $p = 5000\text{ psi}$, $td = 30\text{-min}$.

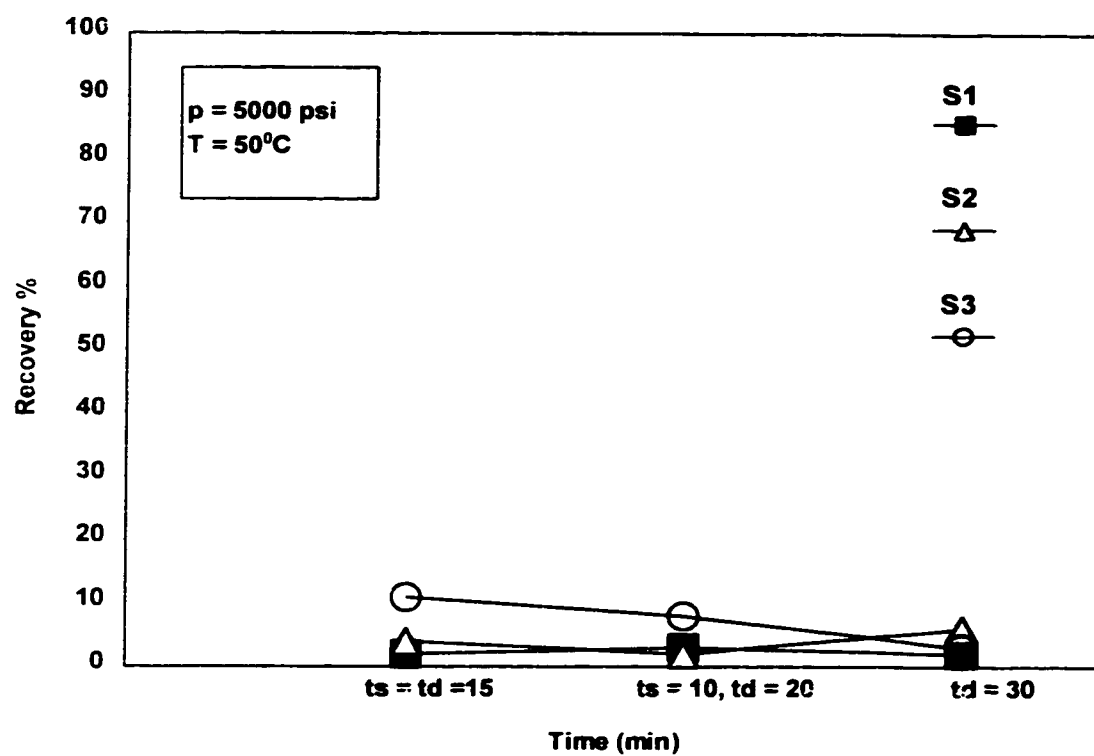


Figure 4.27. Recovery of phenanthrene from specimens S1, S2, S3 vs. time
Conditions: without modifier, $T = 50^\circ\text{C}$, $p = 5000 \text{ psi}$.

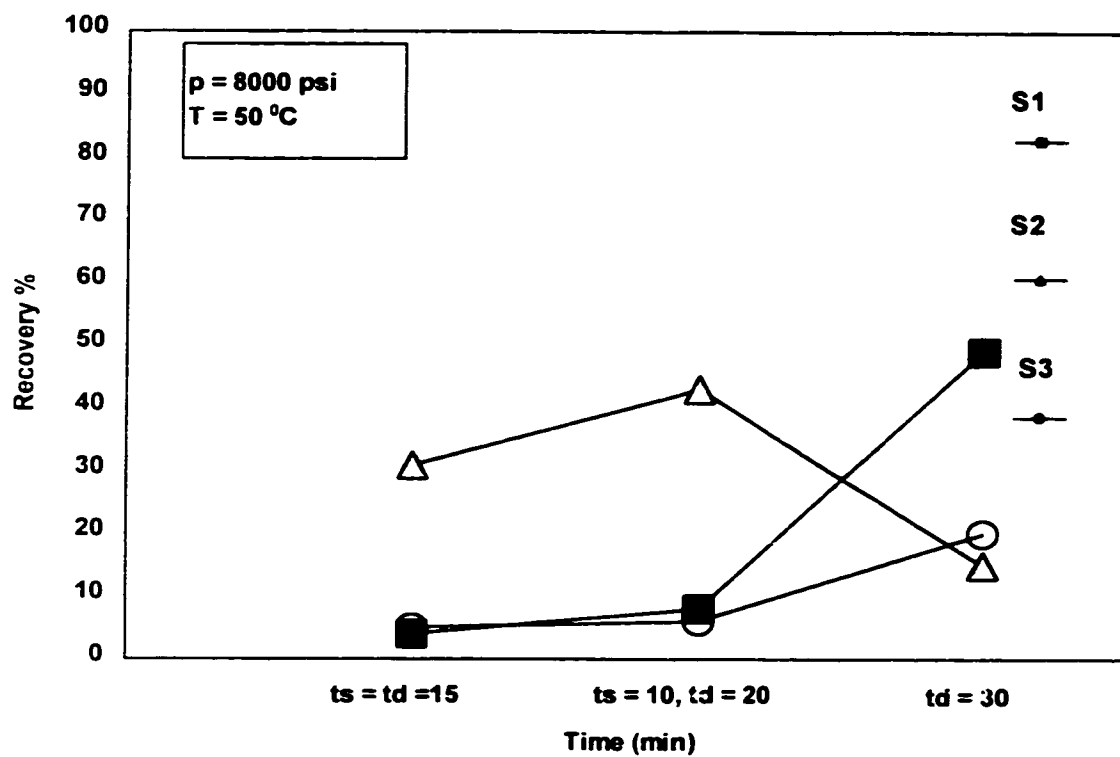


Figure 4.28. Recovery of phenanthrene from specimens S1, S2, S3 vs. time.
Conditions: without modifier, $T = 50 \text{ }^{\circ}\text{C}$, $p = 8000 \text{ psi}$.

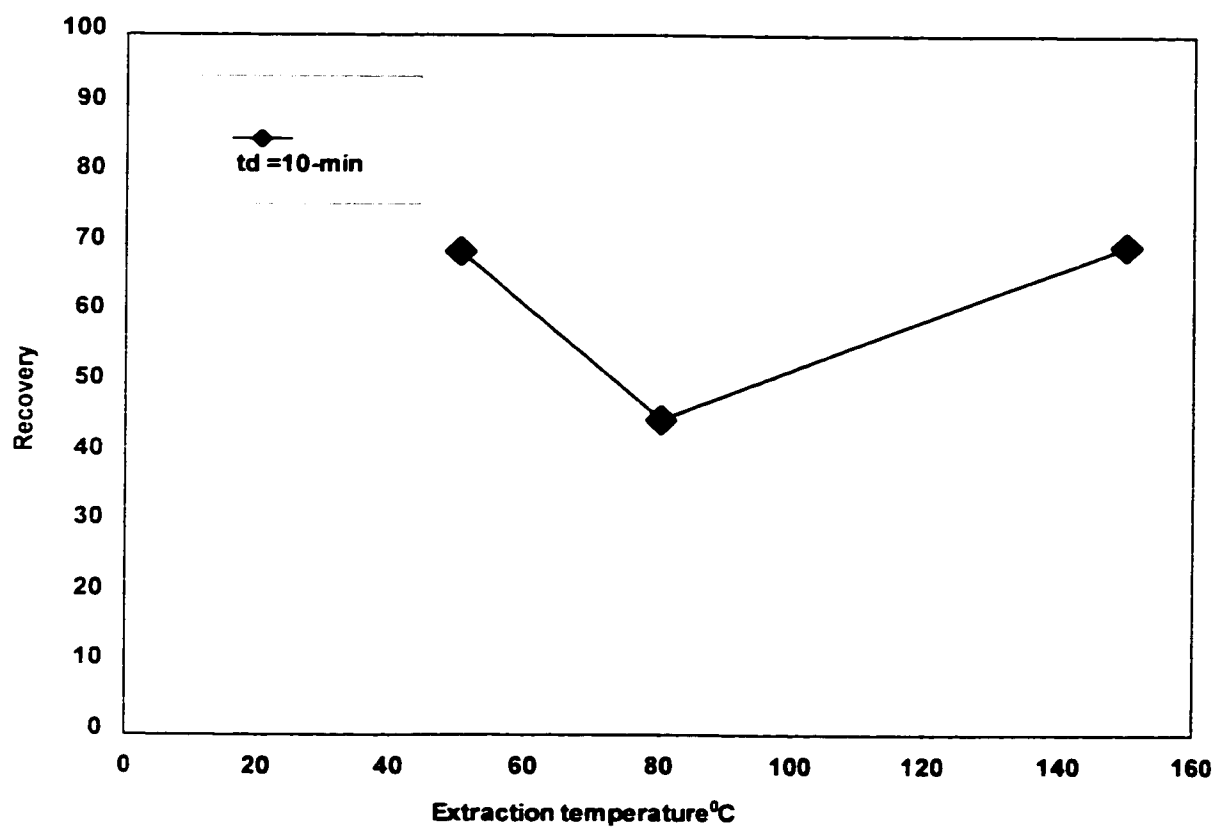


Figure 4.29. Recovery of phenanthrene from specimen S4 (100% fine sand) vs. $T = 50, 80, 150^{\circ}\text{C}$.

Conditions: without modifier, $p = 5000$ psi, $td = 10$ -min.

CHAPTER 5

Modeling of supercritical fluid extraction of phenanthrene from soil

Supercritical fluids have proved to be effective in some extraction of HOCs from soils due to their unique characteristics. They have liquid-like densities, gas-like viscosities, and diffusivities at least an order of magnitude higher than liquids which may result in superior mass-transfer characteristics. Further, the SCF density can be controlled by small changes in temperature and pressure. The desorption of phenanthrene from soil can be described through three consecutive mass-transport steps. They are: intraparticle diffusion from the interior to the outer surface of the particle, mass-transfer of the organic from the outer surface of the particle to the mobile (supercritical fluid) phase and the bulk transport of the phenanthrene in the mobile phase. In addition, the thermodynamic equilibrium of the phenanthrene in the soil to the phenanthrene in the fluid phase seems to play a crucial role in the desorption process.

5.1 Literature survey

Many investigators have employed a simple local equilibrium model, using the Freundlich isotherm and neglecting mass-transfer effects to interpret the regeneration data [54]. The model successfully estimated the amount of carbon dioxide needed to achieve the required extraction, but could not simulate the shape of the desorption profiles accurately. Tan and Liou [55] investigated the desorption of ethyl acetate from activated carbon and proposed a single parameter model assuming linear desorption kinetics to interpret their regeneration data. Recasens [56] modeled the data of Tan by two different parameter models: (1) an equilibrium model where the rate of desorption is controlled by external and intraparticle mass transfer; (2) a kinetic model where the intraparticle mass transfer as well as a first-order irreversible desorption step control the overall process. Later, Srinivasan [57] studied the desorption characteristics of the same system as a function of pressure, temperature,

flow rate, and particle size. They modeled the system based on a well-mixed reactor and first-order reversible desorption kinetic model. Giridhar Madras [58] modeled the desorption of heavy molecular weight organic from soil and activated carbon by supercritical carbon dioxide without the use of any adjustable parameters.

Above-mentioned works does not adequately describe the extraction of phenanthrene from clayey soil. This chapter proves a contribution to model the extraction of HOC from soil by using SFE.

5.2 Model description

Consider a cylindrical packed bed (cartridge) of cylindrical particles. Pure solvent fluid is introduced to the cartridge. Initially the solvent rapidly fills the pores of the particles.

The assumptions of the model are:

- The flow is axially dispersed.
- The system is isothermal during the run.
- The adsorbed and fluid concentrations are in equilibrium at interior sites
- Adsorption represents linear isotherm.

For these conditions mass conservation equations for the adsorbate in the void region, in the pore, and on the particles are described by equation (1), (2), (3) consequently.

$$\varepsilon \frac{\partial C}{\partial t} + u \frac{\partial C}{\partial z} - D_L \frac{\partial^2 C}{\partial z^2} = (1 - \varepsilon) k_m (C - C_a) / L \quad (1)$$

Where:

C = concentration of phenanthrene in bulk fluid, mg/ml

C_a = concentration at the surface of the particle, mg/ml

ε = void fraction

u = superficial velocity in the cartridge, m/s

D_L = axial dispersion coefficient, m²/s

k_m = mass transfer coefficient, m/s.

L = cartridge length, m.

Z = vertical coordinate along the axis of cartridge.

The boundary conditions for this equation are given by Smith, 1981.
[59]:

$$dC/dz = Lu/ D_L (C - C_o) \text{ at } z = 0$$

$$dC/dz = 0 \text{ at } z = L$$

For desorption, the initial condition is given by:

$$C = C_o \text{ when } t = 0 \text{ for all } z$$

$$n\partial C_i/\partial t = D_e(1/r (\partial/\partial r(r\partial C_i/\partial r))) + \rho k_d C_a - \rho k'_a C_i \quad (2)$$

where

C_i = concentration in pores, mg / ml

D_e = effective diffusivity in the porous media, m^2/s

r = radial coordinate from center of particle, m.

n = porosity of media

ρ = density of particles, mg/cm^3 .

k_d = first-order desorption rate constant, $cm^3/mg.s$

k'_a = pseudo first-order adsorption rate constant, $cm^3/mg.s$

C_a = adsorbed concentration, mg / ml.

The boundary conditions for this equation are:

$$dC_i / dr = k_m[C - C_a]/D_e \text{ at } r = r_p$$

$$dC_i / dr = 0 \text{ at } r = 0$$

$$C_i = C_o, \text{ when } t = 0 \text{ for all } r$$

r_p = is the radius of particle

$$dC_a/ dt = k'_a C_i - k_d C_a \quad (3)$$

If the desorption rate is irreversible so that $\rho k'_a C_i$ in Eq. 2 is negligible
and Eq. 3 becomes

$$dC_a/ dt = - k_d C_a \quad (3a)$$

If the adsorbed and fluid concentration are in equilibrium and the pores are fully saturated, the adsorbed concentration on the particle is equal the concentration in the pore and it can be assumed that

$$C_a = C_i \quad (4)$$

5.3 Solution technique

Several methods are available to solve the system, Eq. (1), (2). However, in this study the finite difference method has been used to solve this problem.

In equation (1), C is a function of z and t , the z - t plane can be subdivided into equal

- rectangles of sides $dz = h$, $dt = k$

with co-ordinates (z, t) : $z = ih$, $t = jk$

Where i, j are integers, $C(ih, jk) = C_{ij}$

By using Taylor's theorem:

$$(d^2C/dz^2)_{ij} = (C_{i+1,j} - 2C_{i,j} + C_{i-1,j}) / h^2 \quad (5)$$

$$(dC/dz)_{ij} = (C_{i+1,j} - C_{i-1,j}) / h \quad (6)$$

$$\text{Similarly, } (dC/dt)_{ij} = (C_{i,j+1} - C_{i,j}) / k \quad (7)$$

Eqs. (5), (6), (7) applied finite difference approximation to (1):

$\varepsilon \partial C / \partial t = D_L \partial^2 C / \partial z^2 - u \partial C / \partial z + (C - C_a)(1 - \varepsilon) k_m / L$ becomes

$$(C_{i,j+1} - C_{i,j}) \varepsilon / k = D_L (C_{i+1,j} - 2C_{i,j} + C_{i-1,j}) / h^2 - u (C_{i+1,j} - C_{i-1,j}) / h + ((1 - \varepsilon) k_m / L) C_{i,j+1} - (1 - \varepsilon) k_m / L C_{i,j}$$

The results are shown in Appendix 5 (2.3.4).

Finite difference approximation to Eq.(2)

$$n \partial C_i / \partial t = D_e (1/r) (\partial / \partial r (r \partial C_i / \partial r)) + \rho k_d C_a \quad \text{then}$$

$$n \partial C_i / \partial t = D_e (\partial^2 C_i / \partial r^2) + (D_e / r) \partial C_i / \partial r + \rho k_d C_i$$

By substitute in $dC_a / dt = -k_d C_a$

By using Taylor's theorem:

$$(d^2Ca/dr^2)_{ij}=(C_{i+1,j}-2C_{ij}+ C_{i-1,j}) / h^2 \quad (2a)$$

$$(dCa/dr)_{ij}=(C_{i+1,j}-C_{i-1,j})/h \quad (2b)$$

$$\text{Similarly, } (dCa/dt)_{ij}=(C_{ij+1}-C_{ij})/ k \quad (2c)$$

By substitute Eq. (2a), (2b), (2c) in Eq. (2) :

$$(n / k + \rho / k)Ca_{ij+1} = Ca_{ij} (\rho / k + n / k -2 D_e/h^2) + Ca_{i+1,j} (2 D_e / h^2)$$

The results are shown in Appendix 5 (5).

The value of constant D can be found from the Stokes-Einstein equation [60]:

$$D_m=KT/6\pi\mu R' \quad (8)$$

Where:

R' = is the radius of the solute molecule

K = is the Boltzmann constant, $1.38 \cdot 10^{-23}$ joule/ $^{\circ}K=1.38 \cdot 10^{-23}$ kg.m²/s². $^{\circ}K$

μ = is the solvent viscosity

T = the temperature of the system

The value of the solvent viscosity [61]

$$\mu = \mu_r \mu_c \quad (8a)$$

where

μ_r = is the critical viscosity

μ_c = is the reduced viscosity

$$\mu_c = 7.70 M^{0.5} p_c^{0.66} T_c^{-0.166} \quad [61] \quad (8b)$$

where

p_c = is the critical pressure (atm.)

T_c = is the critical temperature ($^{\circ}K$)

M = molecular weight of carbon dioxide

μ_r = is the viscosity of the solvent (CO_2) (micropoises = 10^6 g /cm. sec.)

μ_r can be obtained from the chart [x]

The value of the void fraction [4] can be calculated from

$$\epsilon = (V / V_s) - 1 \quad (9)$$

where:

V per gram = the total volume.

V_s per gram= the volume of the particle.

To find the value of porosity, n:

$$n = \epsilon / (1 + \epsilon) \quad (10)$$

To calculate D_e which is pore diffusivity in the particle [59].

$$D_e = (n / \tau_p) D_m \quad (11)$$

where

τ_p = is the tortuosity factor .

The density of the solvent can be found from

$$\rho = \rho_{ccO_2} \quad (12)$$

where:

ρ_{ccO_2} = is the critical density of the carbon dioxide = 0.47gcm⁻³

The mass transfer coefficient can be estimated using the Wakao and Kaguei empirical correlation equation [62]

$$r_p k_m / D_e = 2 + 1.1 (\mu / \rho D_m)^{0.3} (5 r_p u \rho / \mu)^{0.6} \quad (13)$$

where

r_p = is the particle radius, m.

D_e = is the effective diffusion coefficient, m²/s.

μ = is the solvent viscosity.

ρ = is the solvent density kg/m³.

u = is the solvent velocity, m/s.

D_m is the molecular diffusion coefficient, m²/s

k_m = is the mass transfer coefficient.

The axial dispersion coefficient (D_L) in supercritical carbon dioxide were measured by Tan and Liou [63]. They proposed an empirical correlation involving nondimensionless groups. Correlation based on dimensionless groups such as:

$$r_p u / D_L = 0.817 (2 r_p u \rho / \mu)^{0.265} (\mu / \rho D_m)^{-0.919} \quad (14)$$

The calculation of phenanthrene solubility in the solvent by using the following equation [64]:

$$Y_2 = P_i^{sat}(T) \exp[(p - P_i^{sat})v_i^{os} / RT] / p\phi_2^v \quad (15)$$

where:

P_i^{sat} = is the vapor pressure, kPa .

ϕ_1^v = is the fugacity at vapor pressure kPa

ϕ_2^v = is the fugacity at the pressure of the system kPa.

p = is the pressure of the system kPa.

v_i^{os} = is the molal volume, $m^3/kg - m^3$

R = ideal gas constant

T = is the temperature of the system, °K

The vapor pressure can be calculated by using the following equation [65]

$$\text{Log } P_i = A - B / (T+C) \quad (16)$$

where T is the temperature, and A , B , C constants characteristic of the substances

5.4 Verification of the model

Verification of the model base of the data from experimental phase. Three cases were verified, for this purpose the program in computer language c was developed (Appendix 5.1)

5.4.1 Case1- SFE extraction over $t_d = 30\text{min}$

First case was related to extraction over $t_d = 30\text{ min}$ under the pressure 8000 psi, and extraction temperature 150 °C

- rectangles of sides $dz = h = 0.255\text{ cm}$, $dt = k = 0.025$

- co-ordinates (z,t) :

$z = ih$, $t = jk$

Where i, j are integers, $C(ih, jk) = C_{ij}$

By using Taylor's theorem:

$$(d^2C/dz^2)_{ij} = (C_{i+1,j} - 2C_{ij} + C_{i-1,j}) / h^2 \quad (5)$$

$$(dC/dz)_{ij} = (C_{i+1,j} - C_{i-1,j}) / h \quad (6)$$

$$\text{Similarly, } (dC/dt)_{ij} = (C_{ij+1} - C_{ij}) / k$$

The constants (D_L , ϵ , n , D_e , ρ , μ , k_m) were calculated as follows

Equation (8b) can be determined the viscosity of carbon dioxide

$$\mu_c = 7.70 (44)^{0.5} (73.3)^{0.66} (305)^{-0.16}$$

From the chart at $p_r = p / p_c = 0.542 / 73 = 0.01$, $T_r = T / T_c = 423 / 305 = 1.38$

Then μ_r is 0.58

$$\mu = 0.58 \cdot 343.87 \cdot 10^{-6} = 1.99 \cdot 10^{-4} \text{ g / cm. sec (Eq. 8a)}$$

Equation (8) regards the solute molecule (phenanthrene) as moving in a continuum of solvent (carbon dioxide).

$$\begin{aligned} D_m &= 1.38 \cdot 10^{-23} \cdot (150 + 273) / (6 \cdot \pi \cdot 1.99 \cdot 10^{-5} \cdot 2.6 \cdot 10^{-8}) \\ &= 5.98 \cdot 10^{-10} \text{ m}^2/\text{s} \end{aligned}$$

The value of void fraction can be obtained from Eq. (9)

$$V = 10.0 \text{ cm}^3, V_s = 5.75 \text{ cm}^3.$$

Where the particle density = 0.4 g/cm^3

The mass of the particle = 2.3 g

$$\epsilon = 0.74$$

The porosity from Eq. (10)

$$n = 0.42$$

The tortuosity factor of porous medium is in the range from 2 to 8. For Eq. (11), it was held constant at a value of 2 in case 1.

$$D_e = (0.42 / 2) \cdot 5.98 \cdot 10^{-10} = 1.25 \cdot 10^{-10} \text{ m}^2/\text{s}$$

The value of mass transfer coefficient was obtained from Eq. (13).

$$k_m = 0.097 \text{ m / s}$$

The value of axial dispersion coefficient was obtained from Eq. (14)

$$D_L = 1.5 \cdot 10^{-6} \text{ m}^2/\text{s}$$

The results of the calculation of case 1 are presented in Appendix 5.2

5.4.2 Case2- SFE extraction over $t_d = 20$ min

Case 2 was related to extraction of phenanthrene over $t_d = 20$ min under the pressure 8000 psi, and extraction temperature 150 °C.

The following data are applied to case 2.

- rectangles of sides $dz = h = 0.255$ cm, $dt = k = 0.016$

The constants (D_L , ϵ , n , D_e , ρ , k_m) are calculated in section 5.3.1.

The results of the verification of case 2 in Appendix 5.3

5.4.3 Case3- SFE extraction over $t_d = 10$ min

Case 3 was related to extraction over $t_d = 10$ min under the pressure 8000 psi, and extraction temperature 150 °C

- rectangles of sides $dz = h = 0.255$ cm, $dt = k = 0.0082$

The constants (D_L , ϵ , n , D_e , ρ , k_m) are calculated in section 5.3.1.

The results of the verification of case 3 in Appendix 5.4

The consequently between results and results from the model comparison have been performed and efficiency of the recovery under the extraction of the phenanthrene in effluent was done, as shown in Figure1.1. Table 5.1 demonstrates the comparison between experimental results and modeling results.

Table 5.1. Comparison between experimental results and modeling.

Concentration after SFE extraction and concentration from the model
at $p = 8000$ psi, $T = 150$ °C in 10, 20 and 30 min.

Dynamic time Of extraction (min)	{a} Concentration After SFE extraction (mg/ml)	(b) Concentration from the model (mg/ml)	Divergence $ a - b / b$
10	0.1	0.77	0.87
20	1.43	1.14	0.25
30	1.64	1.72	0.046

Supplementary calculations have been done to estimate the effect of particle size on the axial dispersion, diffusivity and mass transfer coefficients, as shown in Table 5.2, The axial dispersion, effective diffusivity and mass transfer coefficient have been calculated from the model.

Table 5.2. The effect of the particle size on D_L , D_e and k_m .

r_p (particle radius) (m)	D_L (axial dispersion) (m^2/s)	k_m (mass transfer coefficient) (m/s)
$1.2 \cdot 10^{-6}$	$1.5 \cdot 10^{-6}$	0.097
$0.5 \cdot 10^{-6}$	$7.5 \cdot 10^{-7}$	0.159
$2 \cdot 10^{-9}$	$4 \cdot 10^{-7}$	0.282

5.5 Solubility

Solubility of phenanthrene in carbon dioxide is influenced by the temperature and the pressure. It requires verification. The verification is performed to achieve the extraction conditions: such as $T = 150$ °K, $p = 8000$ psi and dynamic extraction time, $t_d = 30$ min.

To calculate the vapor pressure:

- The following constants are applied for phenanthrene [66]:

$$A = 7.47774, B = 2581.568, C = 223.199$$

The vapor pressure at $T = (150 + 273) = 423 \text{ }^{\circ}\text{K}$

By substitute in Eq. (16), then

$$\log P_i = 3.4827, P_i = 3.038 \text{ kPa}$$

- The molal volume, v ($\text{C}_{14}\text{H}_{10}$)

$$\text{For } C = 14 \times 14.8 = 207.2, H = 3.7 \times 10 = 37$$

$$v(\text{C}_{14}\text{H}_{10}) = 37 + 207.2 = 244.2 \text{ cm}^3 / \text{g} = 0.244 \text{ m}^3 / \text{kg}$$

- For phenanthrene: critical temperature = $869.25 \text{ }^{\circ}\text{K}$

$$\text{Critical pressure} = 2900 \text{ kPa}$$

The pressure of the system is $8000 \text{ psi} = 55.120 \text{ kPa}$

$$Pr = 55.120 / 2900 = 0.019$$

$$Tr = 423 / 869.25 = 0.4866$$

- From the [67]: $\phi_2^v / p = 0.008$ then $\phi_2^v = 0.008 \times 55.120 = 0.440 \text{ kPa}$

The fugacity of phenanthrene at the vapor pressure

$$Pr = 3.038 / 2900 = 0.001$$

$$Tr = 423 / 869.25 = 0.4866$$

- From the [67]: $\phi_i^v / p = 0.0005$ then $\phi_i^v = 0.0005 \times 3.038 = 0.0015 \text{ kPa}$

- By substitute in Eq. (15),

The solubility $Y_2 = 1.9 \times 10^{-4}$ was obtained.

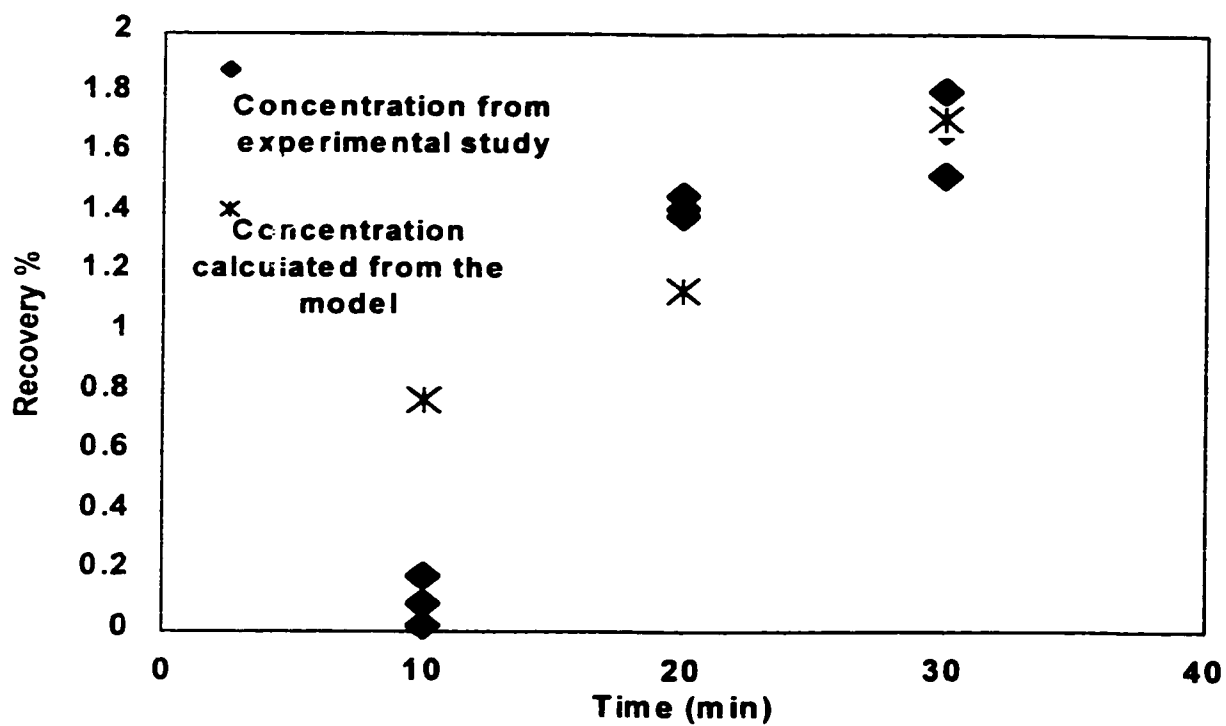


Figure 5.1. Concentrations of phenanthrene in effluent obtained from the model and from the experimental.

Conditions: specimen S4, $p = 8000$ psi (55158.4 kPa), $T = 150$ °C in $t_d = 10$, 20 and 30 min.

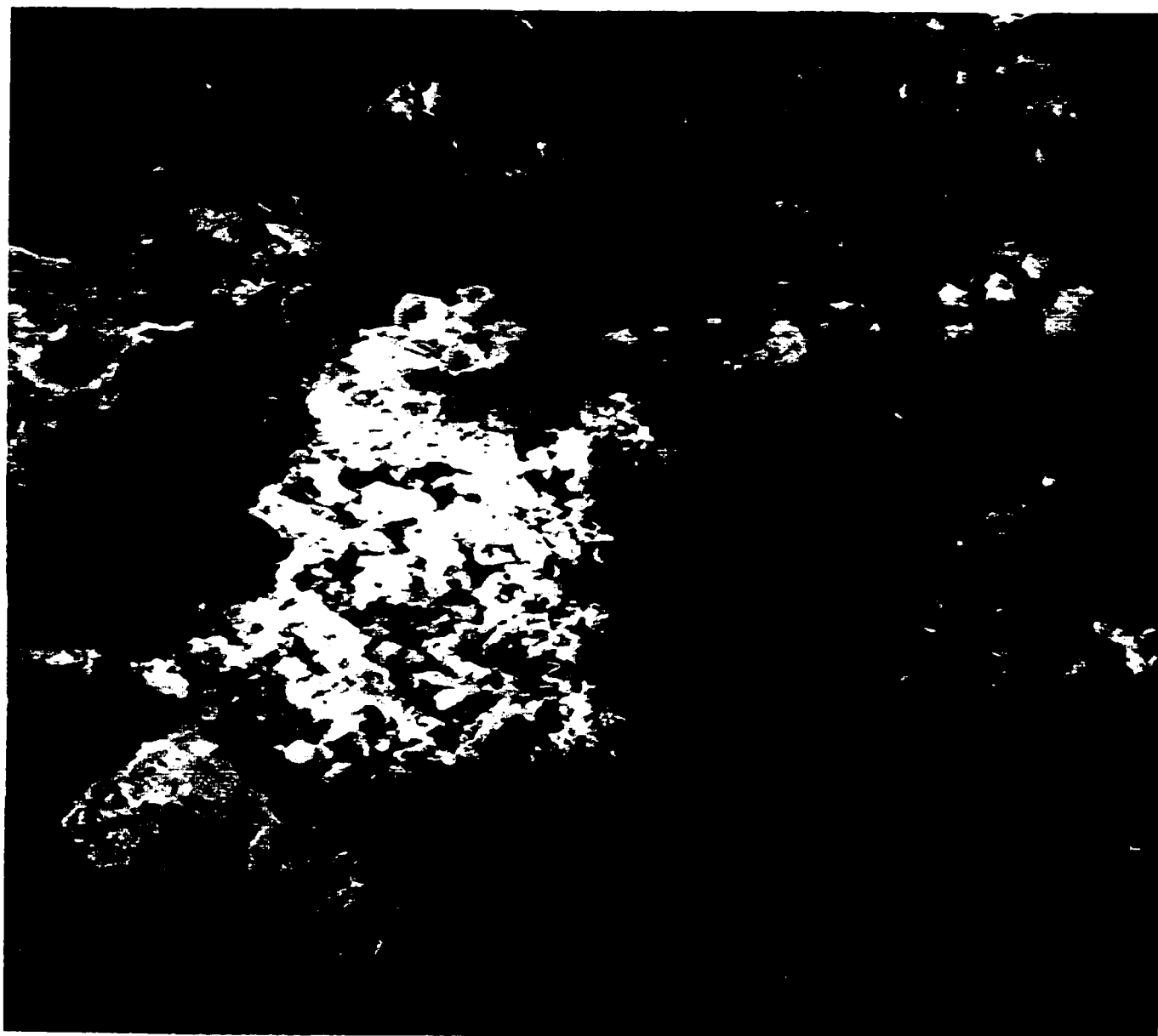


Figure 5.2. A micrograph of non-contaminated illite.

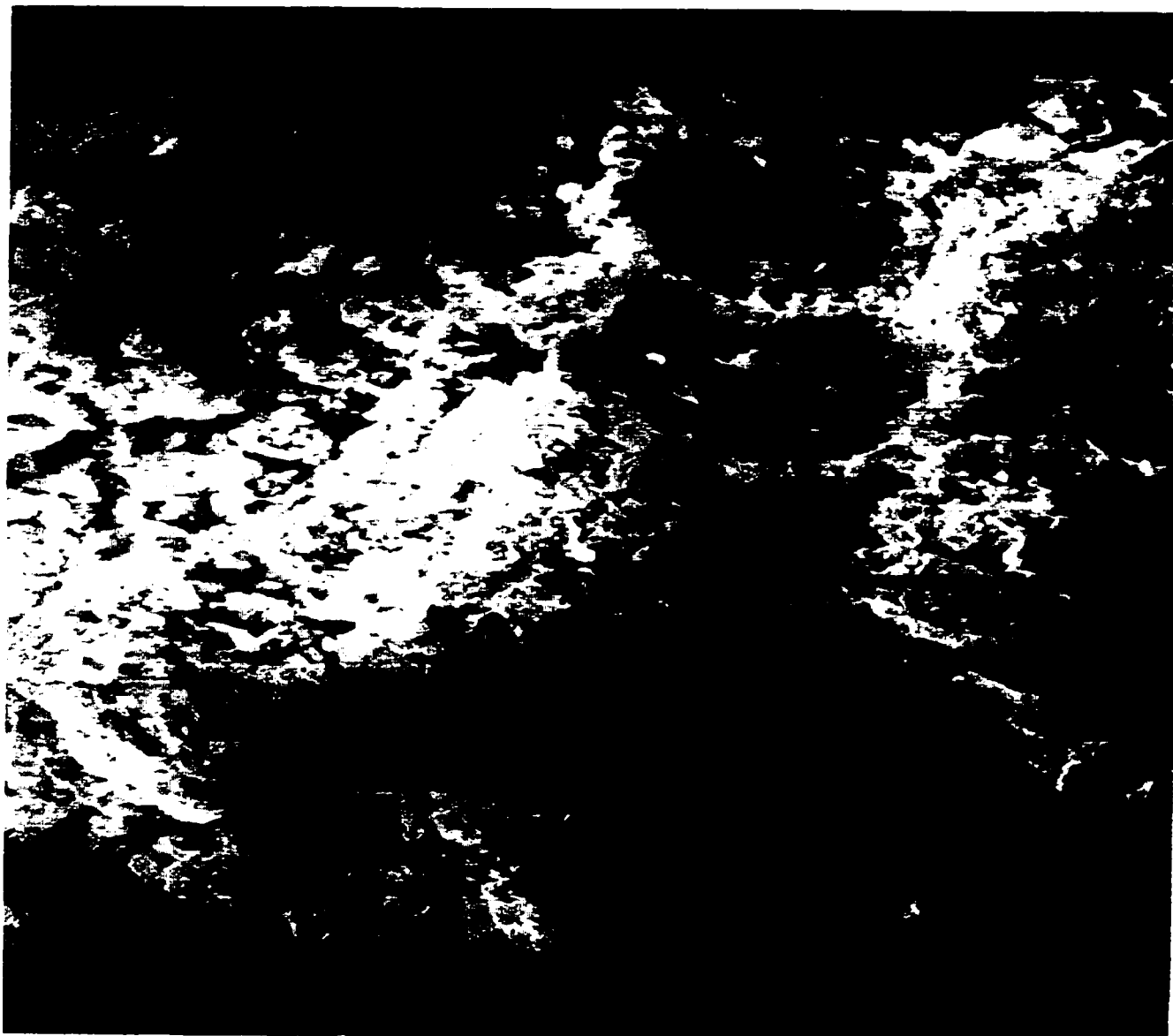


Figure 5.3. A micrograph of contaminated illite with phenanthrene.

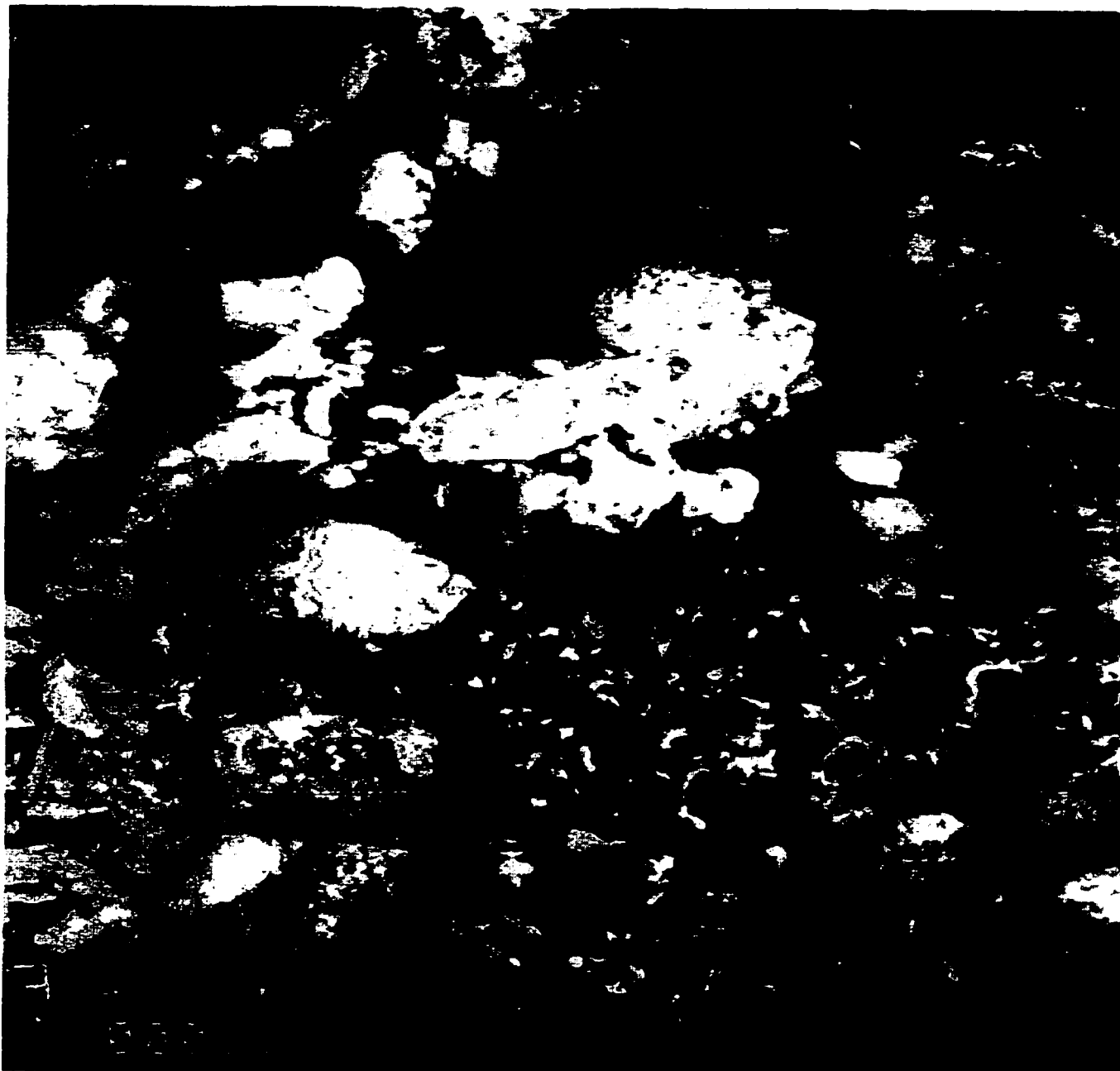


Figure 5.4 A micrograph of illite after extraction at high temperature ($T = 150$ °C), high pressure (8000 psi), with modifier 5% (mol) methanol for $t_d = 30$ min.

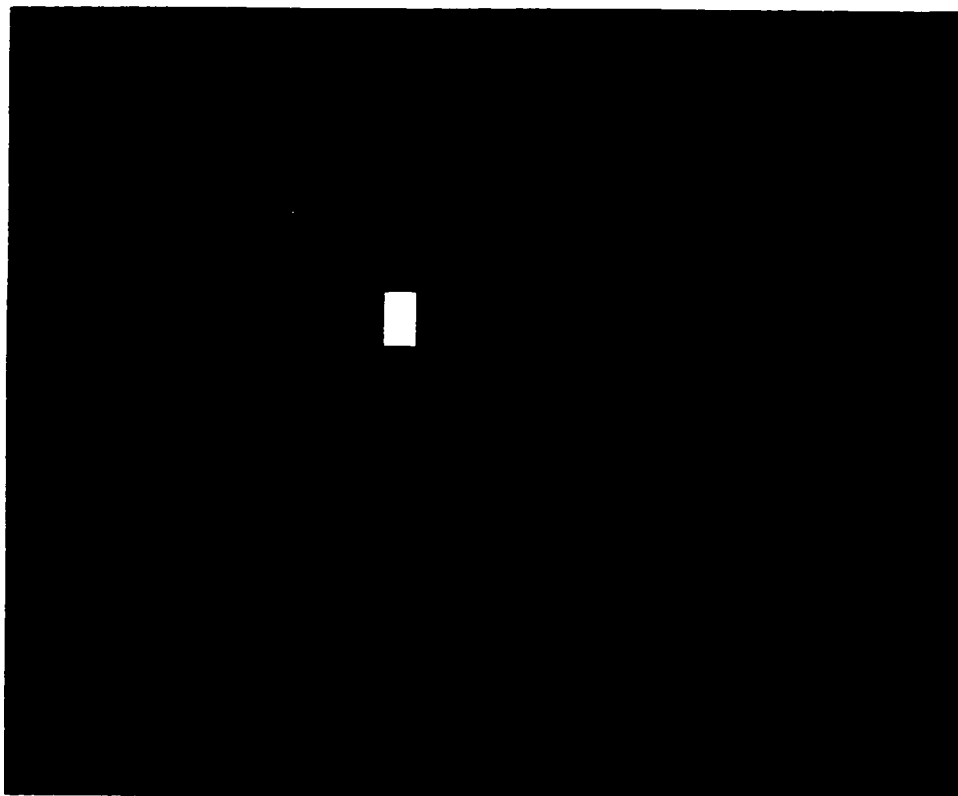


Figure 5.4a. Image of contaminated illite with phenanthrene after extraction using (SFE) at $p = 8000$ psi (55120Kpa) and $T = 150$ °C for $t_d = 30$ min.

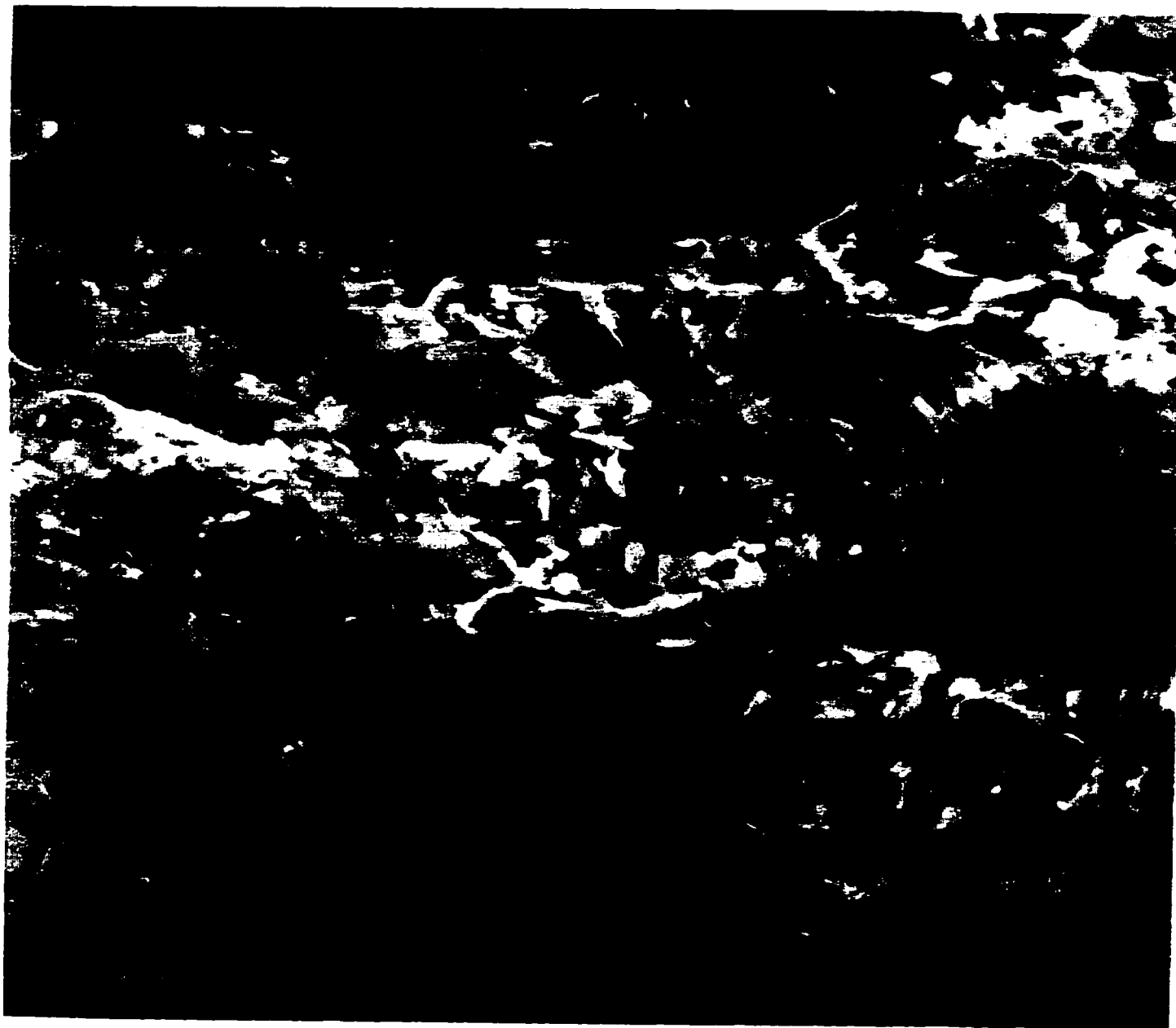


Figure 5.5 A micrograph of illite under temperature (50 °C), pressure (5000 psi) by supercritical fluid extraction for $t_s : t_d = 15 : 15$ min.



Figure 5.6 A micrograph of an extracted illite under temperature (50 °C), pressure (8000 psi) by supercritical fluid extraction for $t_s : t_d = 15 : 15$ min.

CHAPTER 6

Discussion

Discussion of the effect of SFE technological parameters on the removal efficiencies

6.1 Introduction

Supercritical fluid extraction is a technique that employs a fluid phase having intermediate properties between a gas and liquid, to effect the solubilization of solutes. The advantages that can be gained by employing SFE are related to the unique physical properties that these fluids possess. Compared to liquid solvents, supercritical fluids have lower viscosities and higher diffusivities, thus allowing more efficient mass transfer of solutes from sample matrices [supercritical fluid extraction]. Another advantage of supercritical fluids is that their solvent power can be adjusted through mechanical compression of the extraction fluid. This feature not only permits selective extraction to be accomplished but also allows the concentration of analytes after extraction, free from any contaminating solvent. These advantages could be effectively applied to the extraction of HOC from soil matrix. There are several parameters, which are of key importance in conducting an extraction by SFE. These are 1) the pressure, 2) the temperature, 3) the extraction time, 4) the physical and chemical properties of the solutes that are to be extracted etc. The operation in this work is unsteady state, the characteristic of unsteady-state that the concentration at any point in the cartridge change with the time. This may result from changes in concentrations, flowrate, or conditions of temperature and pressure. In addition, the changes are influenced by soil matrix. The analysis of an accurate extraction rate is based in recognition the effect of all factors in phenomena taking place in the cartridge during the extraction process.

6.2 Physical matrix effects

The morphology of the illite undergoing SFE can have a pronounced influence on the efficiency of the extraction and the rate at which it is desorbed of different specimens. Displacement of fine clay particle versus the coarse sand particle takes place in different extent consequently the variation of pressure affected in different soil matrix represented by specimens (S1 to S4). The micrograph of clay material demonstrated the sensitivity of displacement to all technological parameters of SFE mainly (temperature, pressure, time). The experimental studies demonstrated that the initial condition in which soil was contaminated (e.g. moisture content) influence on soil behavior during extraction process. The calcium content in clay material provoke the formation of calcium carbonate in the presence of water (moisture) and carbon dioxide. A micrograph (Figure 5.4) showed the formation of calcium carbonate crystals. Extraction from soil containing high fraction of clay material represents the highest challenge for analytical work. Dry clay soil is more appropriate to extract than clay soil contains water because water can affect the mechanical performance of SFE by causing restrictor plugging, can also affect the extraction process itself.

In general, as small as the particle size of the matrix, more rapid and the extraction will be completed. This effect is largely due to the shorter internal diffusional path lengths over which the extracted phenanthrene must travel to reach the bulk fluid carbon dioxide phase. An increase in illite porosity will generally promote a more efficient and rapid SFE, as shown in a micrograph (Figure 5.2) illite without contaminant. A micrograph of the contaminated illite of phenanthrene without extraction shows a different texture (Figure 5.3).

6.3 Properties of supercritical fluid carbon dioxide

Carbon dioxide is unique among the supercritical fluids. Its critical temperature of 31 °C is close to room temperature, thereby permitting extractions to be carried out at low temperatures on thermally labile compounds. Modest

compression of CO₂ produces a substantial change in its fluid density due to the high non-ideality exhibited by this fluid.

6.4 The use of Modifier in SFE

Since CO₂ is relatively non-polar, a few percent of a polar modifier. The most common use modifier for SFE propose is methanol. The use of methanol in the amount of 5% improved extraction efficiency around 72% at temperature 150 °C and pressure 8000 psi in $t_d = 30$ min. It was concluded, that the most accurate and reproducible method of modifier addition is to use a separate modifier pump. Modifier affects on the desorption isotherm; since methanol is a poorer solvent for PAHs compared to carbon dioxide. The accurate concentration seems to be close to 5%, the highest concentration can make the extraction fluid too polar for the PAHs [35]. Methanol is often added to increase the ability of the supercritical fluid to better displace phenanthrene from matrix.

6.5 Temperature effect on SFE efficiency

The increased recoveries of the high-temperature were observed in all experiments. This phenomena could be caused by two factors: at first, high temperature can result in higher vapor pressure of the analyte, phenanthrene, thus increasing the phenanthrene solubility despite the decrease in the density of CO₂ at high temperatures (150 °C); second, a certain amount of energy is required to desorb phenanthrene from the matrix experimentally from illite. Increase the extraction temperature can provide more energy to the extraction system, greatly increasing the rate of the desorption process at high temperatures [68]. The lower temperature such as 50 °C or 80 °C did not significantly affect the extraction efficiency, for almost all cases. When the temperature changes from subcritical to supercritical, the physical properties of the solvent such as density and viscosity change significantly. The temperature may affect the diffusion as well as the

mass-transfer behavior. The extraction at high temperature changed the pores voids and increased contact areas within carbon dioxide.

The image analysis done for illite specimens demonstrated differences in voids of soil subjects to the extraction in different temperatures (Figure, 5.4, 5.4a).

6.6 Pressure effects on SFE efficiencies

It was observed that increase pressure (up to 8000 psi) the recovery of phenanthrene is increased. This can be explained by the increase in solvating power of the carbon dioxide caused by higher density. However, the increase density decreases the diffusion coefficient [69]. This decrease of the diffusion coefficient can cause lower recoveries as a result of the kinetics of the extraction process. Hence, the diffusion coefficient also depends on the extraction temperature.

6.7 Effect of the time

While high recoveries were obtained in 30 min dynamic extraction, static (no-flow) / dynamic (flowing) procedure which was suggested by the company yielded lower recoveries of phenanthrene. If the extraction rates are limited by solubility, the 30-min dynamic extraction should yield substantially higher recovery [68]. However, in short time $t_d = 10$ min, it seems that the carbon dioxide has not chance to interfacial contact with a contaminant distributed in the clay particle surface.

6.8 Collection solvent

The collection solvent greatly influences the extraction result sensitivity. If the analyte trapping is insufficient, one can easily get the impression that the extraction is incomplete. Hexane was the only trapping solvent used in this research. The volume of trapping solvent is important because the transition time of the CO₂ bubbles is dependent on the solvent volume. The volume of hexane was 7 - 10 mL. Poor trapping in the solvent was obtained using less than 7 mL or more than 10 mL.

6.9 Effect of diffusion and dispersion phenomena

Diffusion belongs to the main factors influencing on the extraction efficiency. The axial dispersion (D_L) is the spreading of the residence time in unidirectional flow owing to the departure from flow, the fluid particles move forward but at different speeds. The transport of solute (phenanthrene) by these mechanisms is usually described in terms of eddy diffusivity.

The particle radius, the viscosity and the temperature are the most important parameters affect on the diffusivity. As shown from Table 5.2, when the particle size decrease the axial dispersion decrease.

The molecular diffusion (D_m) concerns the movement of individual molecules through a matrix by virtue of their thermal energy. In the case of kinetic theory, a molecule is assumed to travel in a straight line; at a uniform velocity until it collides with another molecule, whereupon its velocity changes both in magnitude and direction. The average distance the molecule travels between collisions is its mean free path, and the average velocity is dependent upon the temperature. The phenomenon of molecular diffusion ultimately leads to a completely uniform concentration of substance, which may initially have been nonuniform [70]

Effective diffusivity is based on a unit of total area (void plus nonvoid) perpendicular to the direction of molecular diffusivity (D_m). It is somewhat limited because of tortuosity factor of the porous medium, which varies from 2 to 8 for soil. The tortuosity is defined as the ratio of the actual path length taken by a solute in a porous medium, over the straight-line distance. In this work, it is determined from the Figures 5.4, 5.5, 5.6 at different extraction conditions at pressure = 8000 psi was applied, temperature = 150 °C in 30 min, the tortuosity factor = 2, while at pressure = 5000 psi, temperature = 50 °C in 15 min static/15 min dynamic, the tortuosity = 4.

6.10 Effect of mass transfer

The fluid motion is related to diffusion and mass transfer coefficient. The mass -transfer coefficient regulates the rate at which equilibrium is approached, it influences the time required for extraction as well as the size of the particle. The assumption of an irreversible reaction used in the model indicates that intraparticle diffusion does not affect the extraction process. The external mass transfer coefficient was estimated from the correlation equation [62]. The particle size affects the mass transfer coefficient, when the particle size decrease the mass transfer coefficient increase.

6.11 Effect of solubility

The rate of removal of a phenanthrene from illite using a SFE is a function of its solubility in the fluid (carbon dioxide) media and the rate of mass transport of the phenanthrene in soil voids. Rate limiting kinetics can adversely impact on the rapid extraction of the phenanthrene despite favorable its solubility characteristics in the supecritical fluid cartridge.

Slight changes in the system temperature or pressure can cause large changes in the solvent density and consequently in its ability to solubilize the solute. The vapor pressure is the most important indicator of solubility. The

correlation which has been used to calculate the solubility of phenanthrene in carbon dioxide is shown in chapter 6.

6.12 Effect of equipment dimensions on extraction efficiency

From the modeling results, the extraction efficiency increases in the axial direction as time increases.

6.13 Sensitivity of the model

A part of the work related to the prediction of the extraction efficiency was done based on the computer programming. The matrix 20×20 was used for those calculations. It was found that the accuracy of results obtained from the program change less than 5% if the matrix will increase to 100×100 or decrease to 5×5 .

As shown in Figure 5.1 the results obtained from experimental data and the model are in good agreement for the dynamic time 20 and 30 min whilst some deviation can be noticed for $t_d = 10$ min.

The model can be used for different types of HOC as well as contaminants like metals in porous media.

Chapter 7

Conclusion and Recommendation

- The illite (clay texture) and the physical properties such as particle size and porosity play the main role in extraction efficiencies.
- Dry clayey soil is more appropriate for extraction than clayey soil with water content.
- Phenanthrene extractions from soil showed that increases the temperature up to 150 °C, and the pressure of the system up to 55 kPa increase the efficiency removal of phenanthrene from the soil up to 72%.
- For soil specimen like illite, better results were achieved with modifier content of 5% (mol) methanol. The combination of modifier and elevated temperature and the pressure is effective.
- The modifier can affect both the desorption isotherm and diffusional - dispersion in pores.
- The extraction efficiencies increased as the time of extraction (dynamic) increased over 30 min at high temperature and pressure for clay material.
- The SCF-PAH model, that best fits the experimental data for the desorption of phenanthrene from illite by using supercritical carbon dioxide
- The results which have been calculated from the model showed that the increase in mass transfer coefficient, when the particle size decrease.
- The viscosity of the solvent which has been affected by the temperature and pressure of the system, particle size, and the velocity of the solvent are the main parameters, which affect on the axial dispersion coefficient
- The results from the model demonstrates that the axial dispersion increase when the particle size increase.
- The tortuosity factor limits the effective diffusivity.
- The results from this work show, that most soil extractions are not limited by solubility of the solute in SCF, but by the soil and contaminant properties.
- The adsorption concentration is constant in the coordinate of the particle radius.
- Extraction efficiency increases in axial direction with time increase.

- The results obtained from the model shows the effect of temperature and the pressure in the solubility of phenanthrene in supercritical carbon dioxide.
- The vapor pressure of phenanthrene, which has been calculated in the model play the most important indicator of solubility of phenanthrene in the solvent.
- SFE for environmental specimen preparation has undergone a very rapid growth supported by the need to perform more rapid and selective extractions.
- The SFE parameters determined in this work with spiked specimens have been shown to be effective starting conditions for real world samples.

This study indicates that, it is recommended to use:

- Different flowrates of carbon dioxide.
- Different types of trapped solvent.
- The use of combination of a modifier and static time.
- Perform investigation, using SFE for soil remediation purposes.

REFERENCES

- 1 EPA Seminar Publication, Cincinnati, OH 45268 and Robert S. Kerr, Transport and Fate of Contaminants in the Subsurface Center for Environmental Research Information. Environmental Research Laboratory.
- 2 Maria Electrowicv, lin ju, 1997, accuracy of PAH's extraction from sensitive clays using in the SFE ISCO system, CSCE/ASCE, Environmental Engineering Conference., 531-572.
- 3 R.N.Yong, A.M.O.Mohamed and B.P, 1992, Principles of Contaminant Transport in Soils.
- 4 Bailey, G. W. and J. L. White, 1964, Soil Pesticide Relationships: Review of Adsorption and Desorption of Organic Pesticides by Soil Colloids, With Implications Concerning Pesticide Bioactivity. J. Agric. Food Chem. 12:324-332.
- 5 Pouchly, J. and E. Erdos, 1958, Kinetic Der Adsorption aus Losungen. I. Gleichzeitiger Einfluss Der Inneren and Ausseren Diffusion. Coll. Czech. Chem. Comm. 23:1706-1719.
- 6 Kiselev, A. V, 1965, Non-Specific and Specific Interactions of Molecules of Different Electronic Structures with Solid Surfaces. Discuss. Faraday Soc. 40:205-218.
- 7 Brownman, M. G. and G. Chesters, 1975, The solid-water Interface. Pre-print Papers, Am. Chem. Soc., Div. Environ. Chem. 15:10-13.
- 8 Singhal, J. P. and C. P. Singh, 1974, Adsorption of 1,2-Dibromo-3-Chloropropane on Alkali Bentonite. J. Indian Soc. Soil Sci. 22:226-230.
- 9 Greenland, D. J., R. H. Laby and J. P. Quirk, 1965, Adsorption of Amino Acids and Peptides by Montmorillonite and Illite. I. Cation Exchange and Proton Transfer. Trans. Faraday Soc. 61:2013-2023.
- 10 Hadzi, D., C. Klotz and S. Oblak, 1968, Hydrogen Bonding in Some Adducts of Oxygen Bases with Acids. Part IV. Basicity in Hydrogen Bonding and in Ionization. J. Chem. Soc., A. pp. 905-908.

- 11 Hammaker, J. W. and J. M. Thomson, 1972, Adsorption. In C. A. I. Goring and J. W. Hammaker (ed.). Organic Chemicals in the Soil Environment. 1:49-143. Marcel Dekker, New York.
- 12 Kohi, R. A. and S. A. Taylor, 1961, Hydrogen Bonding between the Carbonyl Group and Wyoming Bentonite. Soil Sci. 91:223-227.
- 13 Abernathy, J. R. and L. M. Wax, 1973, Bentazon Mobility and Adsorption in Twelve Illinois Soils. Weed Sci. 21:224-227.
- 14 Theng, B. K. G., 1976, Interactions between Montmorillonite and Fulvic Acid. Geoderma 15:243-251.
- 15 Baker, B. R., 1967, Design of Active-Site-Directed Irreversible Enzyme Inhibitors: The Organic Chemistry of Enzymic Active Site. Ch. 2. Wiley, New York.
- 16 Theng, B. K. G., D. J. Greenland and J. P. Quirk, 1967, Adsorption of alkylammonium cations by Montmorillonite. Clay Miner. 7:1-17.
- 17 Mortland, M. M. 1975, Clay-Organic Complexes and Interaction: Aromatic Molecules. In F. Coulston and F. Korte (ed). Pesticides. Environ. Qty. Saf. Suppl. 3:226-229.
- 18 Mott, C. B. 1970, Sorption of Anions by Soils. In Sorption and Transport Process in Soil. Soc. Chem. Ind. Monograph 37:40-53. London.
- 19 Wayaman, C. H. 1963, Surfactant Sorption on Heteroionic Clay Minerals. In Proc. Int. Clay Conf. 1:329-342. I. T. Rosenquist and P. Graff-Petersen (ed.). Stockholm, Sweden.
- 20 Adamson, A. W. 1967, Physical Chemistry of Surfaces. Ch. 14. Interscience, New York.
- 21 Singhal, J. P. and C. P. Singh. 1976, Adsorption and Interaction of 1,2-dibromo-3-chloropropane. Part II. With illites. J. Indian Chem. Soc. 53:251-254.
- 22 Mithyantha, M. S., K. B. Rao, C. C. Biddappa, N. T. Lillaram and N. G. Perur. 1975, Paraquat Adsorption and Clay Minerals. Bull. Indian Natl. Sci. Acad. 50:293-298.
- 23 Kown, B. T. and B. B. Ewing. 1969, Effect of the Organic Adsorption on Clay ion Exchange Property. Soil Sci. 108:321-325.
- 24 Grim, R. E. 1968, Clay Mineralogy. McGraw Hill, New York.

- 25 Wheatley, G. A. and J. A. Hardman. 1968, Organochlorine Insecticide Residues in Earthworms from Arable Soils. *J. Sci. Food Agric.* 19:219.
- 26 Bollen, Witt B., J. E. Roberts and H.E. Morrison. 1958, Soil Properties and Factors Influencing Aldrin- Dieldrin Recovery and Transformation. *J. Econ. Ent.* 51:214-219.
- 27 Mortland, M. M. 1975, Clay-Organic Complexes and Interaction: Aromatic Molecules. In F. Coulston and F. Korte (ed.). *Pesticides. Environ. Qty. Saf. Suppl.* 3:226-229.
- 28 Eltantawy, I. M. and P. W. Arnold. 1972, Adsorption of n-alkanes by Wyoming Montmorillonite. *Nature Phys. Sci.* 237: 123-125.
- 29 Ministry of the environment.
- 30 Ronald G. Harvey, 1997, Polycyclic aromatic hydrocarbons
- 31 Sally E. Eckert-Tilotta, Steven B. Hawthorne and David J. Miller. University of North Dakota, 1992, Supercritical Fluid Extraction with Carbon Dioxide for the Determination of Total Petroleum Hydrocarbons in Soil.
- 32 Michael D. La Grega, Phillip L. Buckingham, Jeffrey C. Evans, 1994, Hazardous Waste Management.
- 33 Bernd Wenclawrak, university-GH Siegen, 1992, Analysis with Supercritical Fluids Extraction and Chromatography.
- 34 John J. Langenfeld, Steven B. Hawthorne, David J. Miller. Department of Chemistry, University of Waterloo, Ontario, 1993, Effects of Temperature and Pressure on Supercritical Fluid Extraction Efficiencies of Polycyclic Aromatic Hydrocarbons and Polychlorinated Biphenyls.
- 35 Susanne Reindl and Frank Hofler, Am Wortzgaten, Germany, 1994, Optimization of the Parameters in Supercritical Fluid Extraction of Polynuclear Aromatic Hydrocarbons from Soil Samples.
- 36 Barde. K. D. Cufford. A. A.. Jatar. S. A. and Shttsrone. G. F. 1991, *J Phys. Chem. Ref. Data*, 20. 713.
- 37 Burford. M. D. Hawthorne. S. B. Milier. D. J. and Braggins, T. J. 1992, *J. Chromatog.* 609,321.
- 38 S.B. Hawthorne, 1990, *Anal. Chem.*, 62, 33A.

- 39 D.E.Raynie, 1993, *Anal. Chem.*, 65, 3127.
- 40 J.M. Levy, E. Storozynsky and R.M. Ravey, 1991, *J. High Resolut. Chromatogr.* 14, 661.
- 41 S.B. Hawthorne, J.J. Langenfeld, D.J. Miller and M.D. Burford, 1992 *Anal. Chem.*, 64,1614.
- 42 G. Klink, A. Buchs and F.O. Gulacar, 1994, *Org. Geo-chem.*, 21,437.
- 43 R.W.Shaw, T.B. Brill, A.A. Clifford, C.A. Eckert and E.U. Franck, 1991, *Chem. Eng. News*, Special Report, December 23, p. 26.
- 44 S.B. Hawthorne, Y. Yang and D.J. Miller, 1994 *Anal. Chem.*, 66,2912.
- 45 Thompson, P. G.; Taylor, L. T.; Porter, N. L.; Richter, B. E. 1993, *Dionex Tech. Note* 204.
- 46 Brunner, G. I. Elsevier: New York, 1985, *Supercritical Fluid Technology*.
- 47 Sunol, A. K.; Hagh, B.; Chen, S. 1985, *Supercritical Fluid Technology*.
- 48 Peter, S. Ber. Bunsen-Ges. 1984, *Phys. Chem.*, 88, 875.
- 49 Hendricks, S. B.; Nelson, R. A.; Alexandar, L. T. *J. Am. Chem. Soc.*, 62, 1457.
- 50 Tarek M.Fahmy, Michael E. Paulaitis, David M. Johnson,1993, *Modifier Effects in the Supercritical Fluid Extraction of Solutes from Clay, Soil, and Plant Materials*, Department of chemical engineering, Delaware.
- 51 Joseph M. Levy, Eugene Storozynsky, 1992, *Use of Modifiers in Supercritical Fluid Extraction*, Suprex Corporation, Pittsburgh.
- 52 Yu Yang, Ahmed Gharaibeh, and David J. Miller, 1995, *Combined Temperature/ Modifier Effects on Supercritical CO₂ Extraction Efficiencies of Polycyclic Aromatic Hydrocarbons from Environmental Samples*, University of North Dakota, North Dakota.
- 53 Lide, D. R., Ed.; CRC Press: Boca Raton, 1991, *Handbook of Chemistry and Physics*.
- 54 Erkey, C., G. Madras, M.Orejuela, and A.Akgerman, 1993, *Supercritical Carbon Dioxide Regeneration of Organics from Soil*, *Environ. Sci. Technol.*, 27,1225.
- 55 Tan, C.S., and D.C.Liou, 1989a, *Supercritical Regeneration of Activated Carbon Loaded with Benzene and Toluene*, *Ind. Eng. Chem. Res.*, 28, 1222.

- 56 Recasens, F., J.M.S mith, and B.J.McCoy, 1989, Desorption Processes: Supercritical Fluid Regeneration of Activated Carbon, AICHE J., 35, 951.
- 57 Srinivasan, M.P.,J.M.Smith, and B.J. McCoy, 1990, Supercritical Fluid Desorption from Activated Carbon, Chem. Eng. Sci., 45,1885.
- 58 Giridhar Madras, Cathrerine Thibaud, Can Erkey, 1994, Modeling of Supercritical Extraction of Organics from Solid Matrices, J. AICHE, 40, 777-785.
- 59 J.M.Smith, 1981, Chemical Engineering Kinetics, Chemical Engineering University of California at Davis.
- 60 V. M. Shenai, B. L. Hamilton, 1993, Diffusion in Liquid and Supercritical Fluid Mixtures, Laramie, Wyoming.
- 61 Wiley, Stewart, W. R. Marshall, 1980, Transport Phenomena.
- 62 Wakao, N., and S. Kaguei, 1982, Heat and Mass Transfer in Packed Beds, Gordon and Breach, Sci. Publications, New York.
- 63 Tan, C. S., and D. C. Liou, 1989, Axial Dispersion of Supercritical Carbon Dioxide in Packed Beds, Ind. Eng. Chem. Res., 28, 1246.
- 64 Mark A. McHugh, , 1994, Supercritical Fluid Extraction Principles and Practice, Department of Chemical Engineering, 2ND Edition.
- 65 Rene P.Schwarzenbach, Philip M. Gschwend, 1993, Environmental Organic Chemistry.
- 66 Reid, R. C.; Prausnitz, J. M.; Sherwood, T. K., 1977, the Properties of Gases and Liquids, 3rd ed.; McGraw-Hill, New York.
- 67 Gordon J.Van Wylen, Richard E. Sonntag, 1978, Fundamentals of Classical Thermodynamics.
- 68 Pawliszyn, j.j. 1993, Chromatography Sci. 31, 31.
- 69 Lee, M.L., Markides, K.E., Eds; Chromatography Confrences Inc.: Provo, 1990, Analytical Supercritical Fluid Chromatography and Extraction.
- 70 Robert E. Terybal, 1980, Mass-Transfer Operations.
- 71 Wartkentin, 1966, Introduction to Soil Behavior, MC Gill University.

APPENDICES

A3.1 shows a U.S.D.A. texture triangle, giving names to soils containing different proportions of sand, silt, and clay [71].

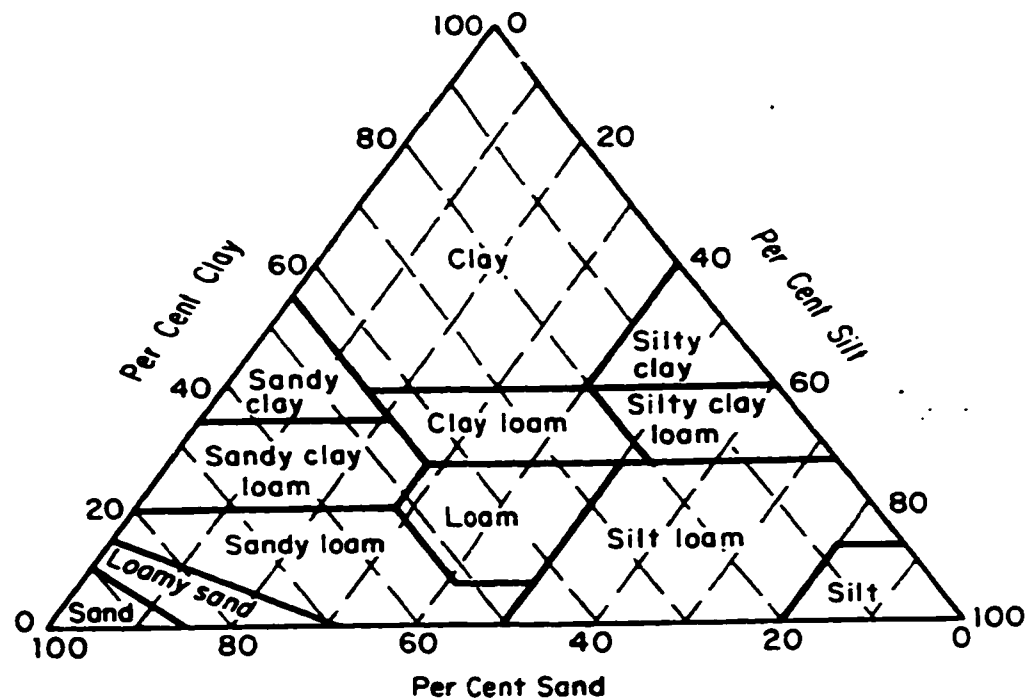


Figure A3.1. Chart Showing Per Cent Clay, Silt, and Sand in the Soil Textural Classes of U.S. Department of Agriculture.

A4.1 Tables of results were measured after extraction using SFE.

Table 4.1. Condition: Clay 100 %, no modifier 5 %.

Time (min)	Pressure (psi)	Temperature (°C)	Recovery (%)
Ts = Td = 15	5000	50	2
Ts = 10 and Td = 20	5000	50	3
Td = 30	5000	50	2
Ts = Td = 15	5000	80	5
Ts = 10 and Td = 20	5000	80	4
Td = 30	5000	80	7
Ts = Td = 15	5000	150	4
Ts = 10 and Td = 20	5000	150	3
Td = 30	5000	150	44
Ts = Td = 15	8000	50	4
Ts = 10 and Td = 20	8000	50	8
Td = 30	8000	50	49
Td = 30	8000	80	6
Td = 10	8000	150	45
Td = 20	8000	150	52
Td = 30	8000	150	53

Table 4.2. Condition: Clay 100 %, modifier 5 %.

Time (min)	Pressure (psi)	Temperature (°C)	Recovery (%)
Td = 10	5000	50	13
Td = 20	5000	50	39
Td = 30	5000	50	46
Td = 10	5000	80	1
Td = 20	5000	80	1
Td = 30	5000	80	3
Td = 10	5000	150	2
Td = 20	5000	150	37
Td = 30	5000	150	58
Td = 30	8000	50	37
Td = 30	8000	80	61
Td = 10	8000	150	4
Td = 20	8000	150	61
Td = 30	8000	150	72
Td = 60	8000	150	6

Table 4.3. Condition: Clay 60 % and sand 40 %, no modifier.

Time (min)	Pressure (psi)	Temperature (°C)	Recovery (%)
Ts = Td = 15	5000	50	4
Ts = 10 and Td = 20	5000	50	2
Td = 30	5000	50	6
Ts = Td = 15	5000	80	5
Ts = 10 and Td = 20	5000	80	7
Td = 30	5000	80	8
Ts = Td = 15	5000	150	27
Ts = 10 and Td = 20	5000	150	24
Td = 30	5000	150	37
Ts = Td = 15	8000	50	31
Ts = 10 and Td = 20	8000	50	43
Td = 30	8000	50	15
Td = 30	8000	80	3
Td = 10	8000	150	34
Td = 20	8000	150	36
Td = 30	8000	150	40

Table 4.4. Condition: Clay 60 % and sand 40 %, modifier 5 %.

Time (min)	Pressure (psi)	Temperature (°C)	Recovery (%)
Td = 10	5000	50	2
Td = 20	5000	50	2
Td = 30	5000	50	2
Td = 10	5000	80	2
Td = 20	5000	80	3
Td = 30	5000	80	3
Td = 10	5000	150	30
Td = 20	5000	150	50
Td = 30	5000	150	51
Td = 30	8000	50	42
Td = 30	8000	80	45
Td = 10	8000	150	25
Td = 20	8000	150	39
Td = 30	8000	150	42

Table 4.5. Condition: Clay 20 % and sand 80 %, no modifier.

Time (min)	Pressure (psi)	Temperature (°C)	Recovery (%)
Ts = Td = 15	5000	50	11
Ts = 10 and Td = 20	5000	50	8
Td = 30	5000	50	3
Ts = Td = 15	5000	80	11
Ts = 10 and Td = 20	5000	80	6
Td = 30	5000	80	5
Ts = Td = 15	5000	150	14
Ts = 10 and Td = 20	5000	150	12
Td = 30	5000	150	31
Ts = Td = 15	8000	50	5
Ts = 10 and Td = 20	8000	50	6
Td = 30	8000	50	20
Td = 30	8000	80	12
Td = 10	8000	150	39
Td = 20	8000	150	63
Td = 30	8000	150	64

Table 4.6. Condition: Clay 20 % and sand 80 %, modifier 5 %.

Time (min)	Pressure (psi)	Temperature (°C)	Recovery (%)
Td = 10	5000	50	2
Td = 20	5000	50	2
Td = 30	5000	50	4
Td = 10	5000	80	4
Td = 20	5000	80	4
Td = 30	5000	80	3
Td = 10	5000	150	2
Td = 20	5000	150	29
Td = 30	5000	150	57
Td = 30	8000	50	16
Td = 30	8000	80	18
Td = 10	8000	150	48
Td = 20	8000	150	50
Td = 30	8000	150	51

Table 4.7. Fine sand with no clay

Material	Time(min)	Pressure(Psi)	Temperature (°C)	Recovery (%)
No modifier	10	5000	50	71
	30	5000	50	65
	10	5000	80	45
	10	5000	150	64
	10	8000	50	69

A5.1 The program used to calculate the desorption concentration and adsorption concentration of several extraction condition.

```
#include <stdio.h>
#include <math.h>
#define k 0.025
#define x 20
#define h 0.255
#define y 20
int i,j;
float c[21][20]
,ca[21][20];
void main()
{
    for(i=0;i<20;i++)
    {
        c[i][0]=0.2;
        ca[i][0]=0.2;
    }
    c[0][0]=0.2;
    ca[0][0]=0.2;
    for(j=1;j<20;j++)
    {
        c[0][j]=0.2;
        ca[0][j]=0.2;
    }
    for (j=0;j<19;j++)
    {
        for(i=1;i<20;i++)
        {
            c[i][j+1]=(c[i][j]*(26.3)+ c[i+1][j]*(-296)+ c[i-1][j]*(302)+ (13553))/(11326);
            if(i==19) c[i+1][j+1] = c[i-1][j+1];
            ca[i][j+1]=(2.35-c[i][j+1])/2;
        }
    }
    printf("\n");
    for (j=0;j<20;j++)
    {
        for (i=15;i<20;i++)
        {
            if(c[i][j]>=0.0 && c[i][j]<=2.5) printf("%4.2f ",c[i][j]);
            else printf(" ");
        }
        printf("\n");
    }
}
```

```

    }
    printf("\n");
    printf("\n");
    for (j=0;j<20;j++)
    {
        for (i=5;i<20;i++)
        {
            if(ca[i][j]>=0.0 && ca[i][j]<=2.5) printf("%4.2f ",ca[i][j]);
            else printf("  ");
        }
        printf("\n");
    }
}

```

A5.2. The output results from the program at P=8000 psi, T=150°C in 30 min.

Time (min)	Z (cm)	Desorped conce. (mg/ml)	Adsorped conce. (mg/ml)
0	0	0	0.2
3	0.51	0.79	0.78
4.5	0.765	0.79	0.78
6	1.02	0.83	0.76
15	1.06	1.275	0.537
21	1.53	1.72	0.315

A5.3 The output results from the program at P=8000 psi, T=150°C in 20 min

Time (min)	Z (cm)	Desorped conce. (mg/ml)	Adsorped conce. (mg/ml)
0	0	0	0.2
1.92	0.51	0.79	0.78
4.8	1.02	0.83	0.76
8.64	1.53	0.87	0.74
14.4	2.04	1.14	0.605

A5.4 The output results from the program at P=8000 psi, T=150°C in 10 min

Time (min)	Z (cm)	Desorped conce. (mg/ml)	Adsorped conce. (mg/ml)
0	0	0.0	0.2
1.992	0.765	0.67	0.84
3.486	1.27	0.71	0.82
4.98	1.785	0.73	0.81
7.47	2.8	0.77	0.79

A5.5. The output from the program in the radial co-ordinate.

r_p , radius of the particle (cm)	Time (min)	adsorped concentration (mg /ml)
$6 \cdot 10^{-10}$	1.5	0.2
$18 \cdot 10^{-10}$	4.5	0.2
$30 \cdot 10^{-10}$	7.5	0.2